



UNIVERSITY of BAYREUTH
Department of Micrometeorology

The Arctic Turbulence Experiment 2006

**Direct measurements of turbulent fluxes in the near
surface environment at high latitudes applying the
eddy-covariance method**



PART 2

**Near surface measurements during the
ARCTEX 2006 campaign
May, 2nd to May, 20th 2006**

**Johannes Lüers
and
Jörg Bareiss**

Work Report
No. 32
Bayreuth, August 2007

Contents

1	Introduction.....	3
2	General Information.....	4
2.1	Location.....	4
2.2	Surface and weather conditions.....	5
3	Overview of measurement sites.....	6
4	Visualization of standard meteorological measurements.....	7
4.1	Synoptic situation.....	7
4.2	Entire observation period.....	20
4.3	Daily charts.....	27
5	Visualization of directly measured turbulence fluxes.....	59
5.1	Calculation of turbulent fluxes with the software package TK2.....	59
5.2	Entire observation period.....	60
5.3	Daily charts.....	69
6	Data archived at Ny-Ålesund (CDs).....	74

1 Introduction

Abstract

Accurate quantification of turbulent fluxes between the surface and the atmospheric boundary layer in polar environments, characterized by frequent stable to very stable stratified conditions, is a fundamental problem in soil-snow-ice-vegetation-atmosphere interaction studies. The observed rapid climate warming in the Arctic requires improvements in the monitoring of energy and matter exchange; accomplished by setting up appropriate (adapted to polar conditions) observation sites to measure turbulent fluxes. To address these problems, it is essential to improve the databases with high-quality in-situ measurements of turbulent fluxes near the surface applying the Eddy-Covariance method.

These direct measurement data (CSAT3 sonic anemometer, KH20 krypton hygrometer, and laser scintillometer) obtained during the first Arctic Turbulence Experiment (ARCTEX-2006) in May 2006 at the French-German Arctic Research Base in Ny-Ålesund (AWI/IPEV) on Spitsbergen (Svalbard) allowed a comparison with simulated results from simple flux gradient-parameterizations used today to force atmosphere-ocean-ice models. In addition, the results of this pilot study shows the problem of direct measurements (e.g. snow drift through the sensor path ways) under rough weather conditions as well as they reveal that the misestimating of sensible heat fluxes can result from inaccurate measurements or calculation of the surface temperature and inappropriate treatment of the neutral and stable conditions (e.g. intermittency, gravity waves) in the bulk parameterization.

The primary goals of the ARCTEX-campaign were:

1. continuous measurements of high-resolution (20 Hz) turbulent heat fluxes near the tundra surface using a ultra sonic anemometer (eddy-covariance method) and an ultraviolet krypton hygrometer,
2. continuous measurements of the turbulent sensible heat flux near the tundra surface using the Laser-scintillometry,
3. measurements of standard meteorological data sampled at 1s intervals using a meteorological gradient tower (6 m and 10 m),
4. pre- and post- processing of high-quality data sets of turbulent fluxes using state of the art flux data quality assessment techniques,
5. understanding of exchange processes and their parameterization for neutral and stable conditions,
6. validation of commonly used sensible and latent heat flux parameterizations (aerodynamic approach, bulk and gradient method).

2 General Information

2.1 Location

Detailed geographic locations of the “Arctic Turbulence Experiment 2006” (ARCTEX-2006) at Ny-Ålesund (Svalbard, Kongsfjorden), May 2006, Universities of Bayreuth and Trier, Germany:

General location	Svalbard, Kongsfjorden, Ny-Ålesund, Position (Center of settlement): 078° 55' 24" N, 011° 55' 15" E	
Eddy-Flux complex UBT (EF):	Coordinates:	078° 55' 02" N, 011° 55' 52" E
	Altitude:	13 m a. s. l.
	Land use:	snow covered tundra
Meteorological tower AWI (MT1):	Coordinates:	078° 55' 04" N, 011° 55' 26" E
	Altitude:	14 m a. s. l.
	Land use:	snow covered tundra
Meteorological tower UBT (MT2):	Coordinates:	078° 55' 03" N, 011° 55' 34" E
	Altitude:	14 m a. s. l.
	Land use:	snow covered tundra
Scintillometer UBT (SLS):	Coordinates:	078° 55' 00" N, 011° 56' 00" E
	Altitude:	13.5 m a. s. l.
	Land use:	snow covered tundra
Tethered balloon AWI (TB1):	Coordinates:	078° 55' 06" N, 011° 55' 23" E
	Altitude:	11 m a. s. l.
	Land use:	snow covered tundra
Tethered balloon AWI (TB2):	Coordinates:	078° 55' 27" N, 011° 56' 07" E
	Altitude:	3 m a. s. l.
	Land use:	Harbor (concrete), fjord (water)
Radiosonde AWI (RS):	Coordinates:	078° 55' 06" N, 011° 55' 23" E
	Altitude:	11 m a. s. l.
	Land use:	snow covered tundra
BSRN AWI (BSRN):	Coordinates:	078° 56' 05" N, 011° 56' E
	Altitude:	11 m a. s. l.
	Land use:	snow covered tundra
Time zone		Central European Time: CET = GMT + 1 h (winter) CEST = GMT + 2 h (summer). Given times and filenames reflect starting time of intervals

UBT=Univ. of Bayreuth; AWI= Alfred Wegener Institute for Polar- and Marine Research; BSRN= Baseline Surface Radiation Network

2.2 Surface and weather conditions

Table 2.1 lists the surface and weather conditions during the ARCTEX-2006 campaign. Noteworthy, is the extreme warm period until evening May 7 and the heavy snow-storm at night, May 7 to May 8.

Table 2.1: **Surface and weather conditions during the ARCTEX-2006 campaign.**

May 3 to May 5	wet melting snow over ice, larger snow free spots (bare soil, tundra), surface melt water, some rain fall and partly cloudy, Arctic Haze event, extremely warm, temperature range: +3 °C to +8 °C
May 6 to May 8	1 st storm and heavy snowfall, heavy snowdrift; overcast weather, extremely warm (+8 °C) until beginning of the 2 nd storm on May 7, 19 h CET and temperature drop of more than 16 K (–10 °C)
May 9 to May 11	fresh snow cover, predominantly sunny weather, temperature range: –5 °C to –2 °C
May 12 to May 14	ongoing snowdrift, snow cover depleting, at 13 th pm temperature around 0 °C, predominantly overcast or partly cloudy weather, temperature range: –4 °C to 0 °C
May 15 to May 16	ongoing snowdrift, some snow free spots, at ground refrozen and compacted thin ice layers, predominantly sunny or partly cloudy weather, temperature range: –4 °C to –1 °C
May 17 to May 19	melting snow over ice, some snow free spots (bare soil, tundra), light to moderate rain and/or snowfall (17 th and 18 th , temperature range: –2 °C to +1 °C)

3 Overview of measurement sites

The map (Figure 3.1) of Ny-Ålesund (Svalbard) shows the measurement sites during the ARCTEX-2006 campaign. The permanent AWI/IPEV sites used for this study are the 10 m meteorological tower of the Alfred Wegener Institute for Polar and Marine Research (MT1), the international standardized radiation measurements of the Baseline Surface Radiation Network (BSRN), the WMO 1004 radiosonde launch site (RS) and the temporary AWI tethered balloon launch sites TB1 and TB2. The temporary sites - build up by the Universities of Bayreuth and Trier - are the 6 m meteorological tower (MT2), the eddy-flux measurement complex with sonic anemometer (EF), and the Laser-scintillometer pathway (SLS).

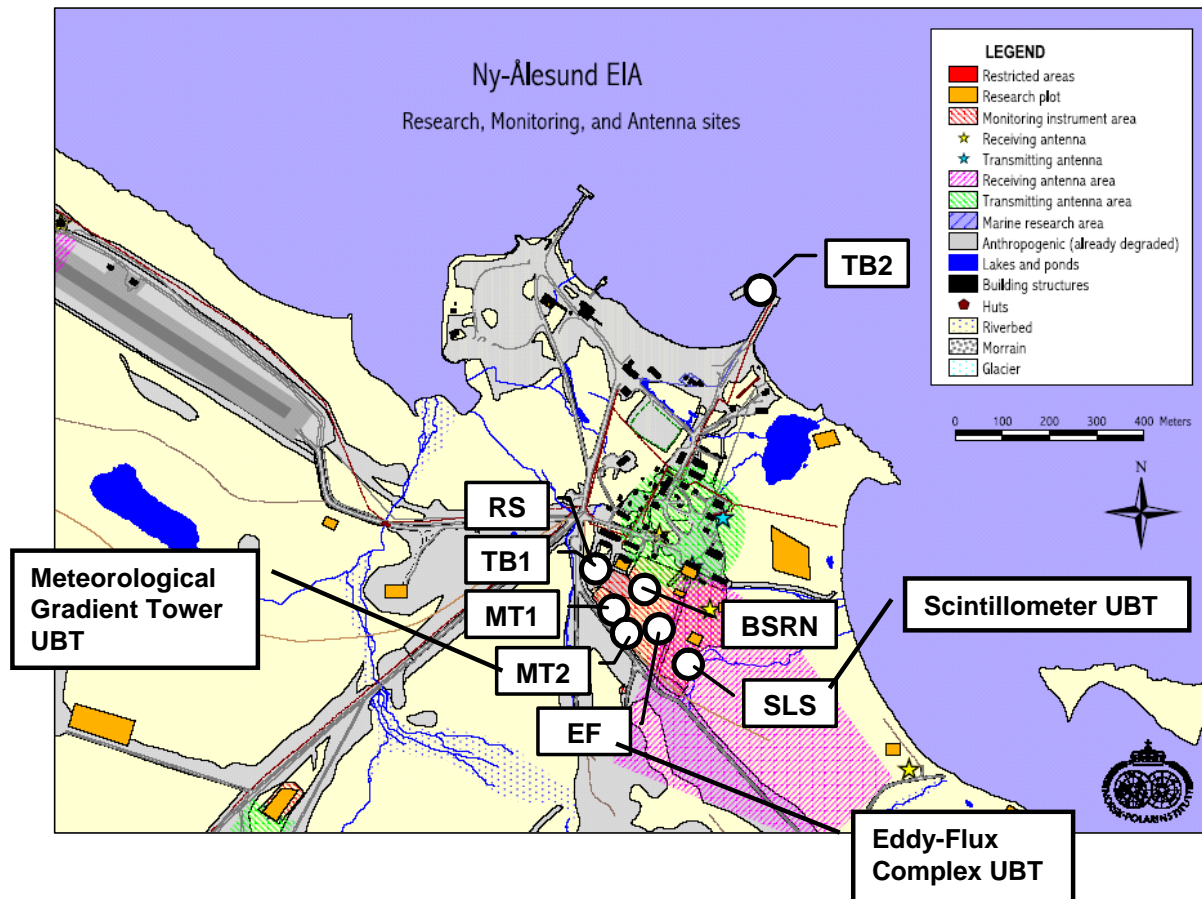
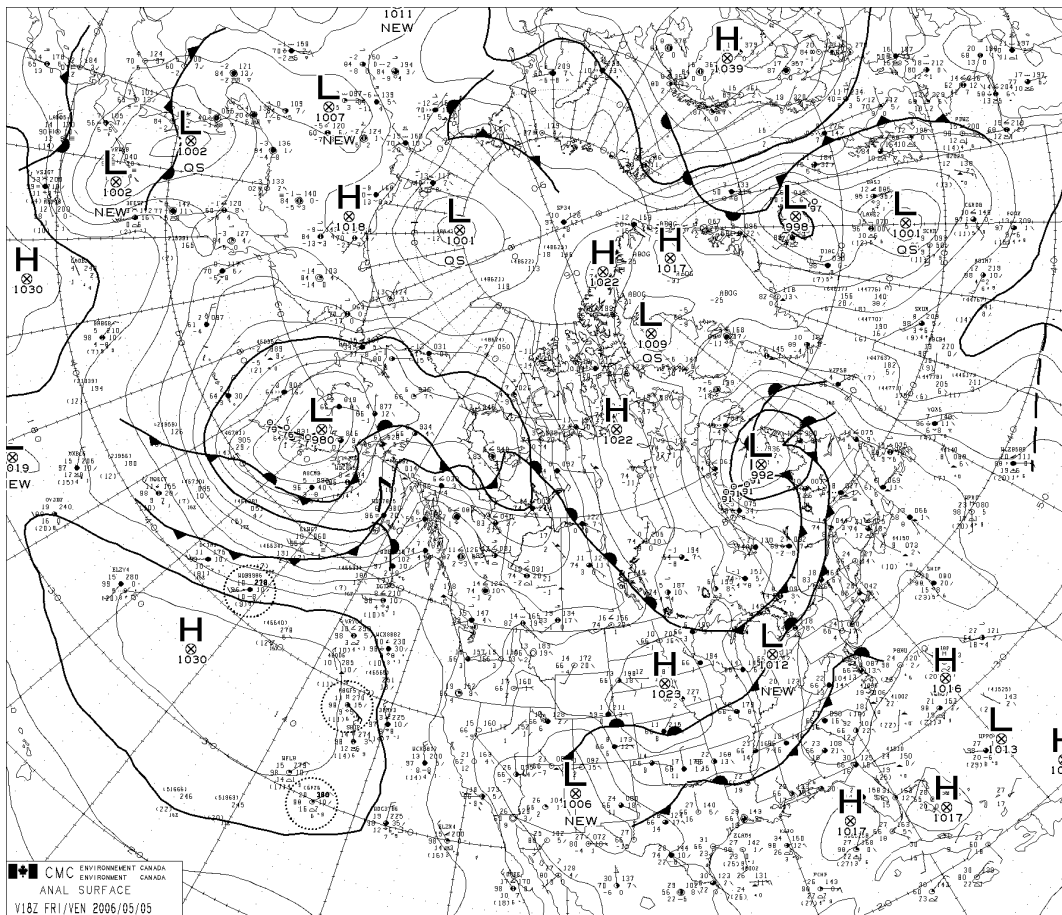


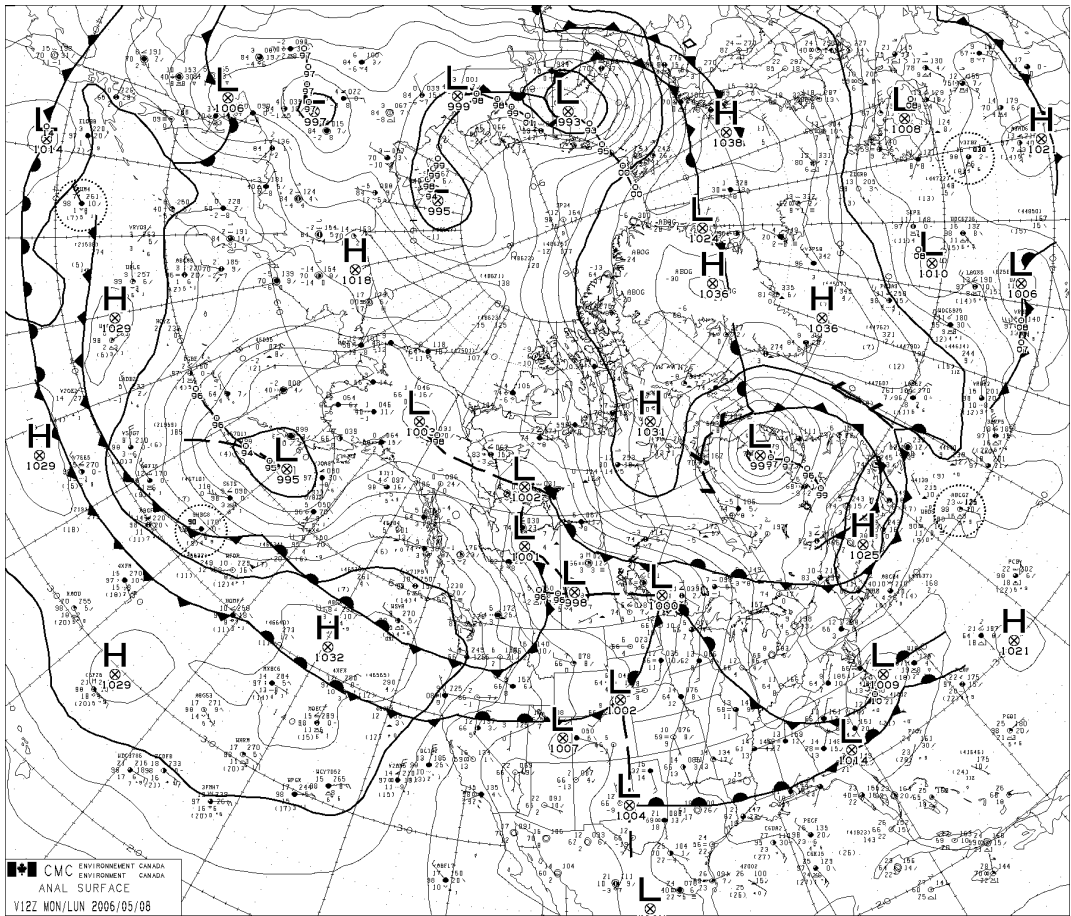
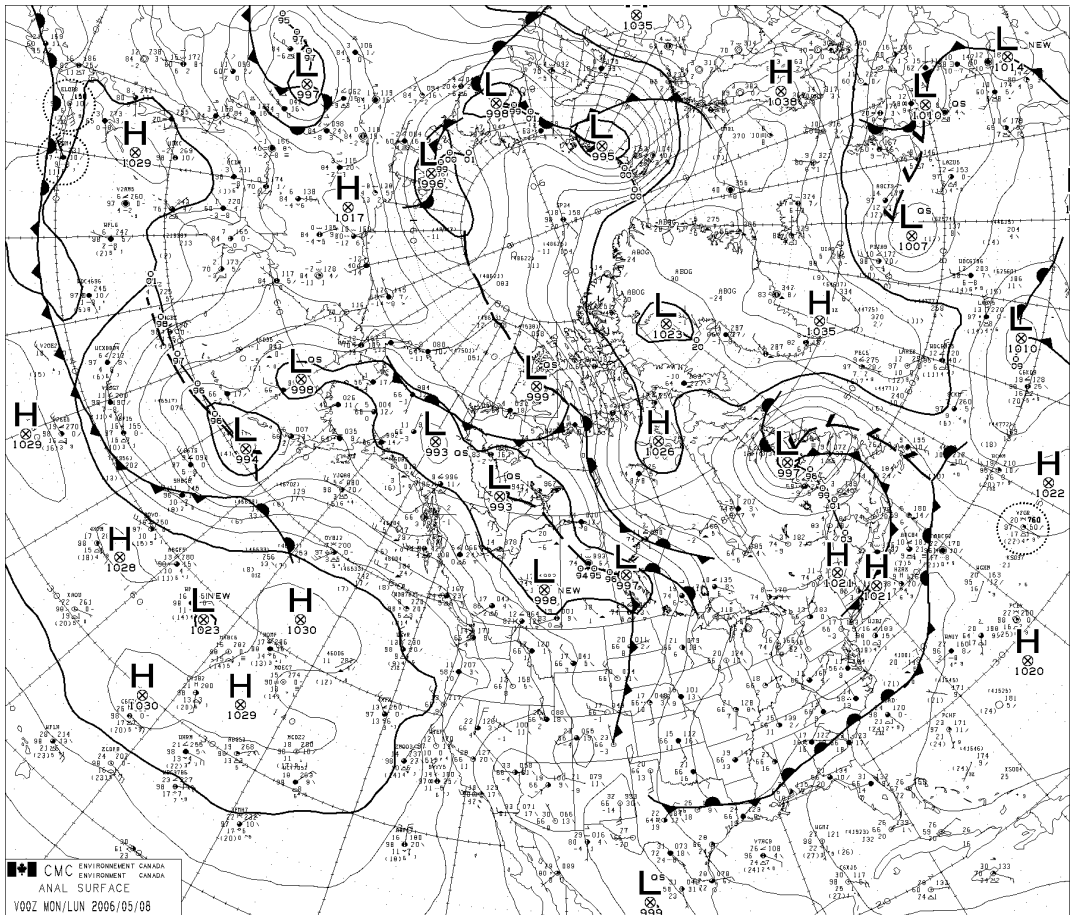
Figure 3.1: Map of Ny-Ålesund (Svalbard, Kongsfjorden) showing the measurement sites during the ARCTEX-2006 campaign: MT1 (10 m meteorological tower of the Alfred Wegener Institute for Polar and Marine Research), MT2 (6 m meteorological tower of the University of Bayreuth), EF (eddy-flux measurement complex), SLS (site for scintillometer measurements), BSRN (radiation measurements of the Baseline Surface Radiation Measurements), RS (radiosonde launch site), TB1 and TB2 (tethered balloon launch sites). The base map was kindly provided by the Norwegian Polar Institute.

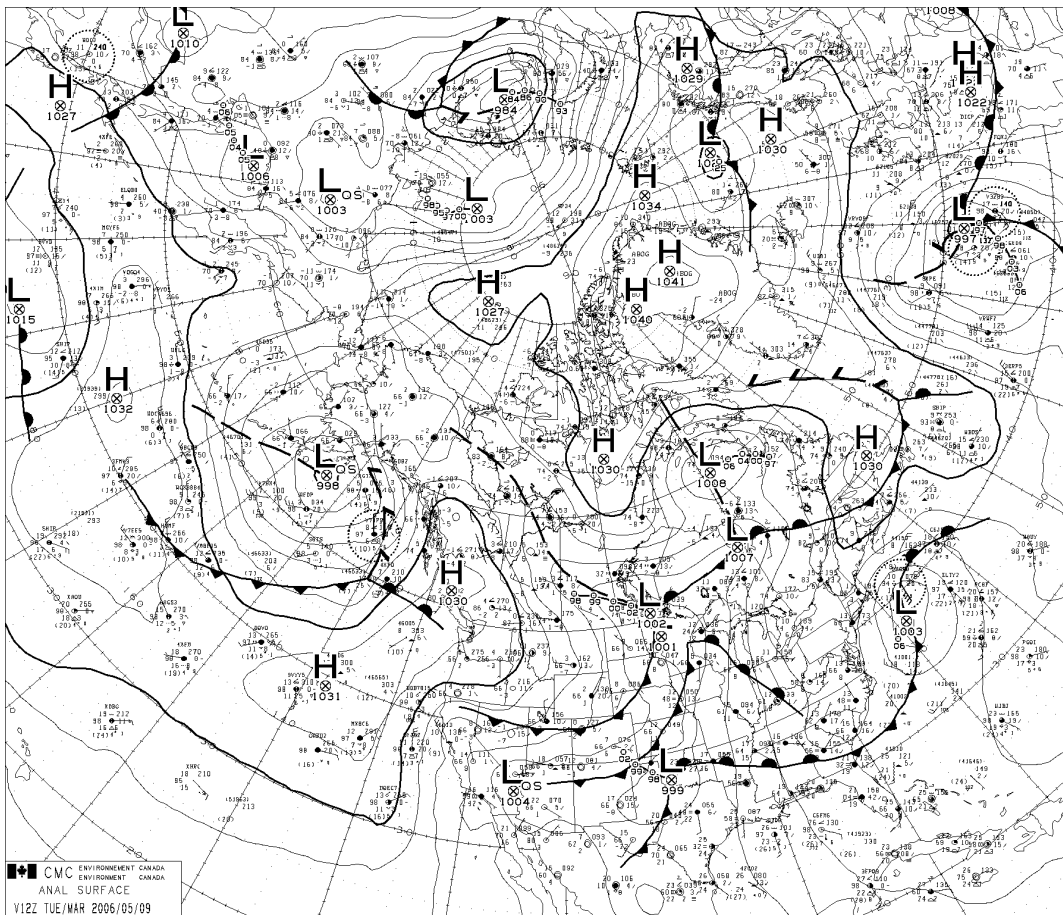
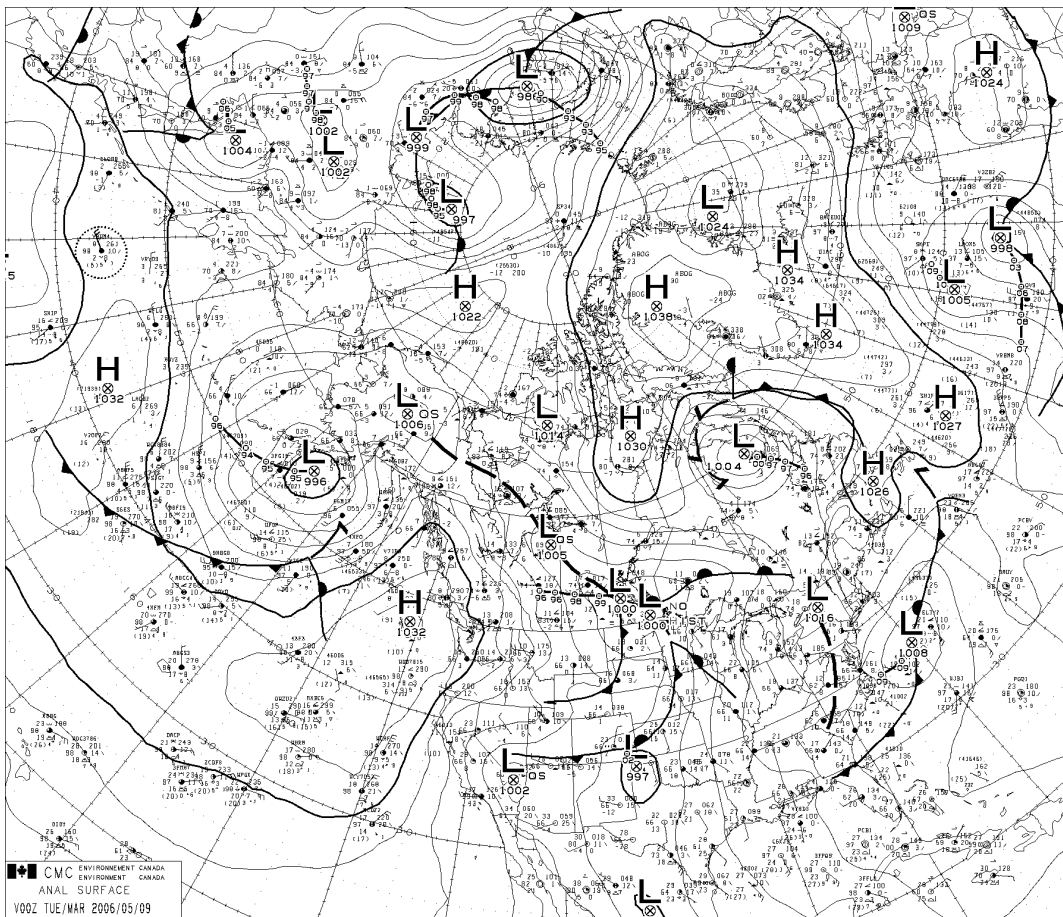
4 Visualization of standard meteorological measurements

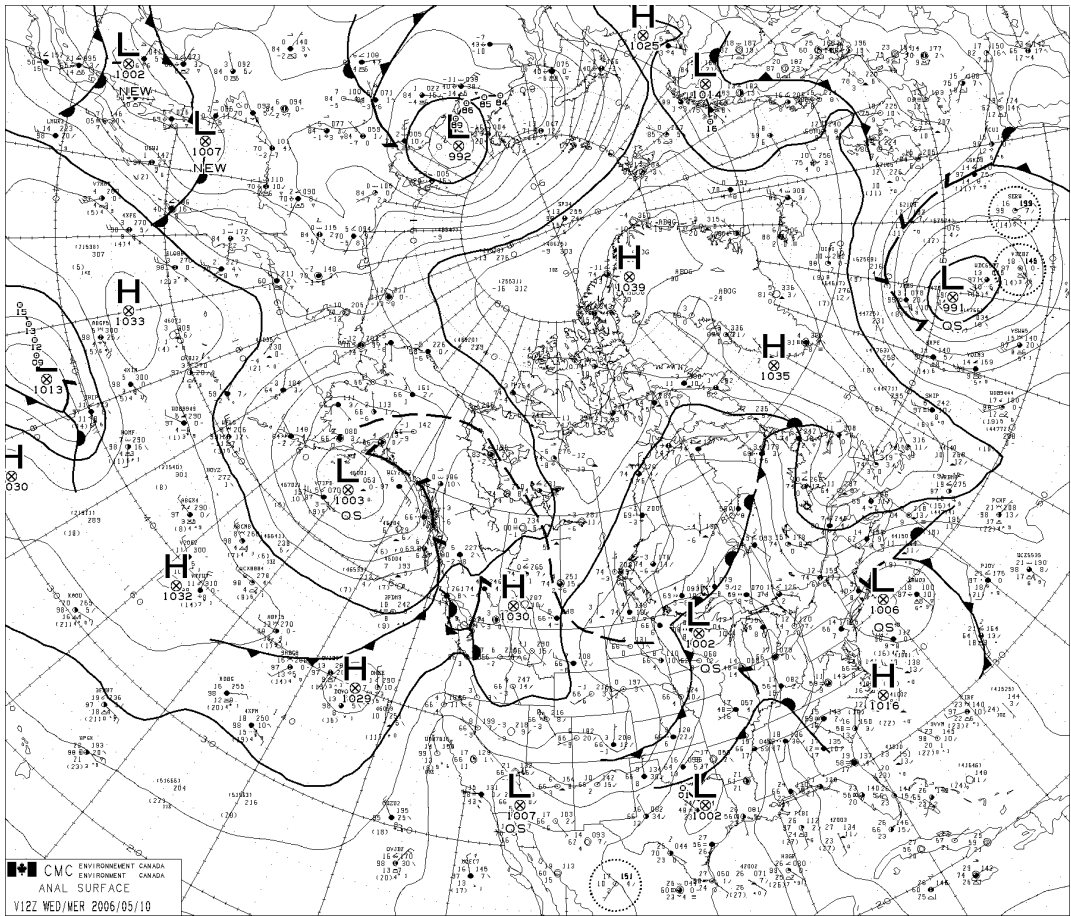
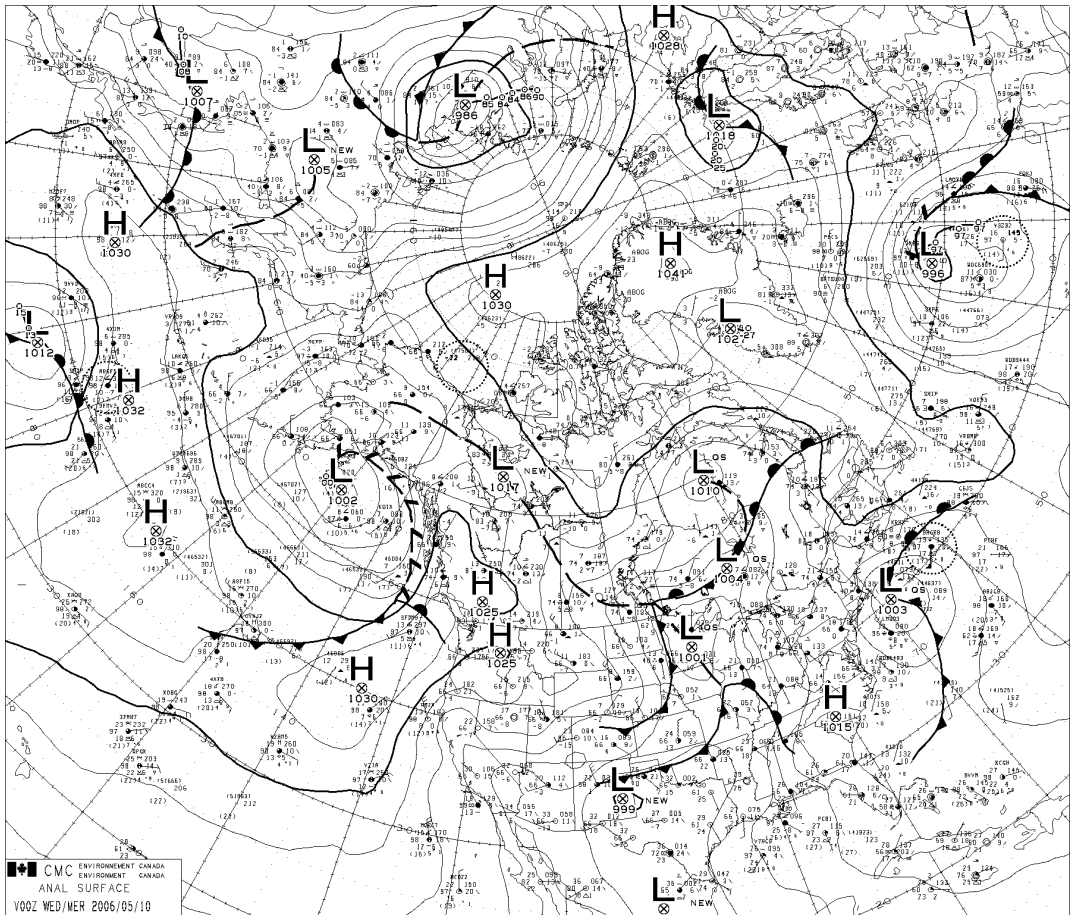
4.1 Synoptic situation

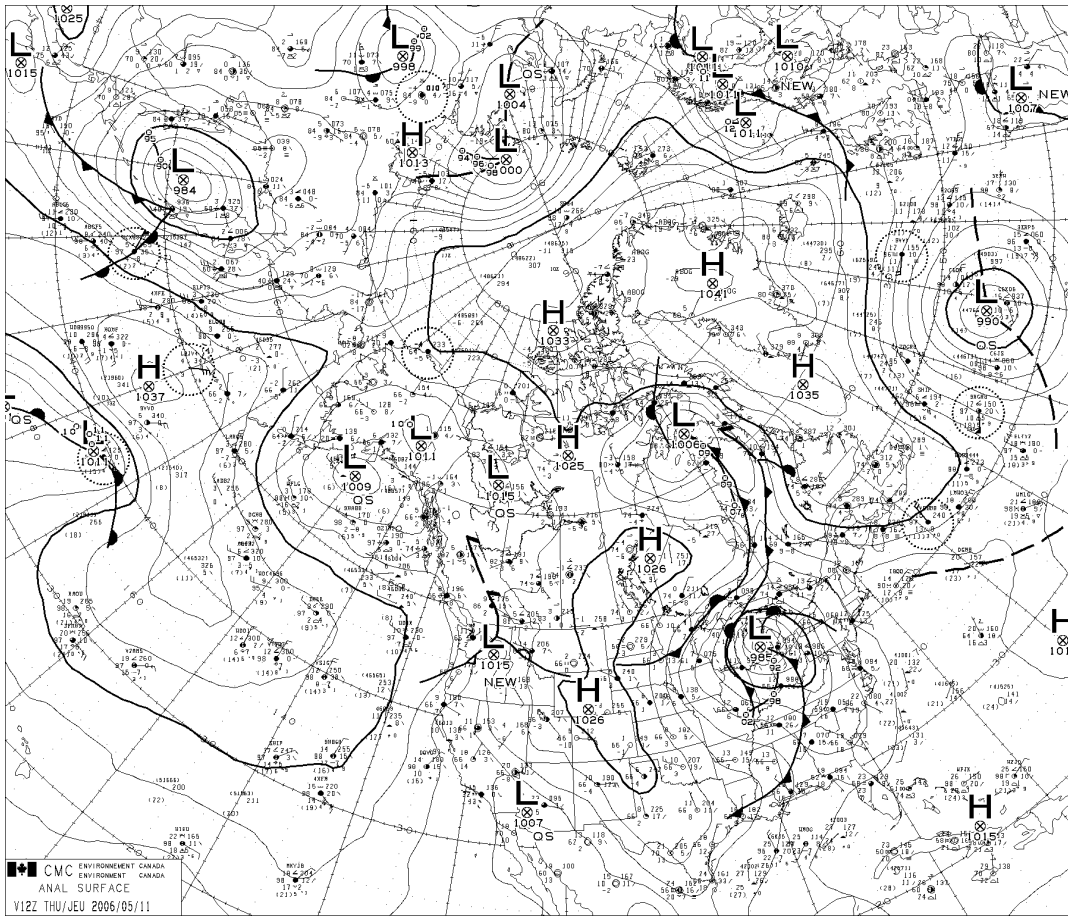
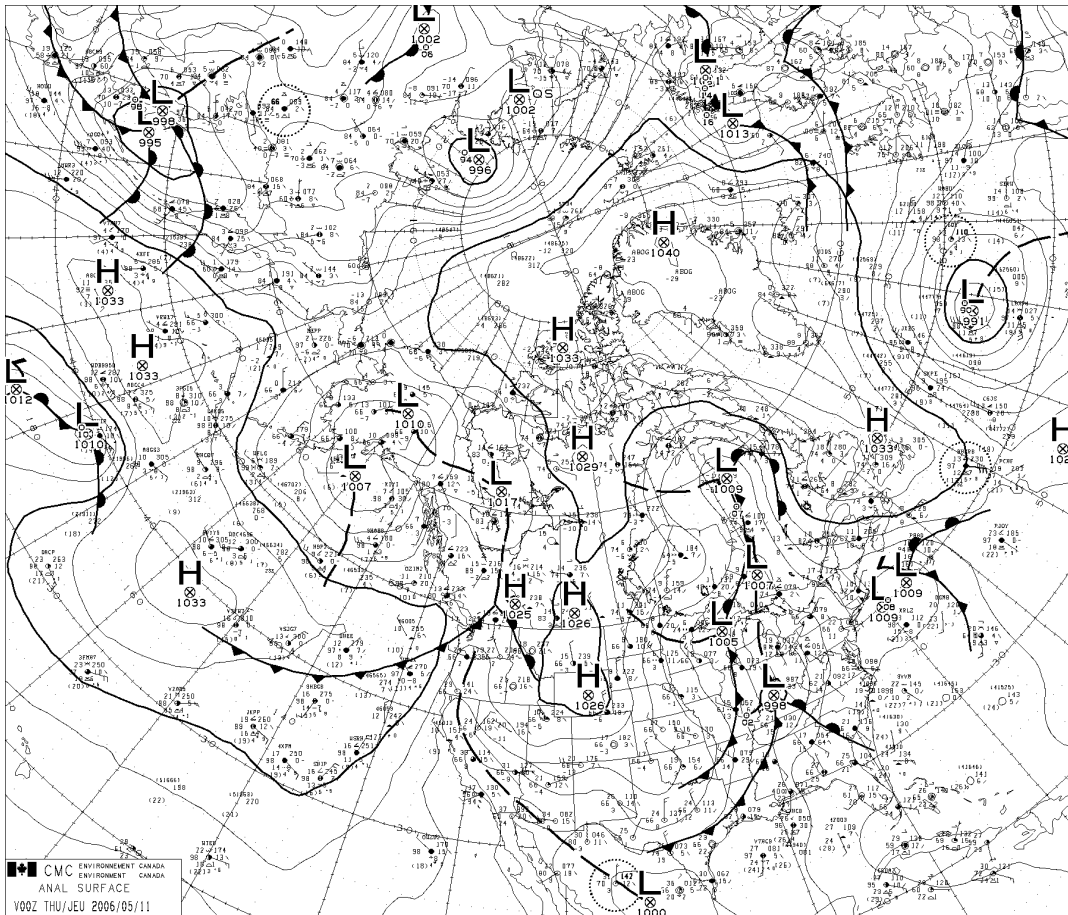
Operational Surface Analysis Charts of the Meteorological Service of Canada, Weatheroffice (www.weatheroffice.gc.ca), complete Northern Hemispheric coverage. The following charts of the Global Environmental Multiscale Model (GEM) outline the synoptic situation between May 5 and May 18, 2006. Remarkable was the passage of an arctic cyclone on May 7 and May 8, 2006 across Spitsbergen causing heavy snow fall and wind speeds up to more than 80 km/h.

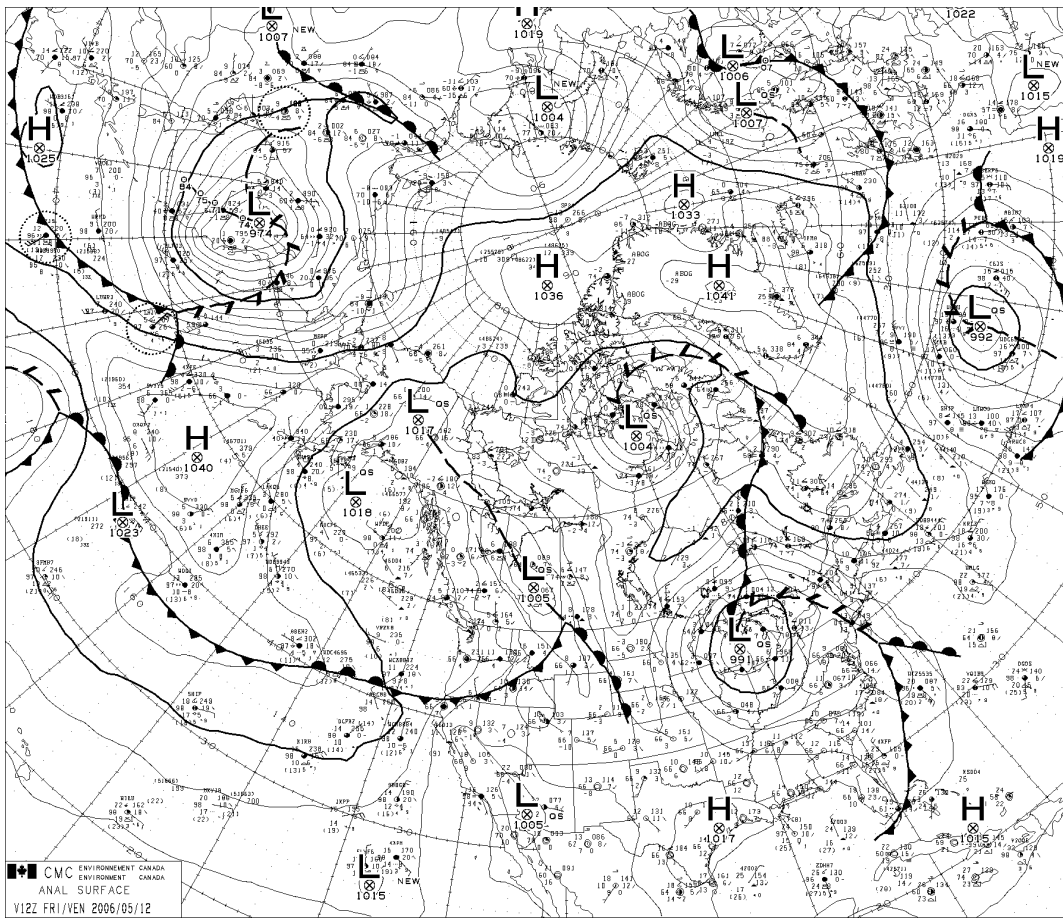
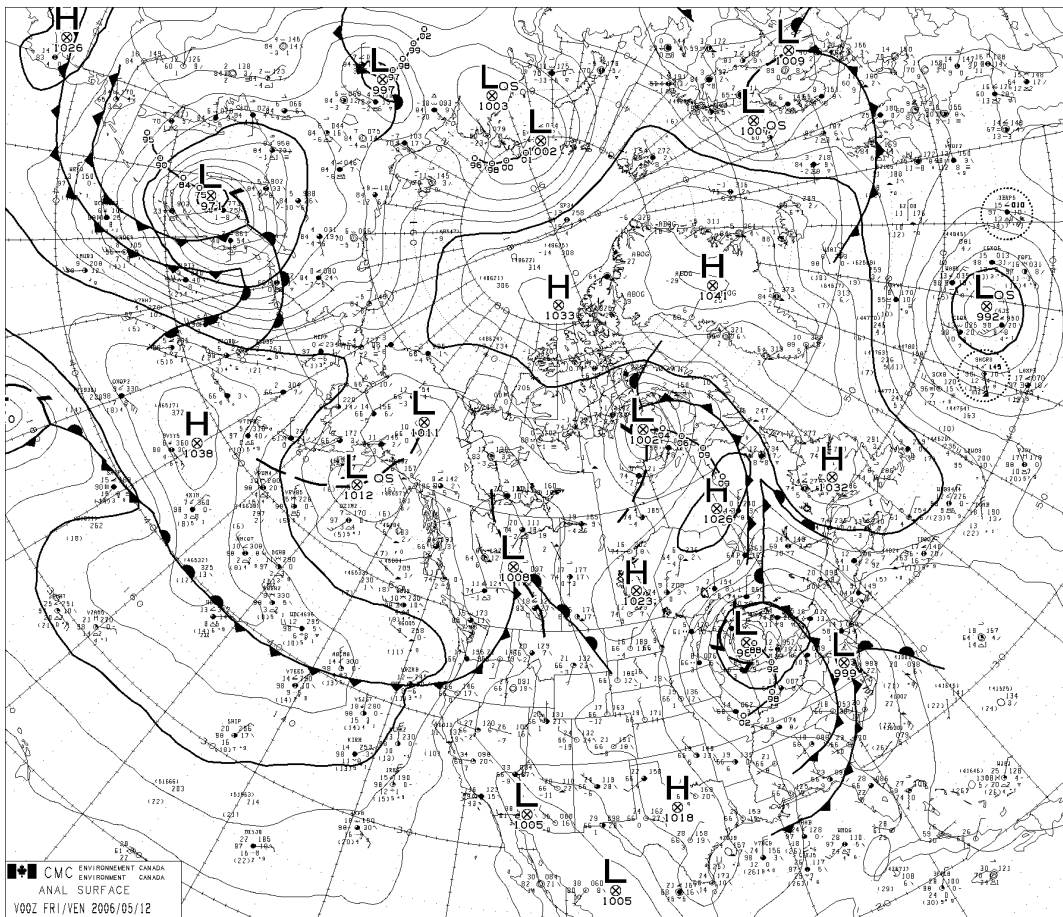


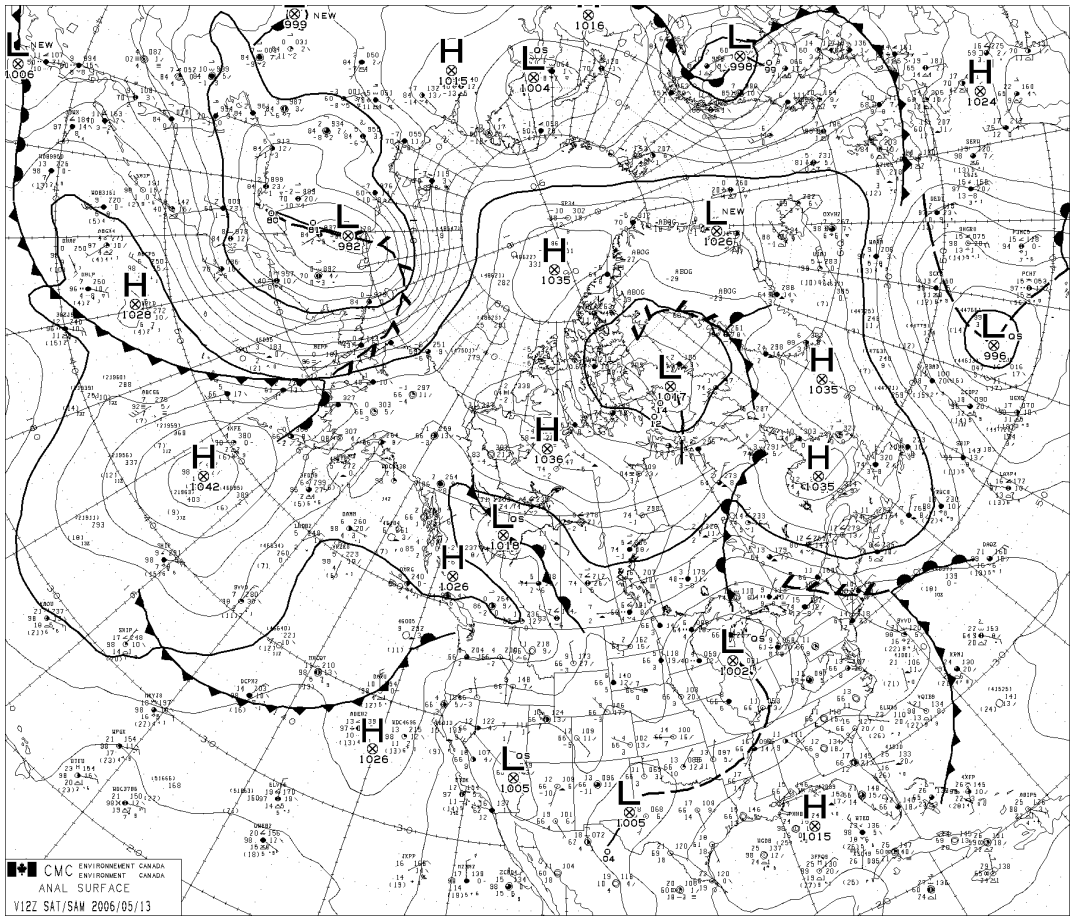
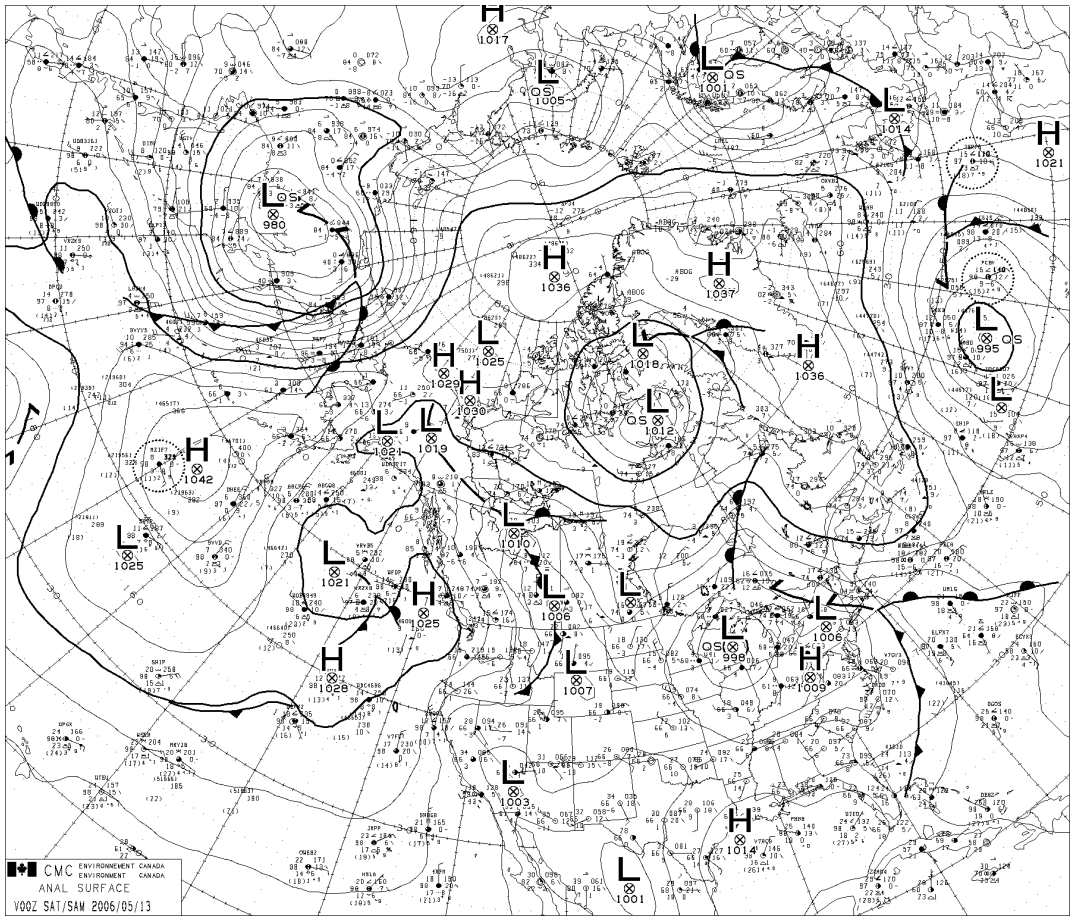


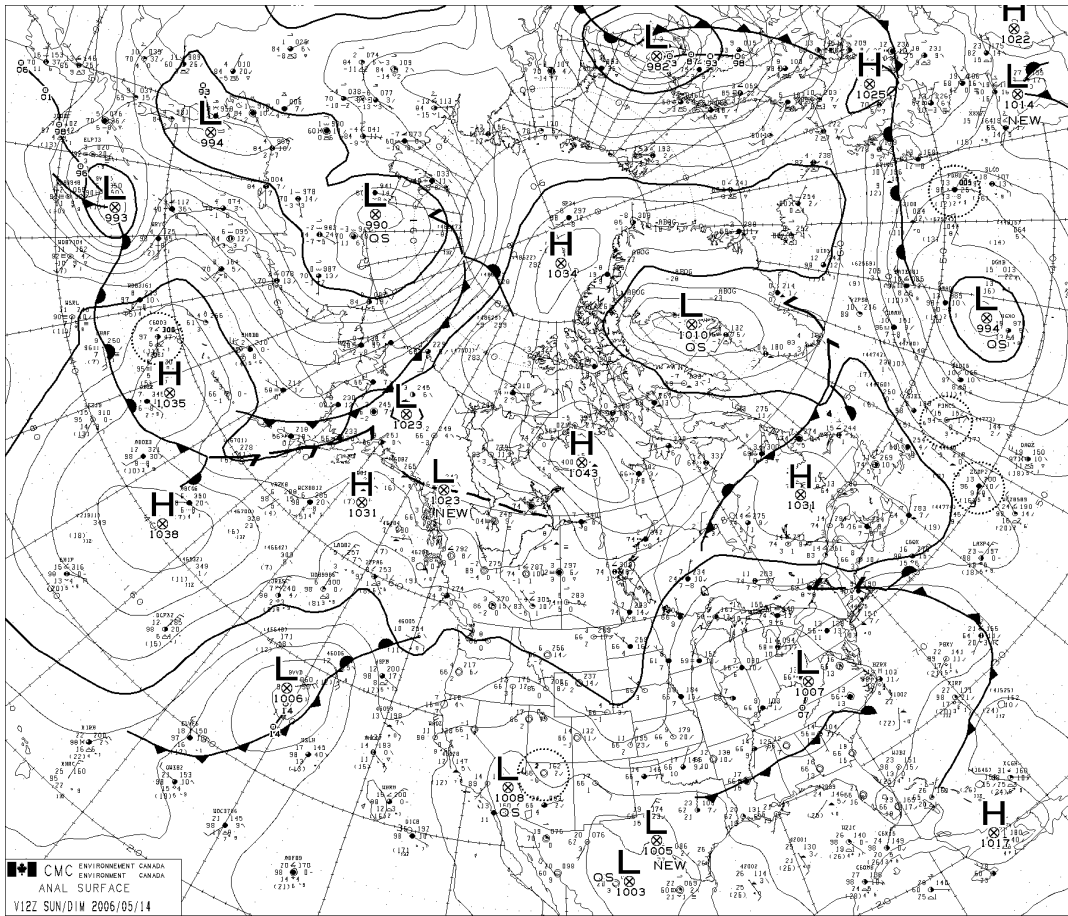
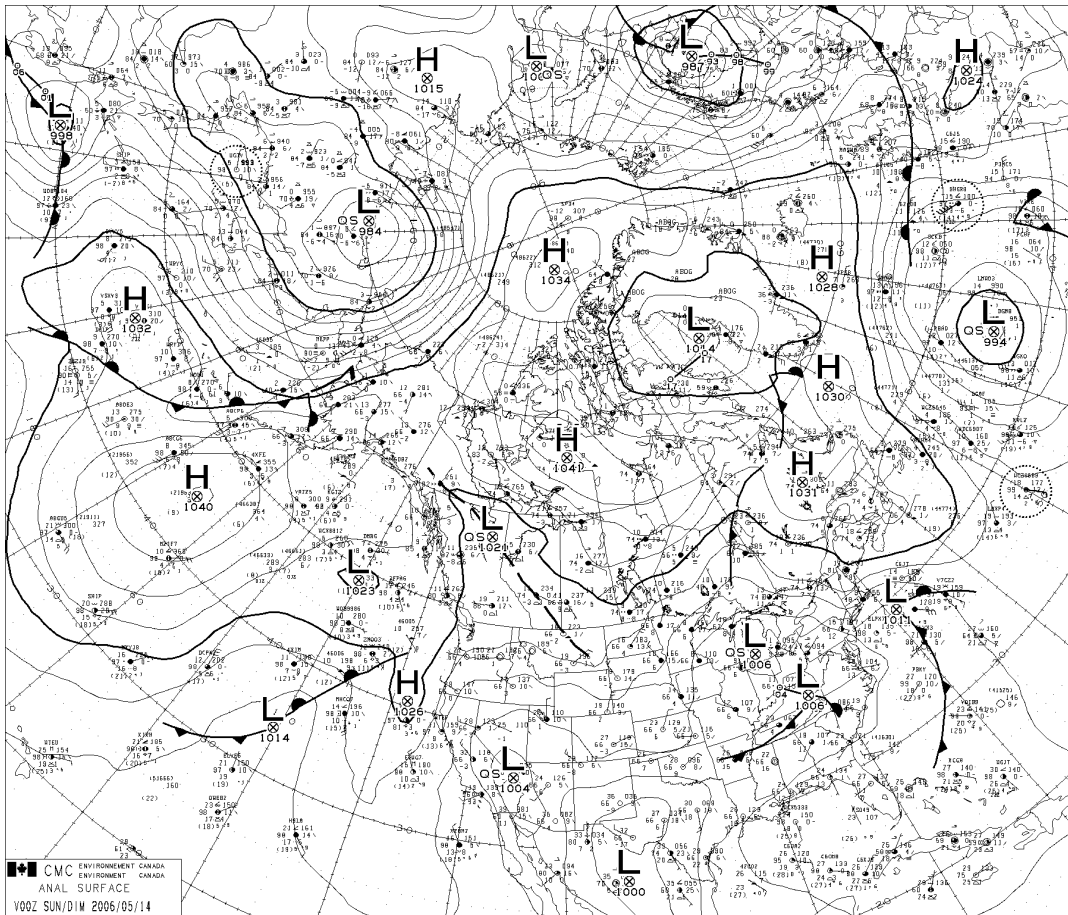


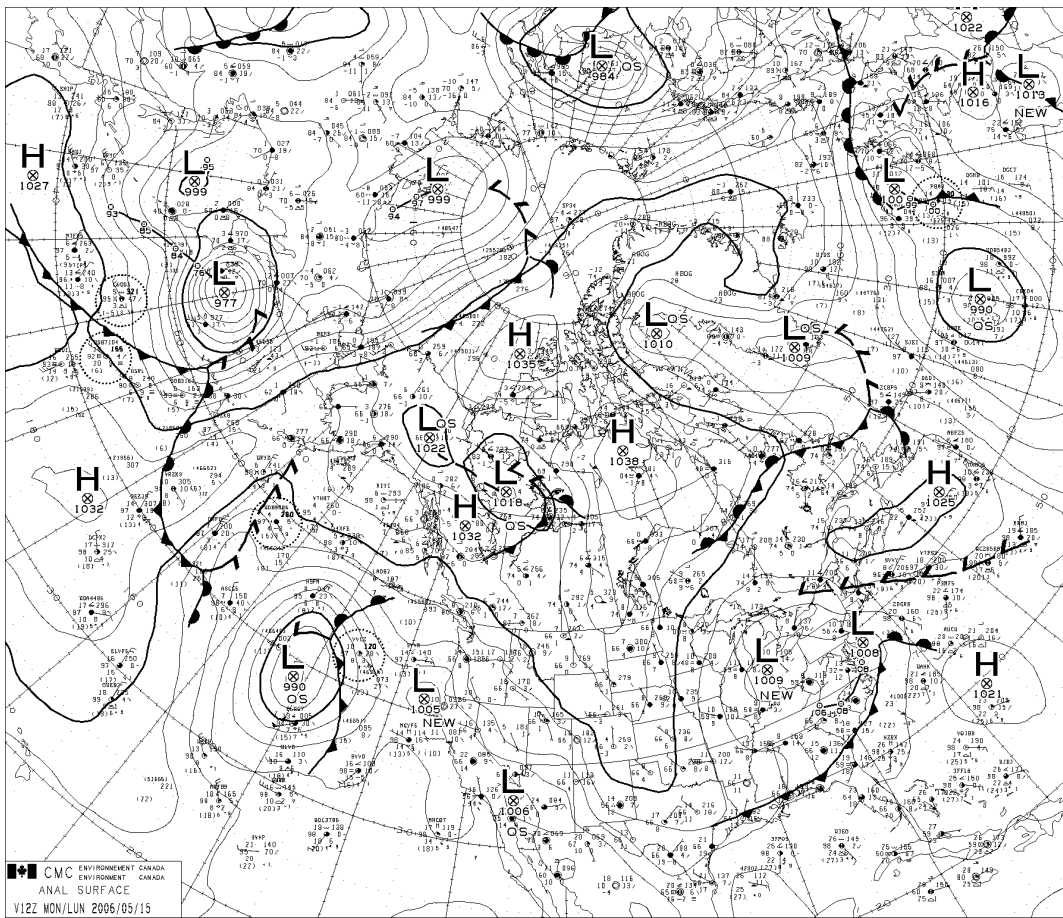
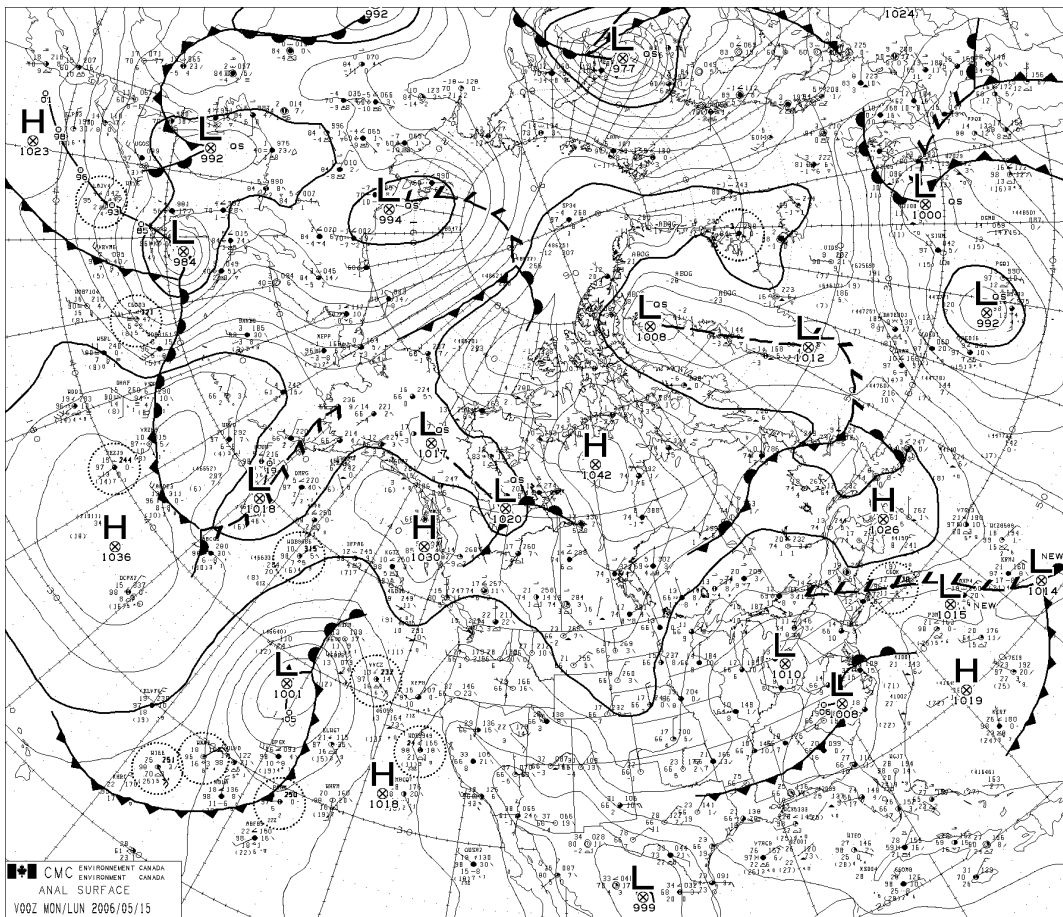


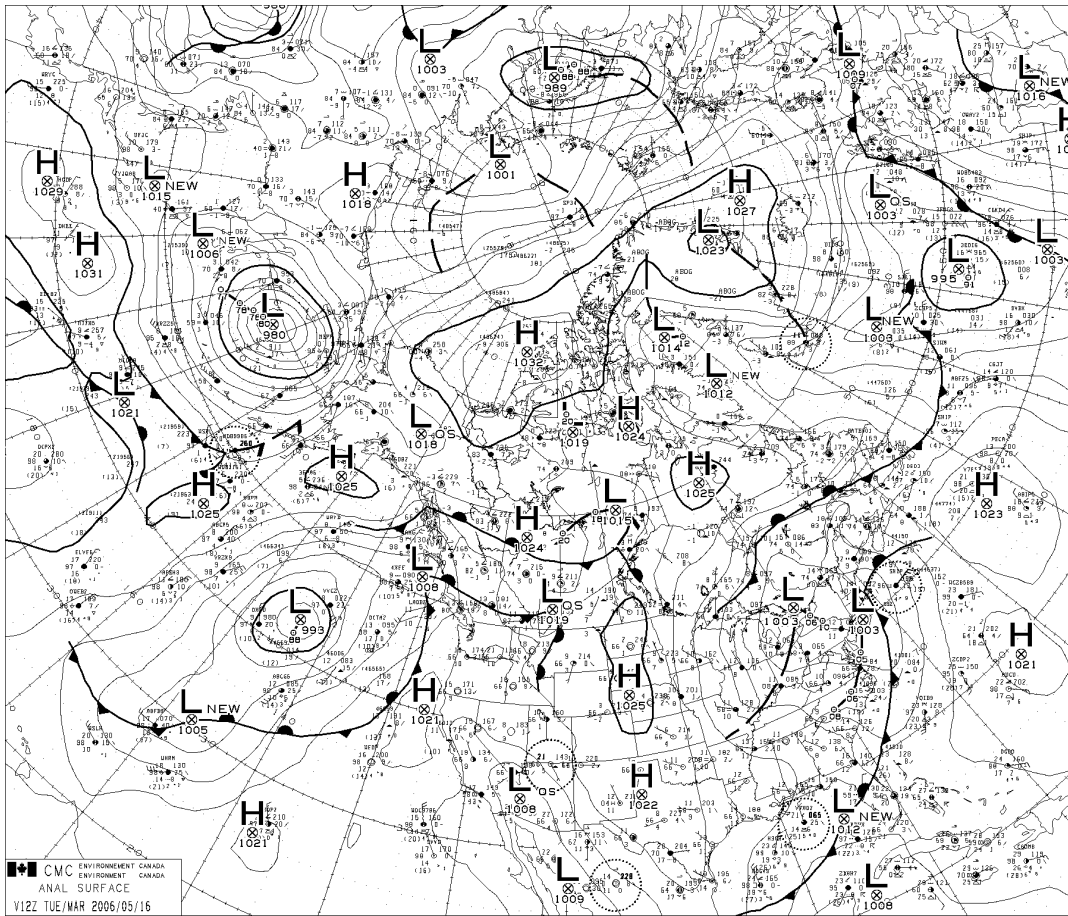
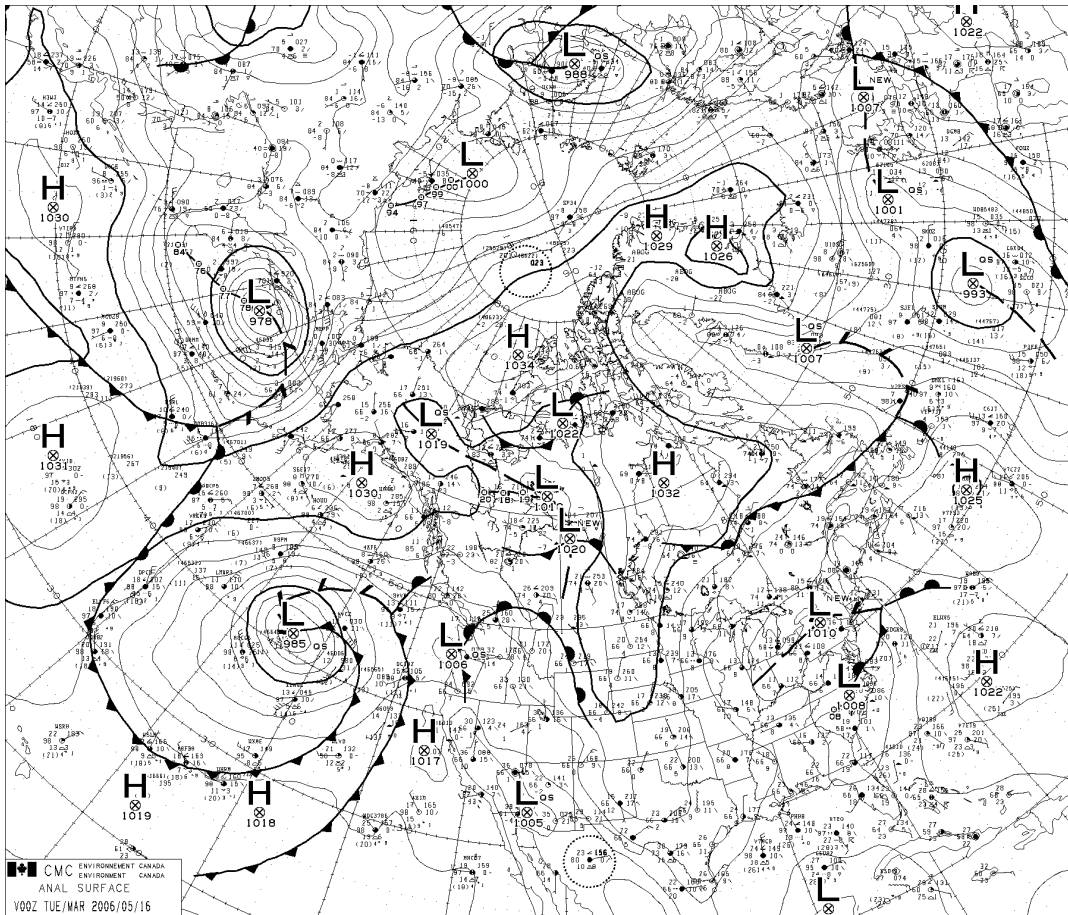


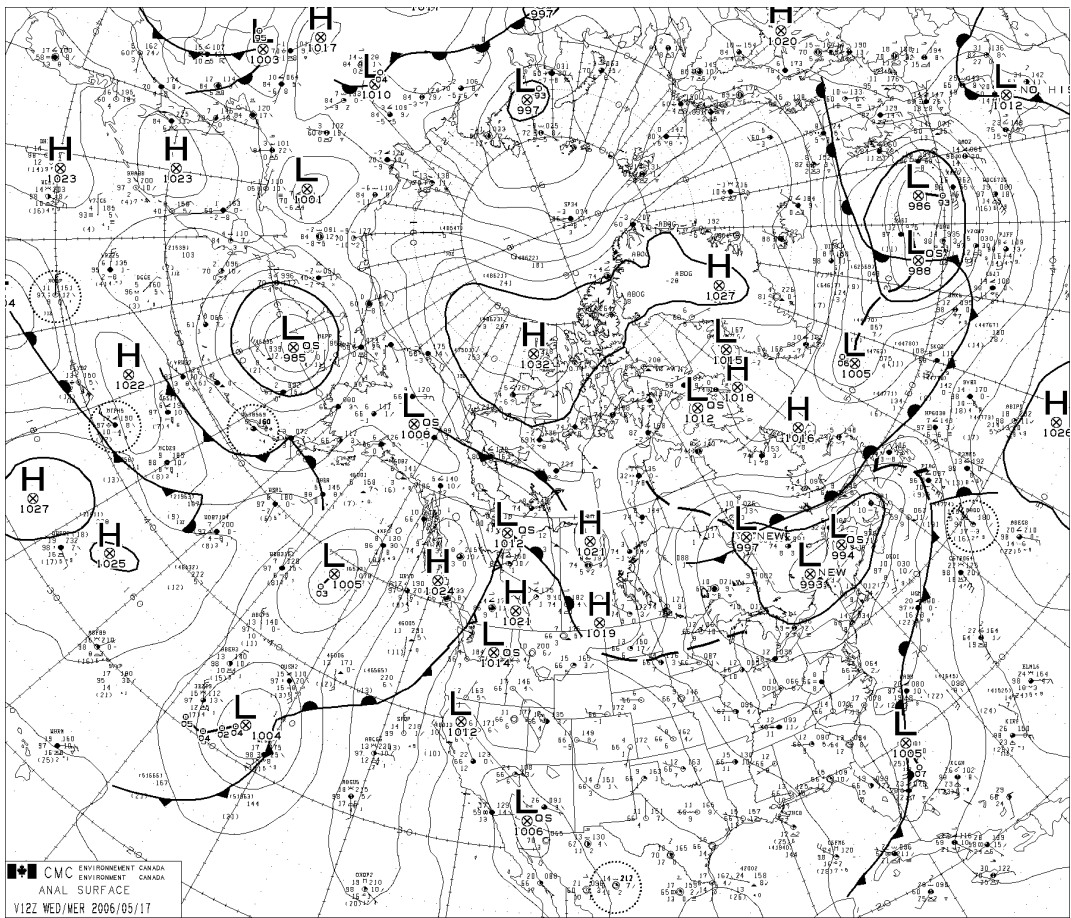
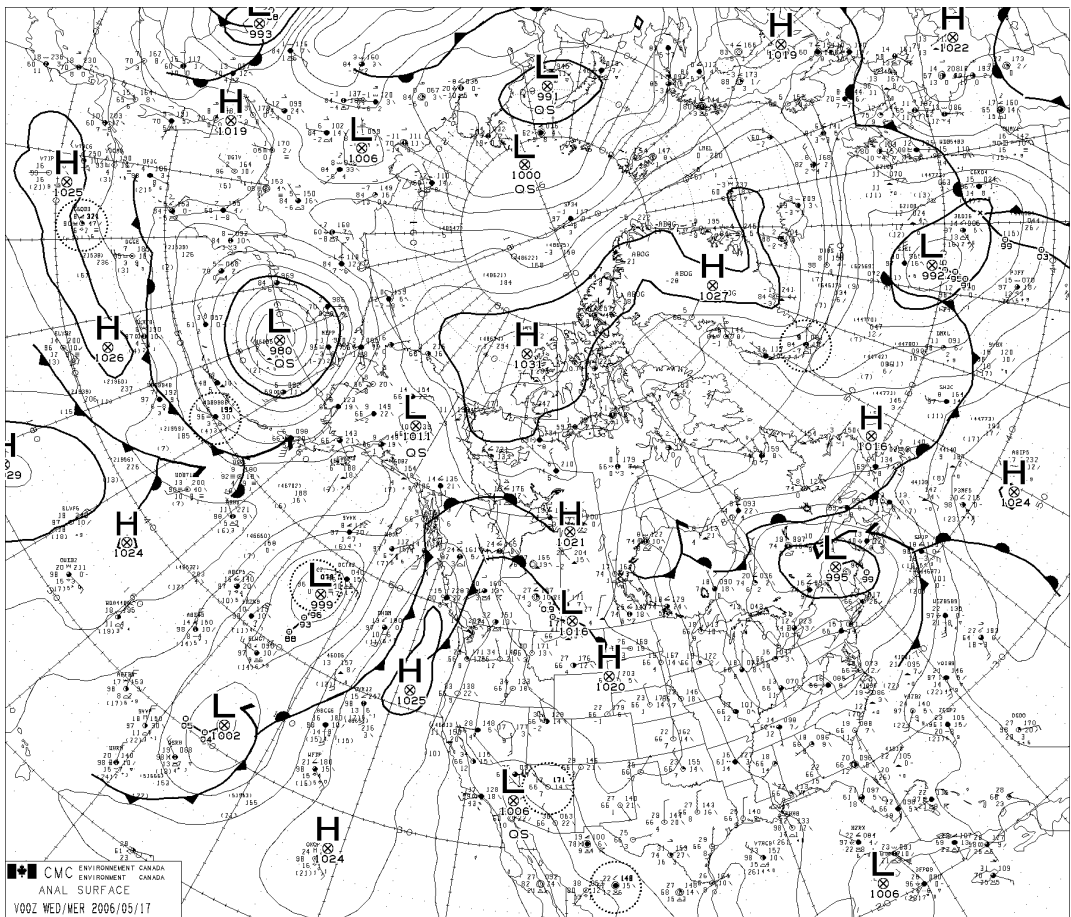












4.2 Entire observation period

Temperature

During the ARCTEX-2006 campaign the temperature drops from +8 °C to –9 °C during the passage of a cold front of an arctic storm cyclone in the night of May 7 to May 8, 2006 (Figure 4.1). Afterwards, until the morning of May 12, a period of sunny, clear sky weather occurs resulting in a strong positive temperature gradient (temperature inversion) and extreme stable stratification in between the first 10 m above the snow cover in the three “nights” May 9 to May 12 (compare Figure 4.1 and Figure 4.2.). Only around noon of May 13, May 14 and May 16 a light negative temperature gradient accompanied by a breakdown of the wind system occurs each time just for few hours resulting in a weak positive heat flux.

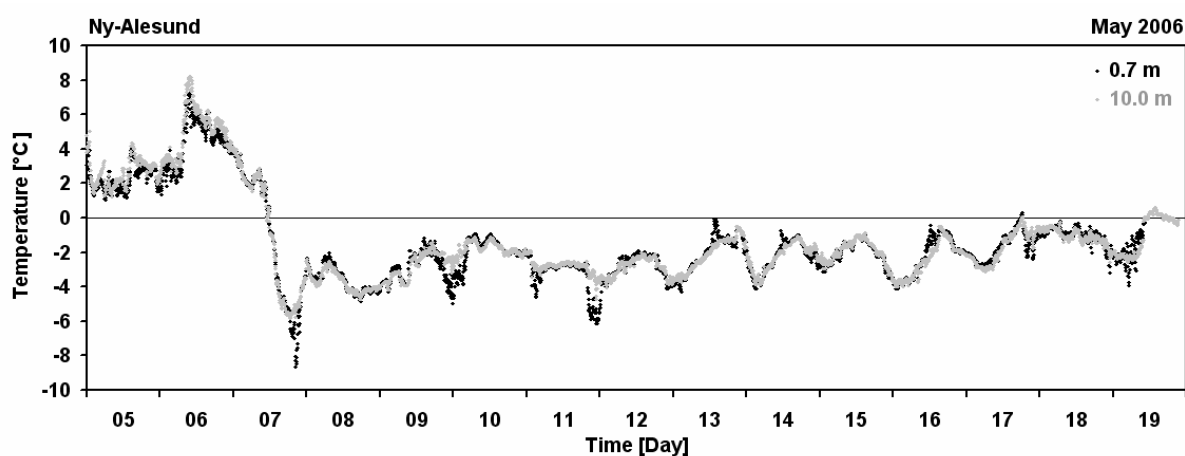


Figure 4.1: Air temperature May 5 to May 19, 2006. Black dots: air temperature in °C at 0.7 m a. g. l. (gradient tower MT2, Univ. of Bayreuth). Grey dots: air temperature in °C at 10.0 m a. g. l. (meteor. tower MT1, Alfred Wegener Institute for Polar and Marine Research). Ny-Ålesund (Svalbard), ARCTEX-2006 campaign.

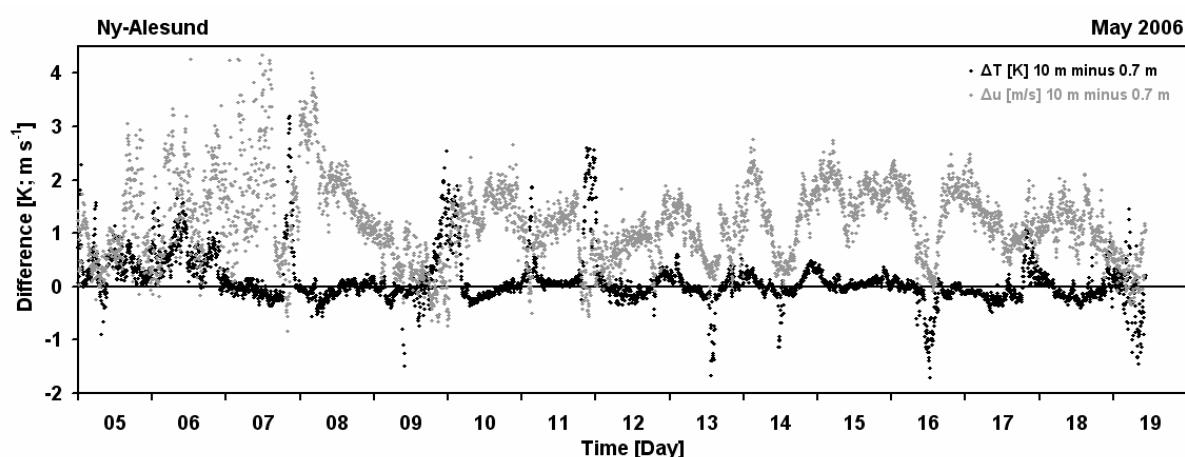


Figure 4.2: Vertical difference of air temperature and wind speed May 5 to May 19, 2006. Black dots: ΔT difference of air temperature in K between 10 m and 0.7 m a. g. l. Grey dots: Δu difference of wind speed in m s^{-1} between 10.0 m and 0.7 m a. g. l. Ny-Ålesund (Svalbard), ARCTEX-2006 campaign.

Humidity

The low level of the absolute humidity amount around 2 to 3 g m^{-3} is typical for a cold arctic air mass. Only under influence of the warm air mass sector of the passing cyclone the water vapor amount increases significant but reaching saturation only during the heavy snow storm at May 7 (Figure 4.3).

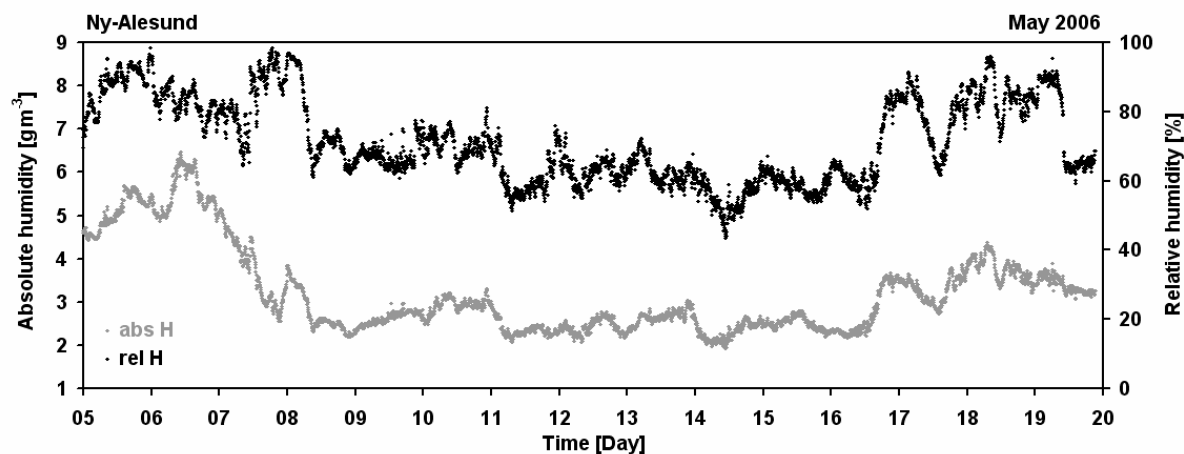


Figure 4.3: Humidity May 5 to May 19, 2006. Black dots: relative humidity in % at 1.5 m a. g. l. Grey dots: absolute humidity in g m^{-3} at 10.0 m a. g. l. (both meteor. tower MT1, Alfred Wegener Institute for Polar and Marine Research). Ny-Ålesund (Svalbard), ARCTEX-2006 campaign.

Wind speed and wind direction

The horizontal wind speed at different heights above ground level (0.7 m up to 10 m) was obtained by the gradient tower of the University of Bayreuth (MT2) using the Climatronics F460 cup anemometers as well by the routine observation of the meteorological tower of the Alfred Wegener Institute for Polar and Marine Research (MT1).

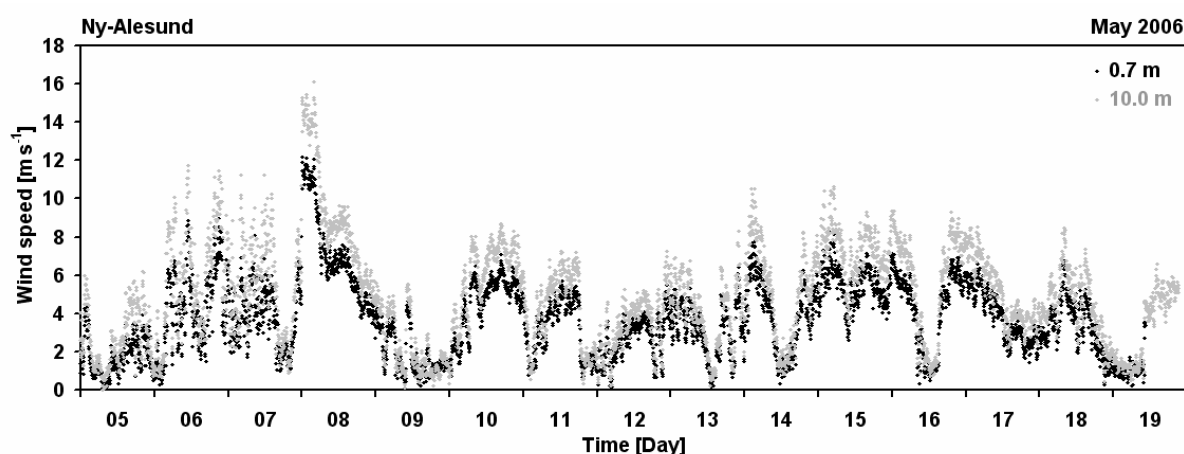


Figure 4.4: Wind speed May 5 to May 19, 2006. Black dots: wind speed in m s^{-1} at 0.7 m a. g. l. (gradient tower MT2, Univ. of Bayreuth). Grey dots: wind speed in m s^{-1} at 10.0 m a. g. l. (meteor. tower MT1, Alfred Wegener Institute for Polar and Marine Research). Ny-Ålesund (Svalbard), ARCTEX-2006 campaign.

The Figure 4.4 indicates that at most of the time the usual vertical wind profile dominates. During few periods between May 7 and May 12 (esp. during the clear sky days) the near surface wind speed (first 3 m) exceeds the speeds at 10 m a. g. l. (compare Figure 4.2). A closer look reveals a more or less 2 m to 3 m thick air flow coming from south-west downhill the slope from the near Zeppelin Mountain Range.

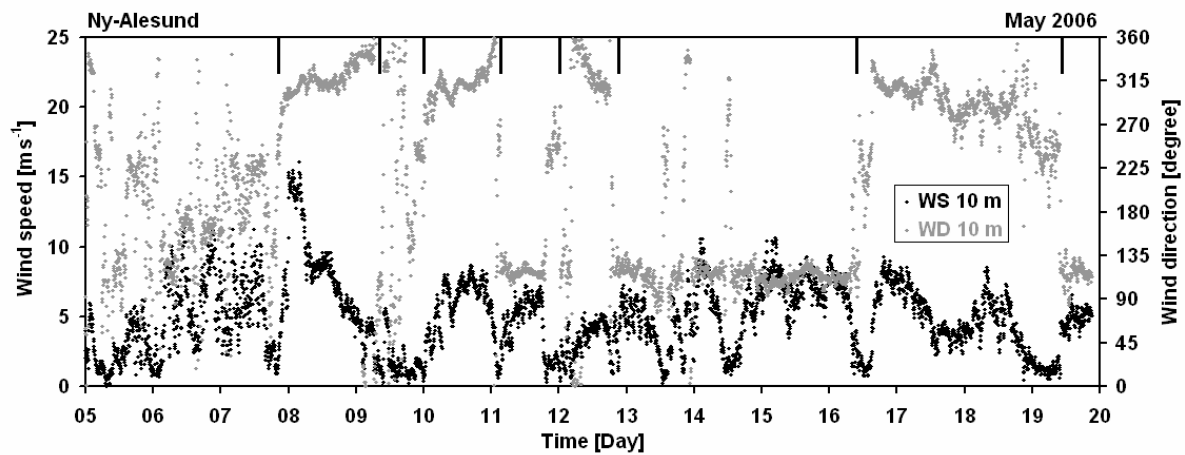


Figure 4.5: Wind direction and wind speed May 5 to May 19, 2006. Black dots: wind speed in m s^{-1} at 10.0 m a. g. l. Grey dots: wind direction in degree at 10.0 m a. g. l. (both meteor. tower MT1, Alfred Wegener Institute for Polar and Marine Research). The small bars at the plot's top boarder indicate significant change of the wind regime (namely SE and NW) or a transition phase. Ny-Ålesund (Svalbard), ARCTEX-2006 campaign.

The Figure 4.5 compares wind speed and the corresponding direction. Between May 8 and May 12 the prevailing wind direction is north-west (upwards the fjord) interrupted at midday May 9 by indifferent directions and relatively calm wind conditions and during May 11 by change to a strong south-east air flow. Beginning around midnight May 12 until noon May 16 the prevailing direction remains south-east (downward the Kongsfjord). At afternoon May 16 a relatively warm and humid air mass arrived in Ny-Ålesund due to a low pressure system across the Barents Sea.

The wind direction (at 2 m and 10 m a. g. l.) was obtained by the meteorological routine observation of the 10 m tall meteorological tower of the Alfred Wegener Institute for Polar and Marine Research (MT1). The used wind sensor is a combined anemometer and wind vane (Thies Clima, Germany). The Figure 4.6 illustrates the both main wind direction sectors at Ny-Ålesund during the ARCTEX-2006 campaign.

This pattern of either south-east or north-west directions (more or less canalized air flow down or upward the Kongsfjord) is typical not only in May but also most of the time during the year. At 2 m and during weak wind an offshore south-west component is distinguishable (compare Chapter 4.3: daily wind rose plots).

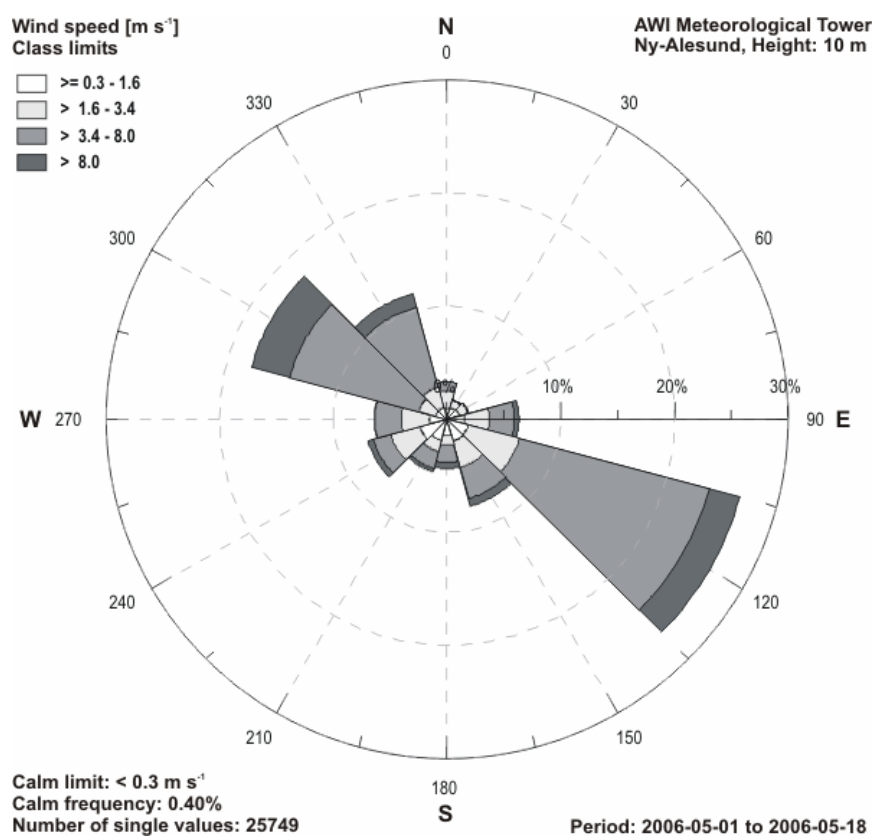
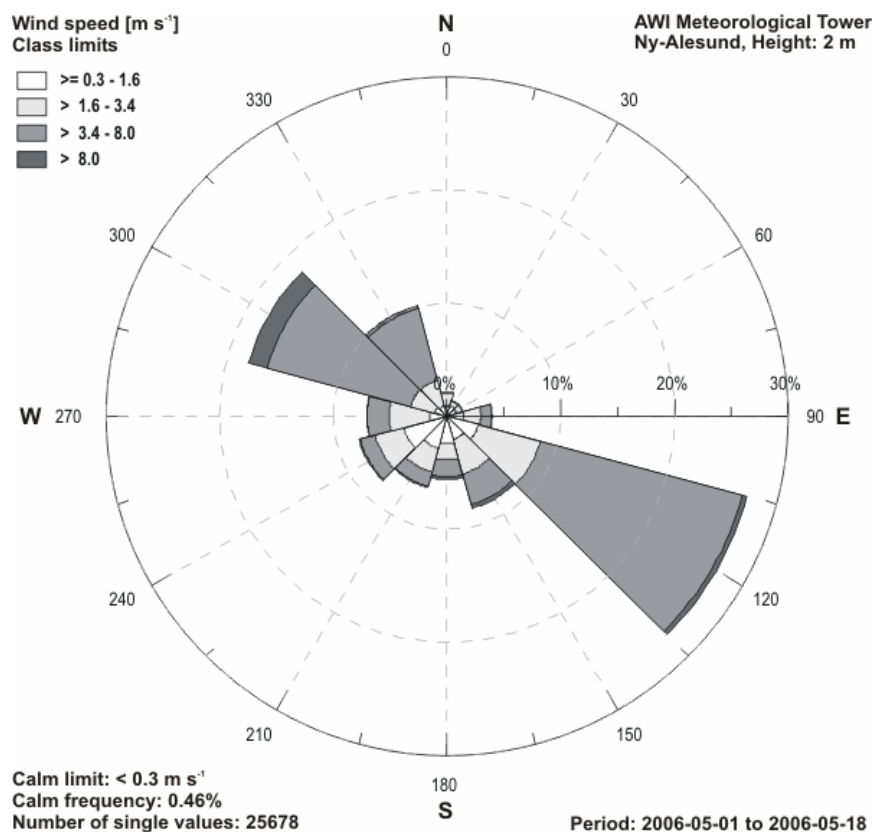


Figure 4.6: Frequency distribution of wind direction separated in 12 wind sectors and classified in 4 wind speed classes, May 1 to May 18, 2006. Above: distribution of the wind directions in degree measured at 2.0 m height a. g. l. Below: distribution of the wind direction in degree measured at 10.0 m a. g. l. (both meteor. tower MT1, Alfred Wegener Institute for Polar and Marine Research). Ny-Ålesund (Svalbard), ARCTEX-2006 campaign.

Radiation

The radiation measurements took place at the routine BSRN-Station (AWI) and at the ARCTEX-2006 measurement field next to the gradient tower of the Univ. of Bayreuth (MT2).

At the latter site the radiation measurement equipment was especially build-up over an adequate thick snow field. At the BSRN site a pattern of more or less snow covered or snow free tundra around the instrument field yields to a slightly reduced amount of reflected shortwave radiation in comparison to the MT2 site whereas the global radiation received at both sites are remarkable similar (compare Figure 4.7 and Figure 4.8).

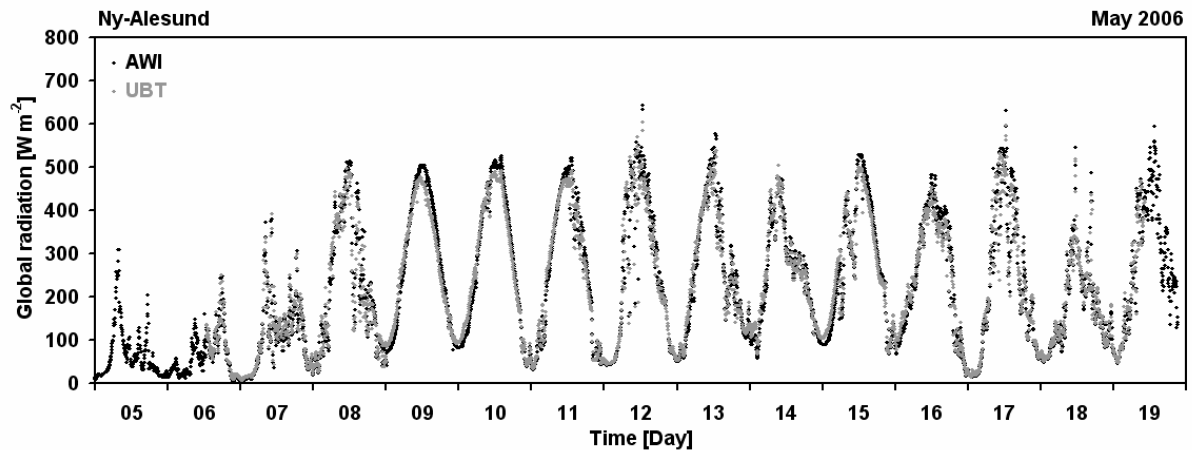


Figure 4.7: Global shortwave radiation May 5 to May 19, 2006. Black dots: global radiation in W m^{-2} measured with a CM11 (Kipp & Zonen) pyranometer (BSRN station, Alfred Wegener Institute for Polar and Marine Research). Grey dots: global radiation in W m^{-2} measured with a CNR1 (Kipp & Zonen) net radiometer (net radiation station Univ. of Bayreuth). Ny-Ålesund (Svalbard), ARCTEX-2006 campaign.

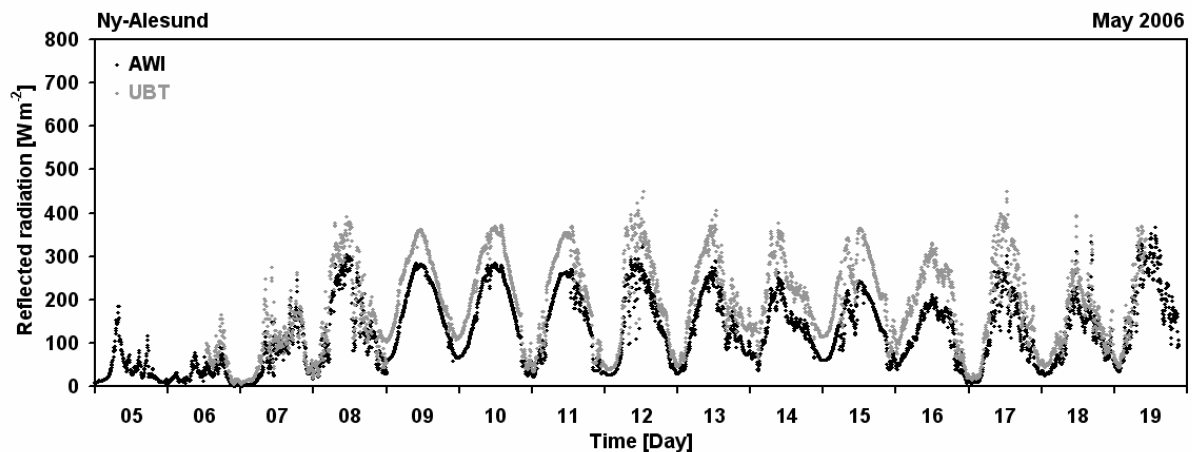


Figure 4.8: Reflected shortwave radiation May 5 to May 19, 2006. Black dots: reflected radiation in W m^{-2} measured with a CM11 (Kipp & Zonen) pyranometer (BSRN station, Alfred Wegener Institute for Polar and Marine Research). Grey dots: reflected radiation in W m^{-2} measured with a CNR1 (Kipp & Zonen) net radiometer (net radiation station Univ. of Bayreuth). Ny-Ålesund (Svalbard), ARCTEX-2006 campaign.

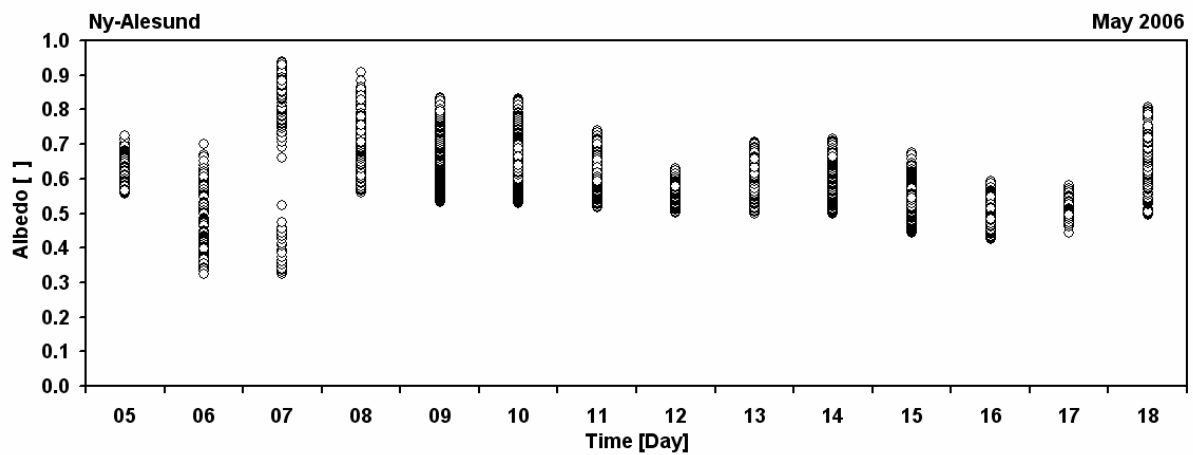


Figure 4.9: Ratio of reflected (only values above or equal 10 W m^{-2}) to global shortwave radiation (albedo) measured with a CNR1 (Kipp & Zonen) net radiometer (net radiation station Univ. of Bayreuth) May 5 to May 19, 2006. Circles show the daily variance of the Albedo due to different elevation angles of the sun and due to different fraction of the half space from which diffuse sky radiation or the - from the surface - reflected radiation can reach the sensors. Ny-Ålesund (Svalbard), ARCTEX-2006 campaign.

The interpretation of the albedo in polar regions especially during snow fall or snow melt seasons is difficult. The Figure 4.9 demonstrates this problem. During snow fall events like between May 6 and May 7, the albedo changed rapidly covering a more or less snow free surface with fresh snow. At times with clear sky weather and lower rate of diffuse radiation and a new fresh and closed snow cover like from May 8 to May 10 the albedo varies in a large range depending on the elevation angle and the superimposed effect of additional reflected radiation receiving the sensor caused by the reflection of the surrounding snow covered earth surface according to the local limitation or extension of the horizon. Otherwise, at days with decreasing snow cover and a higher rate of diffuse radiation like May 12 to May 14 or May 17 the daily variation of the albedo is relatively small.

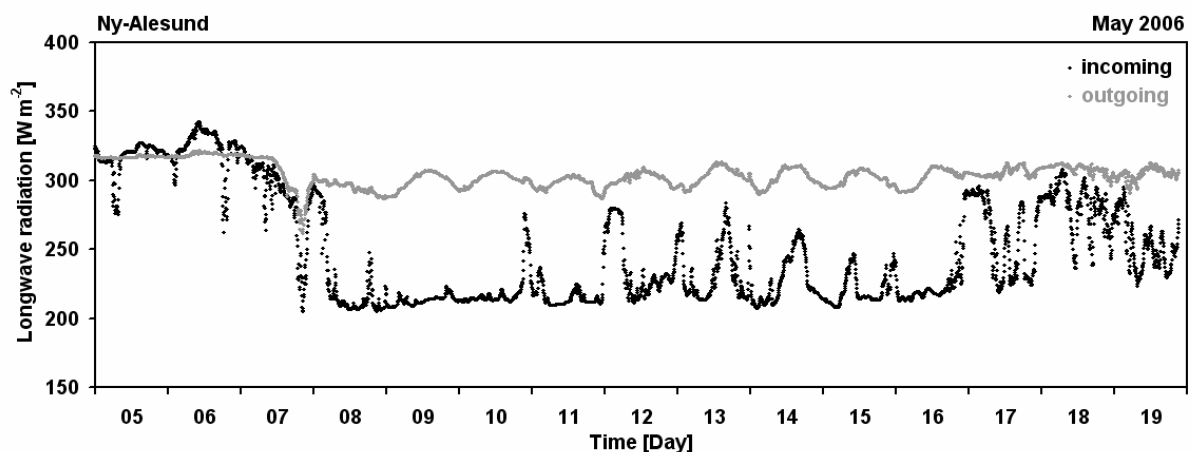


Figure 4.10: Longwave radiation measured with a PIR (Precision Infrared Radiometer, Eppley) Pyrgometer (BSRN station, Alfred Wegener Institute for Polar and Marine Research) May 5 to May 19, 2006. Black dots: incoming long wave radiation in W m^{-2} . Grey dots: outgoing long wave radiation in W m^{-2} . Ny-Ålesund (Svalbard), ARCTEX-2006 campaign.

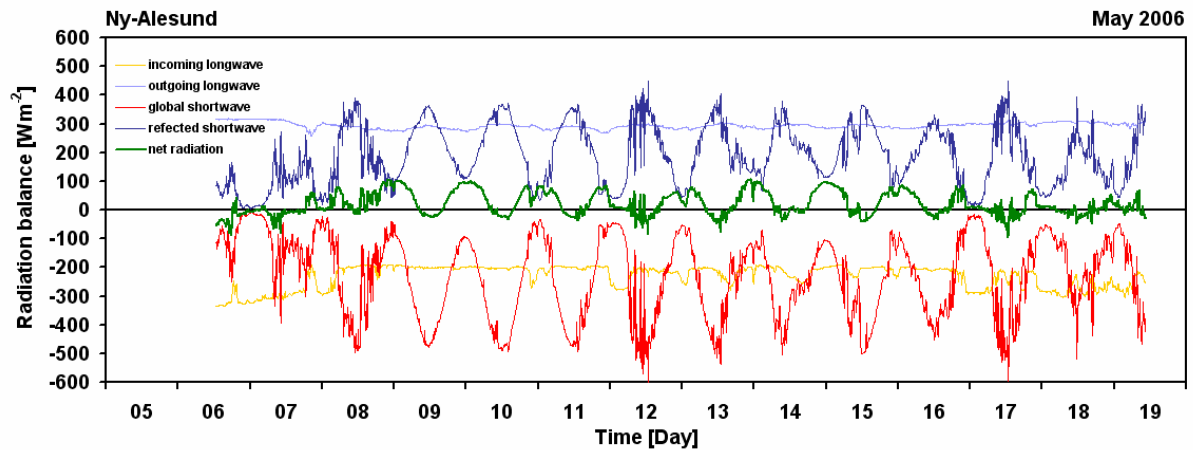


Figure 4.11: Surface radiation balance measured with a CNR1 (Kipp & Zonen) net radiometer (net radiation station Univ. of Bayreuth) May 5 to May 19, 2006. Given the micrometeorological convention, downward directed fluxes (global shortwave and incoming longwave radiation) are negative and upward directed fluxes (reflected shortwave and outgoing longwave radiation) are positive. Ny-Ålesund (Svalbard), ARCTEX-2006 campaign.

Cloud Base height in meter

For cloud base height measurements a laser (LIDAR) based ceilograph LD-40 is used since 1998 with a ceiling range between 23 m and 12 650 m height and with a measuring deviation of ± 23 m (at solid objects). The ceilometer is part of the BSRN measuring field at Ny-Ålesund operated by the Alfred Wegener Institute.

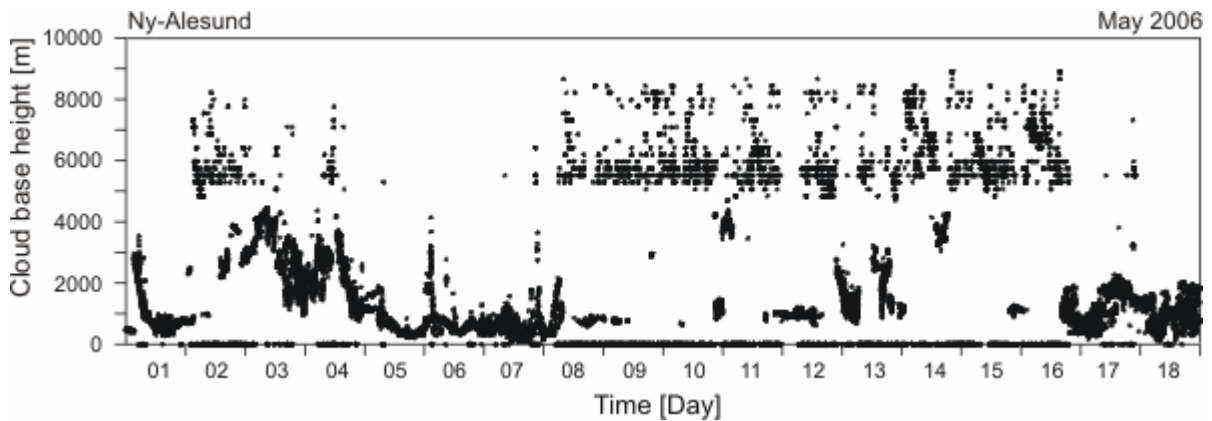
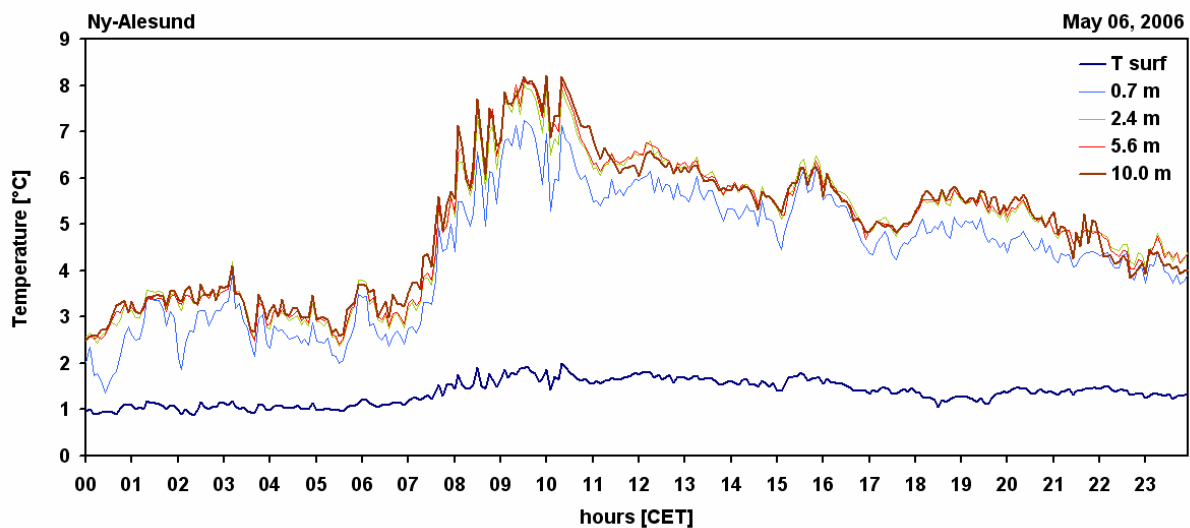
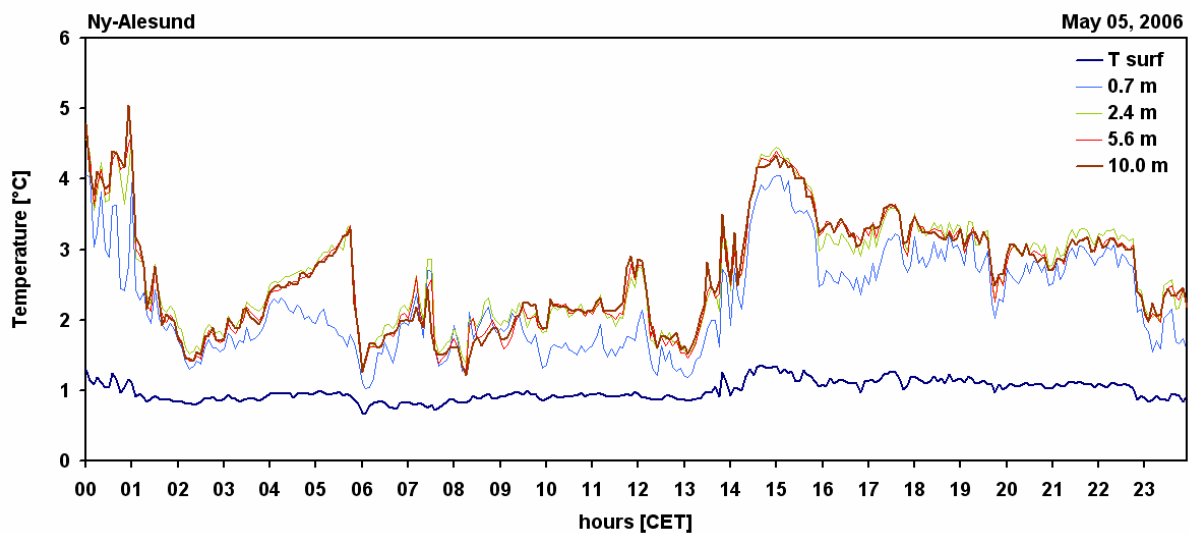


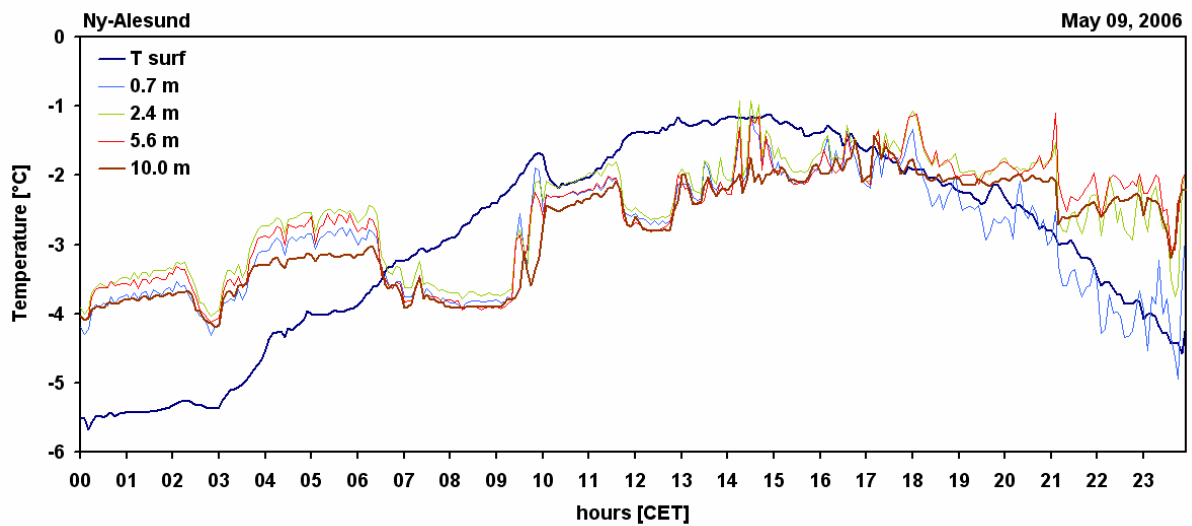
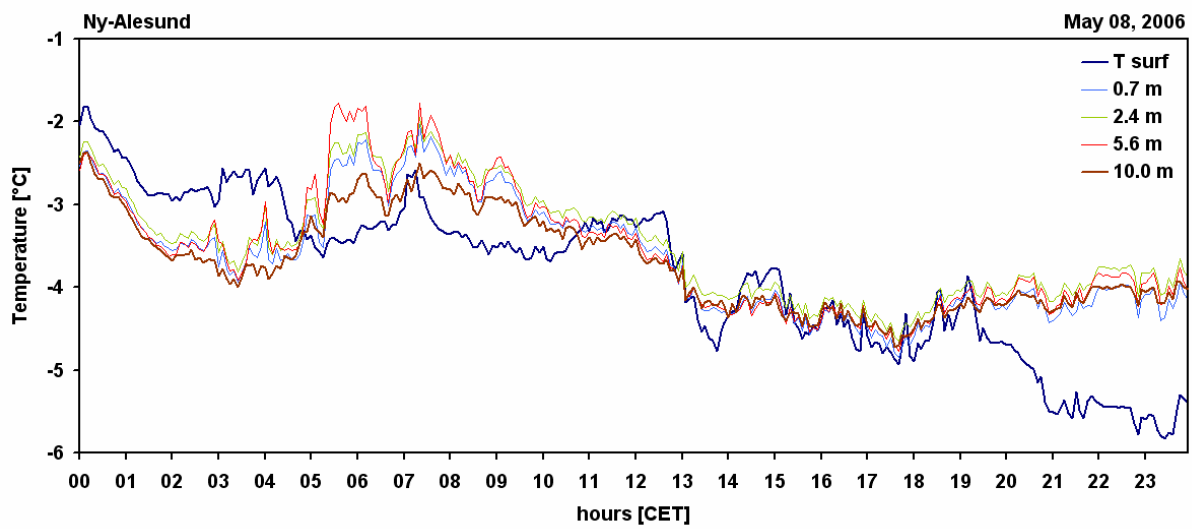
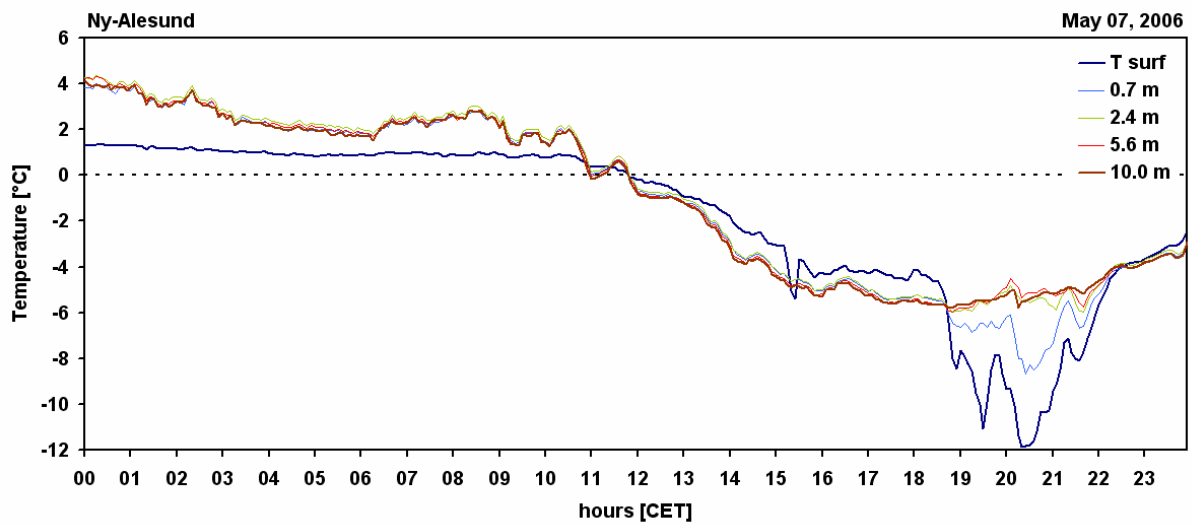
Figure 4.12: Cloud base height in meter above ground May 1 to May 18, 2006. Laser (LIDAR) based ceilograph measurements of the BSRN (Baseline Surface Radiation Network) station Ny-Ålesund operated by the Alfred Wegener Institute. Ny-Ålesund (Svalbard), ARCTEX-2006 campaign.

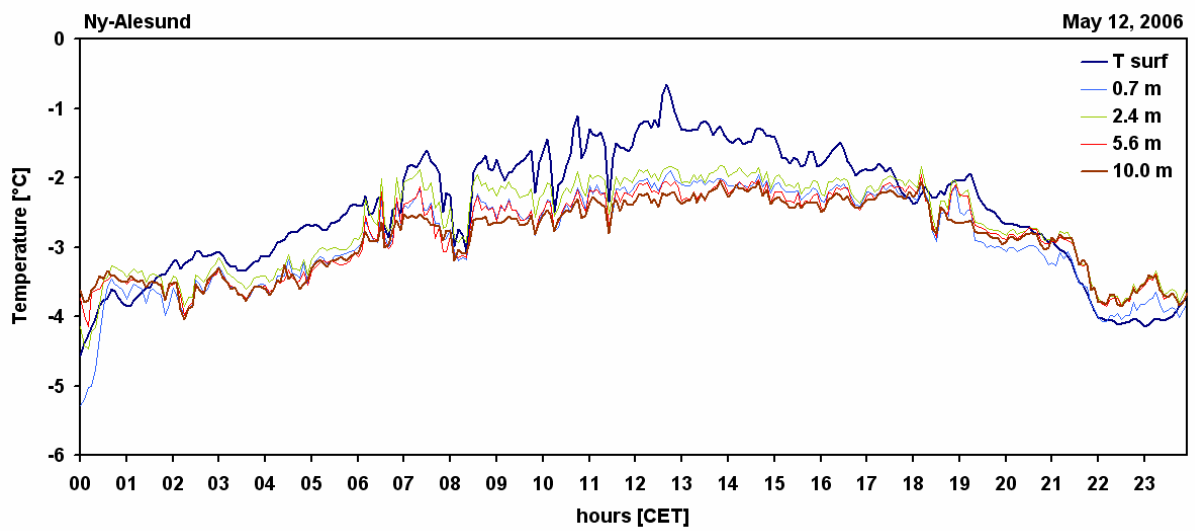
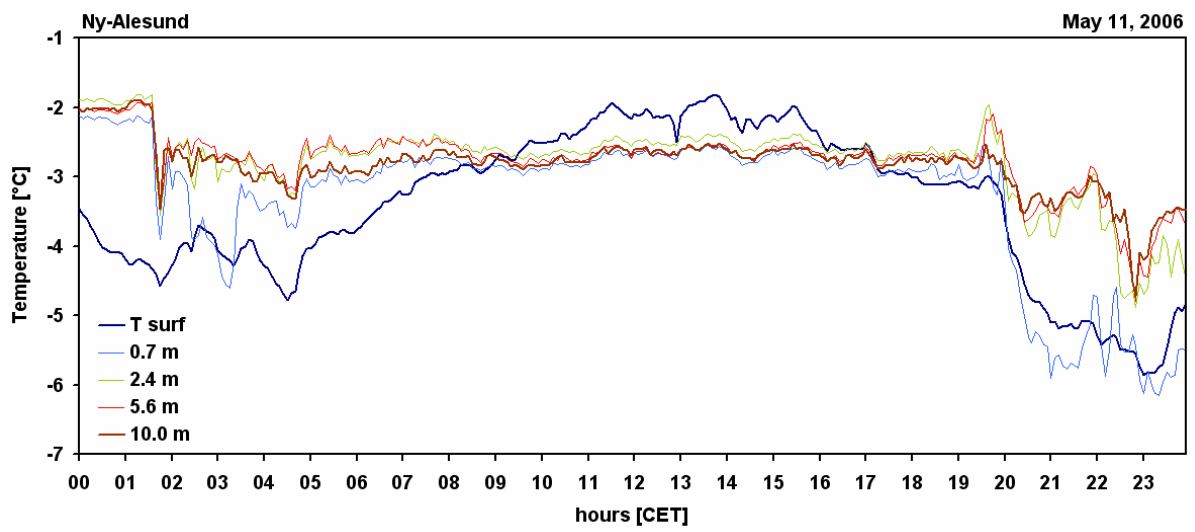
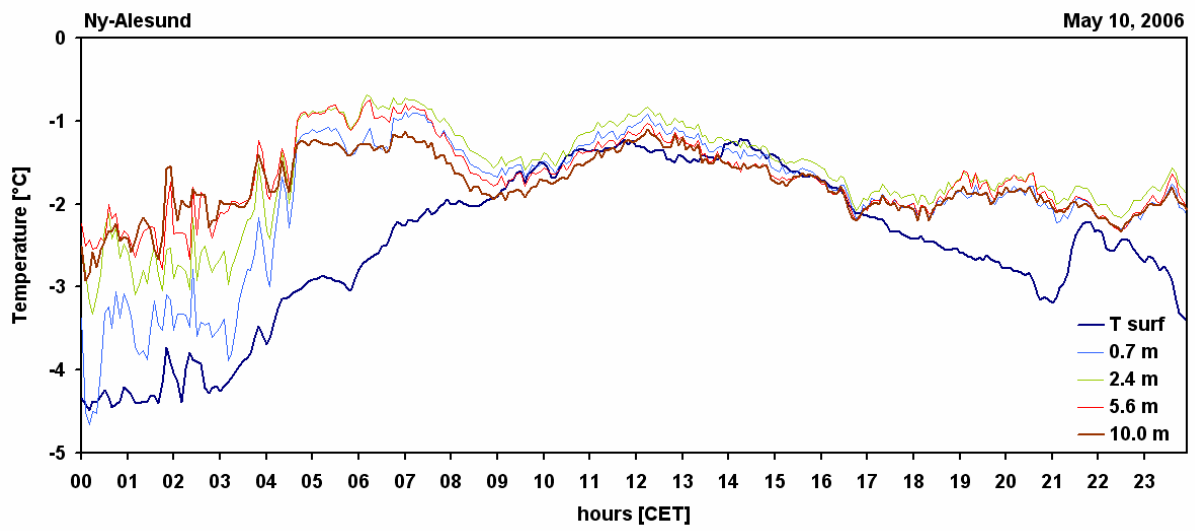
4.3 Daily charts

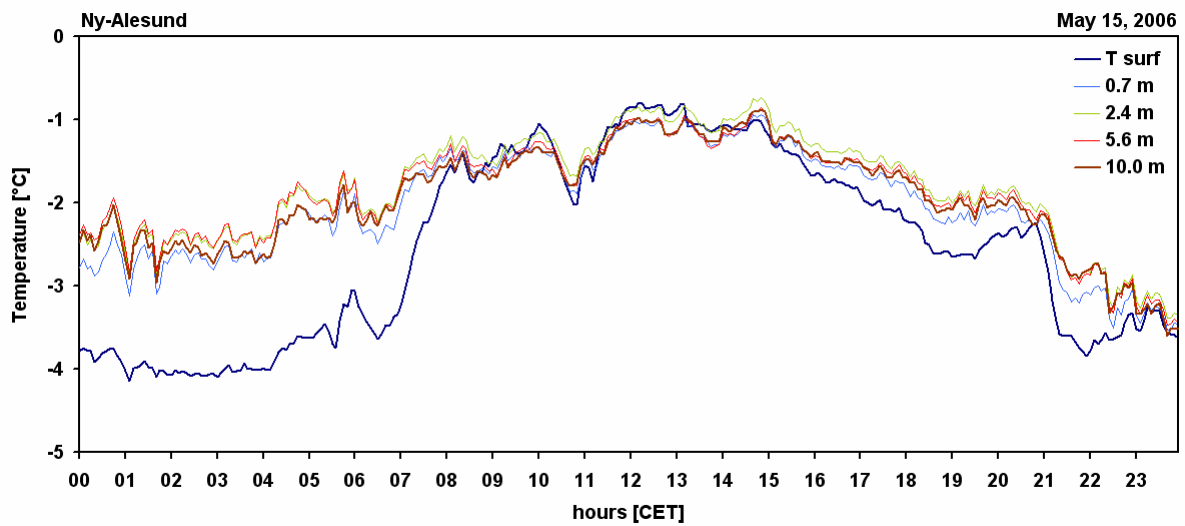
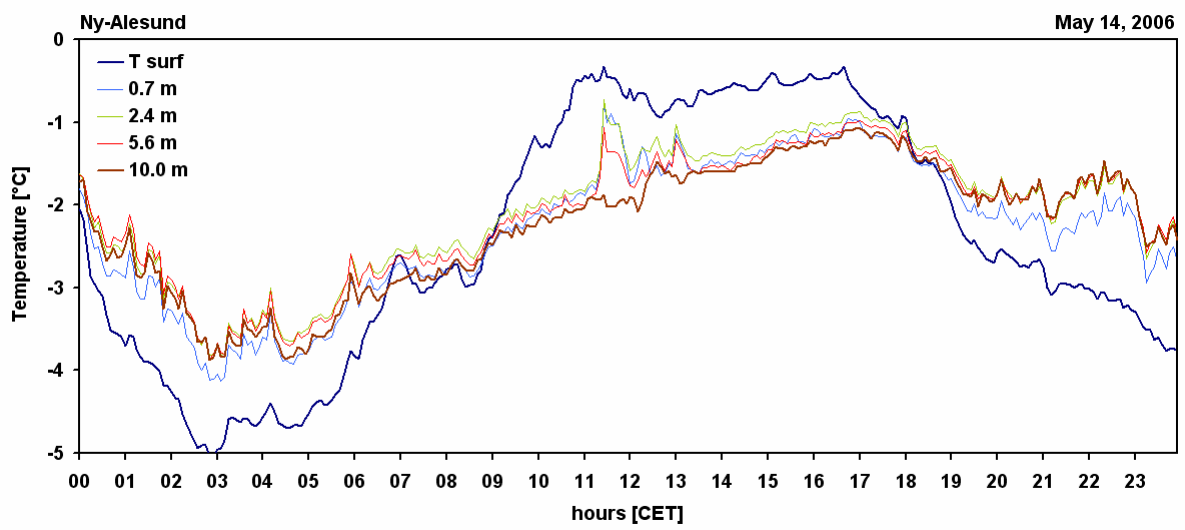
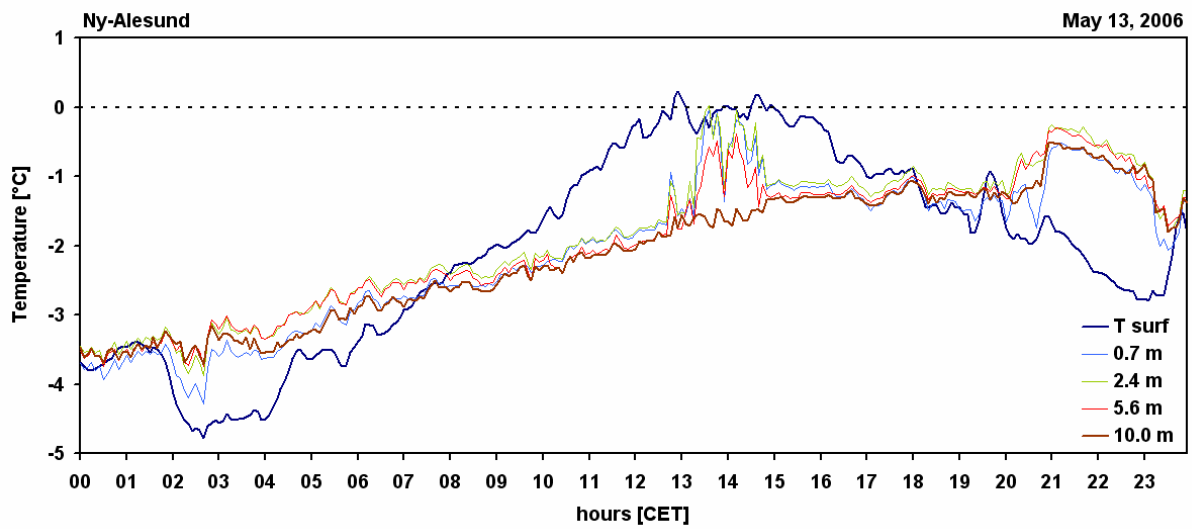
Air temperature

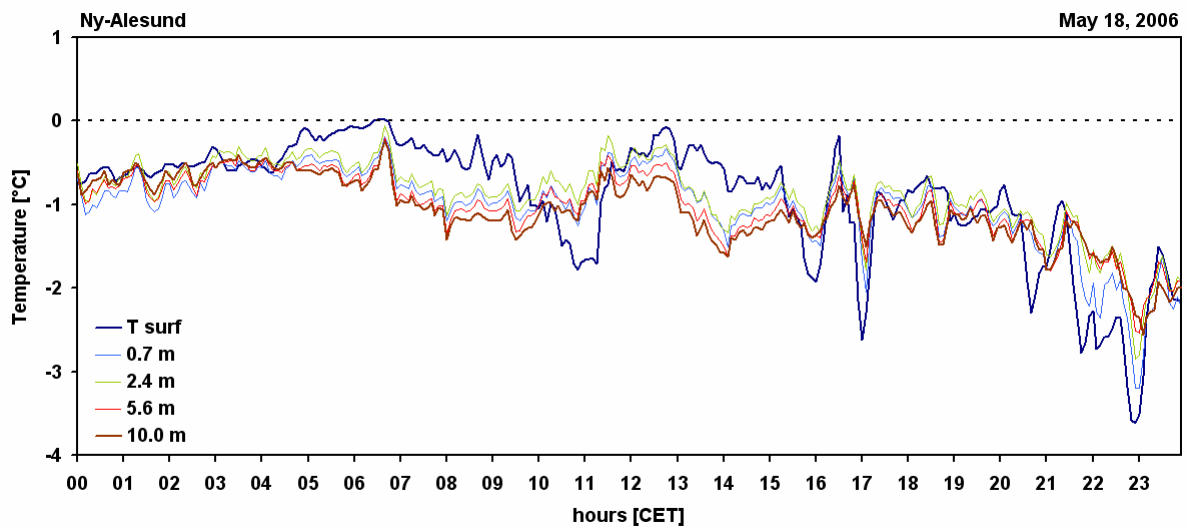
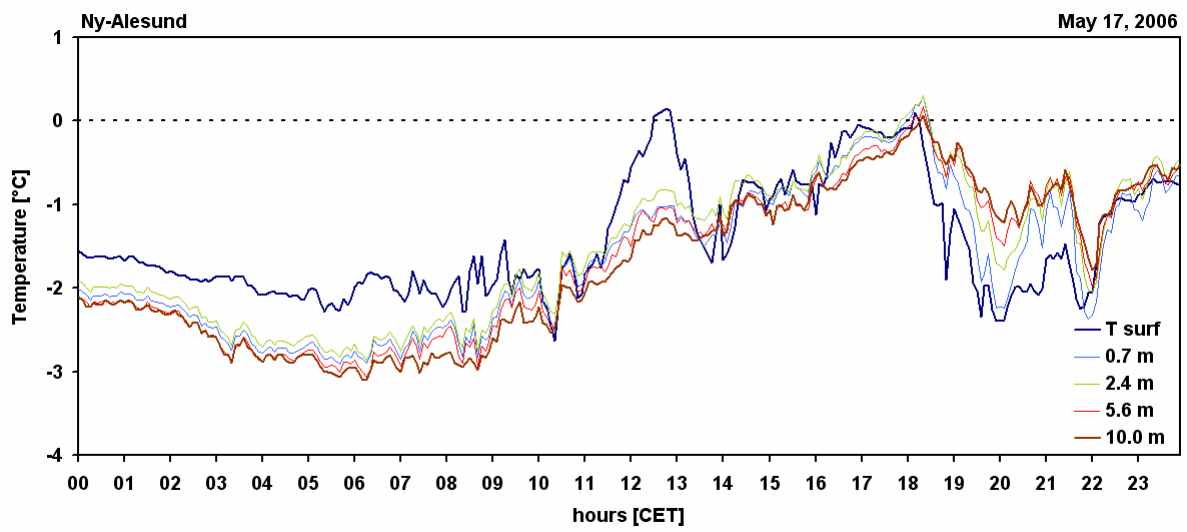
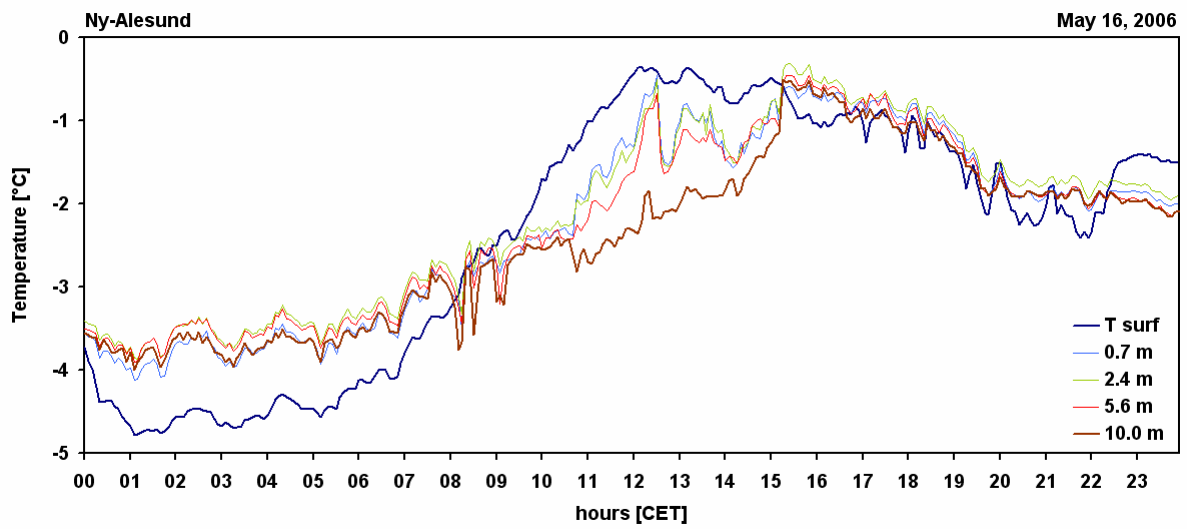
During the ARCTEX-2006 campaign air temperature was recorded in different heights above ground using ventilated and radiation-shielded thermometers. Most of the time the area around the gradient tower of the University of Bayreuth (MT2, measuring heights 0.7 m, 2.4 m and 5.6 m) and around the meteorological tower of the Alfred Wegener Institute for Polar and Marine Research (MT1, 10 m) was covered by 20 cm to 30 cm snow. The ground surface temperature presented in the following figures was derived by recalculation (Stefan-Boltzmann law) of the outgoing longwave radiation obtained by the BSRN-station nearby both towers. Unlike to the tower positions, the area around the BSRN-station was only partly covered with snow or ice especially after May 10, 2006.

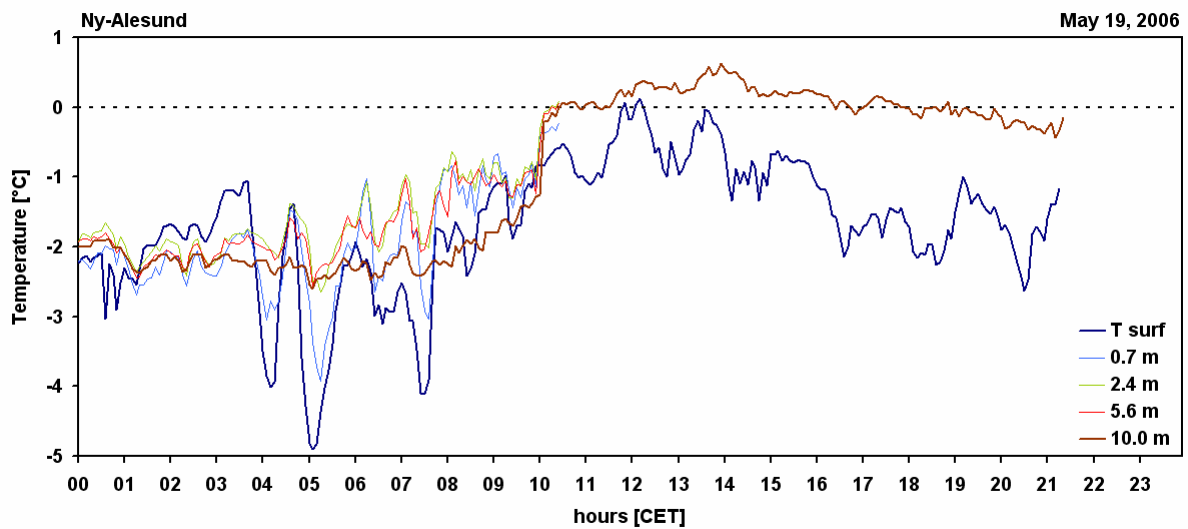






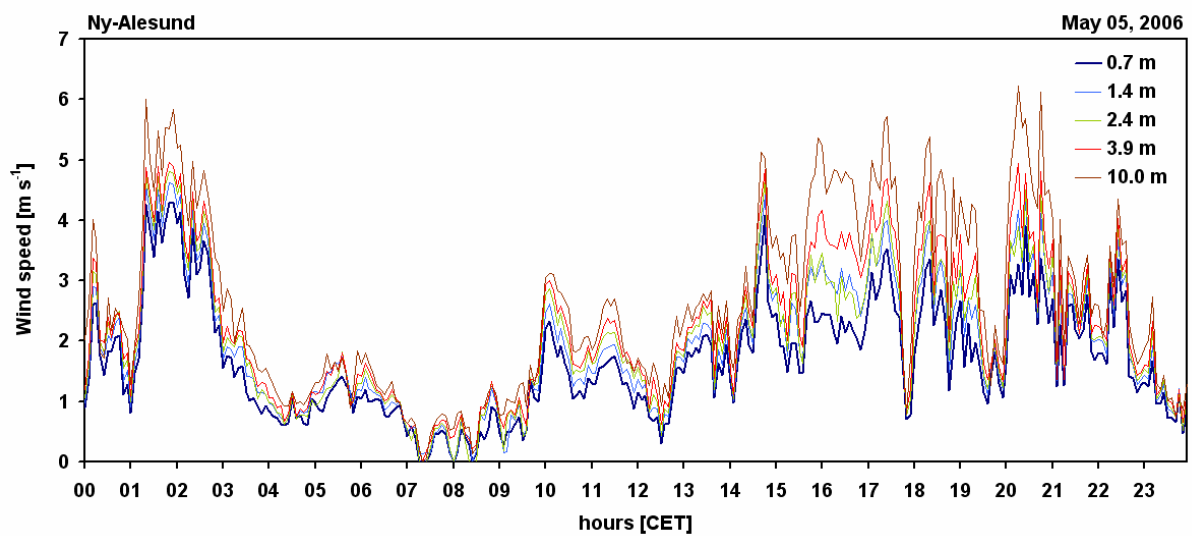


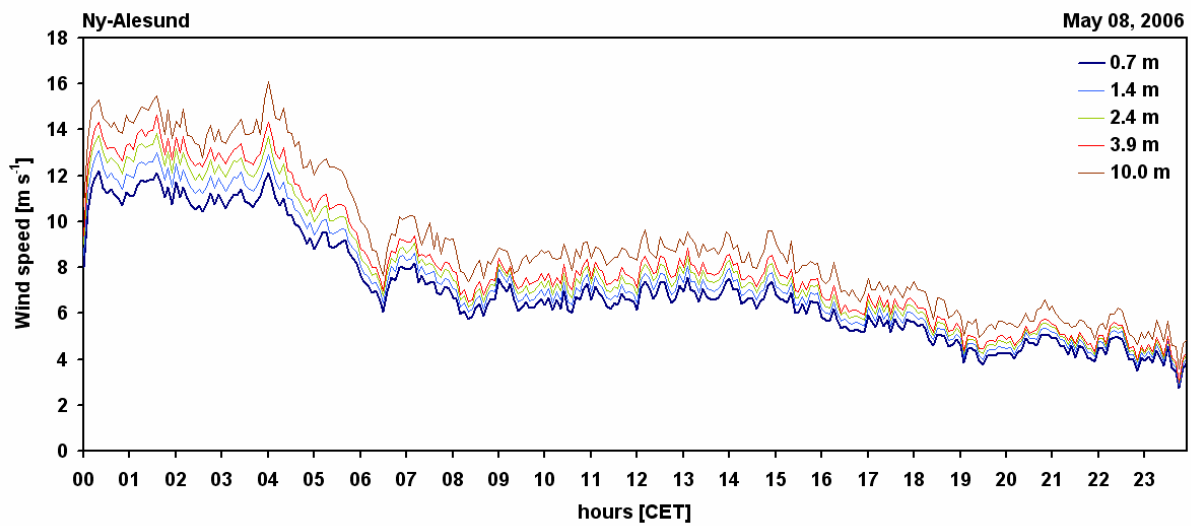
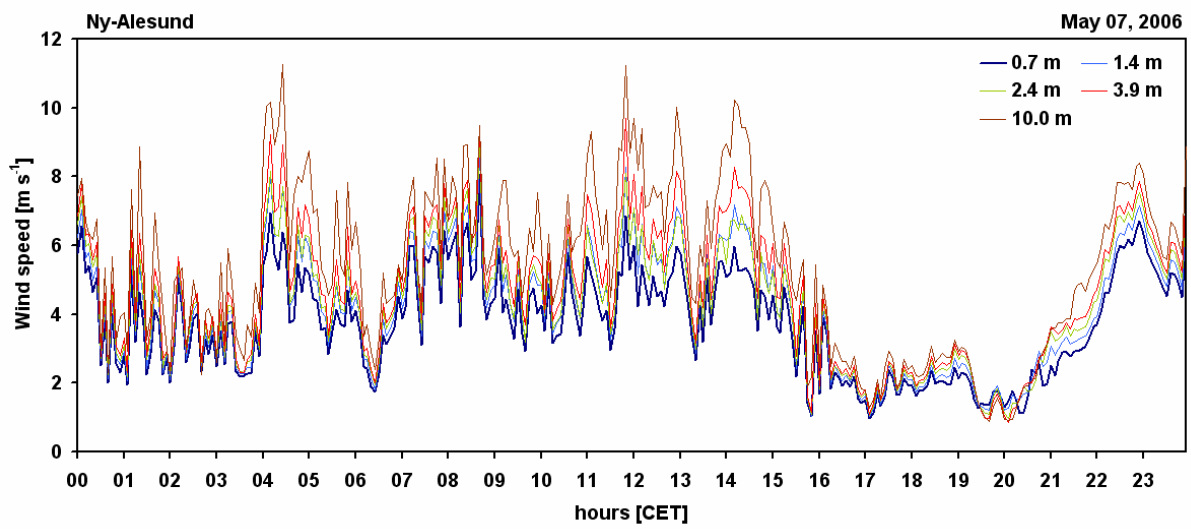
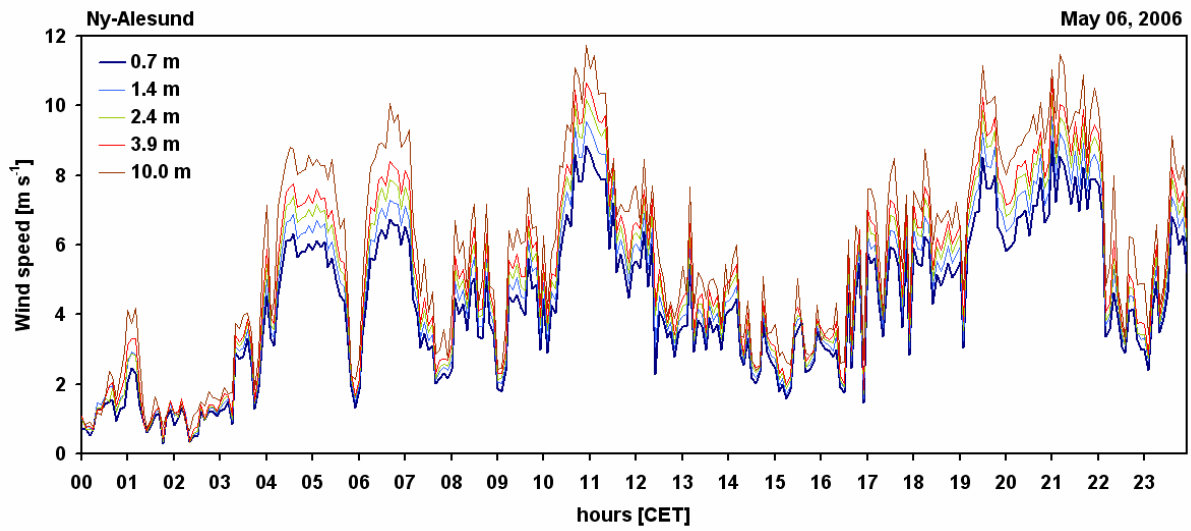


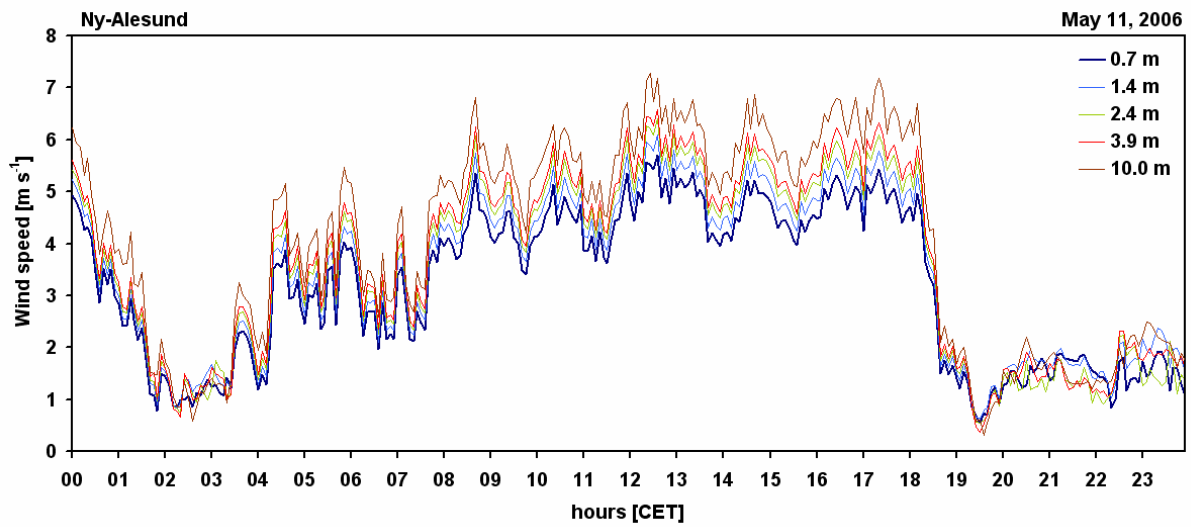
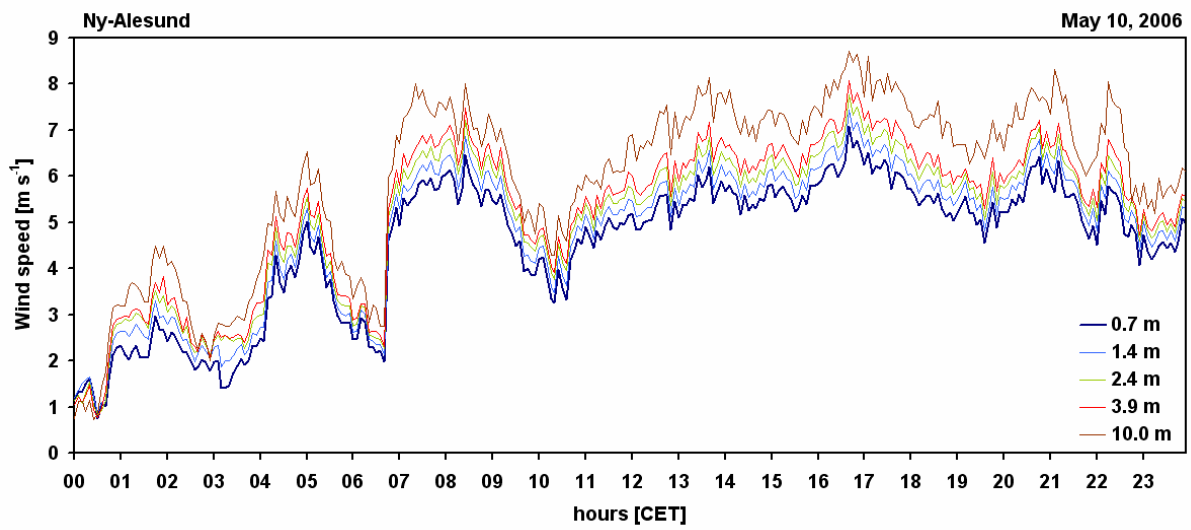
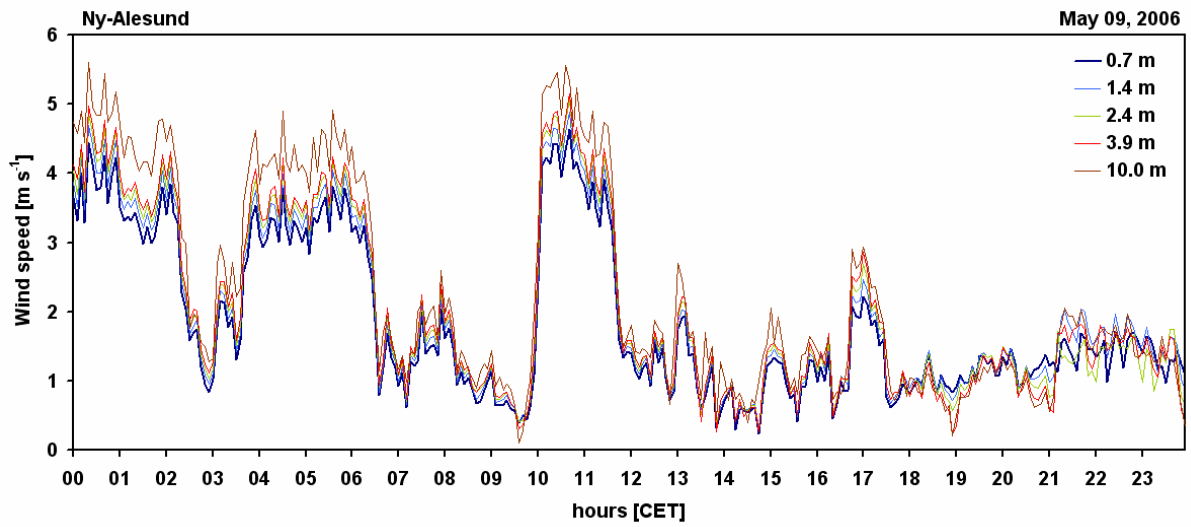


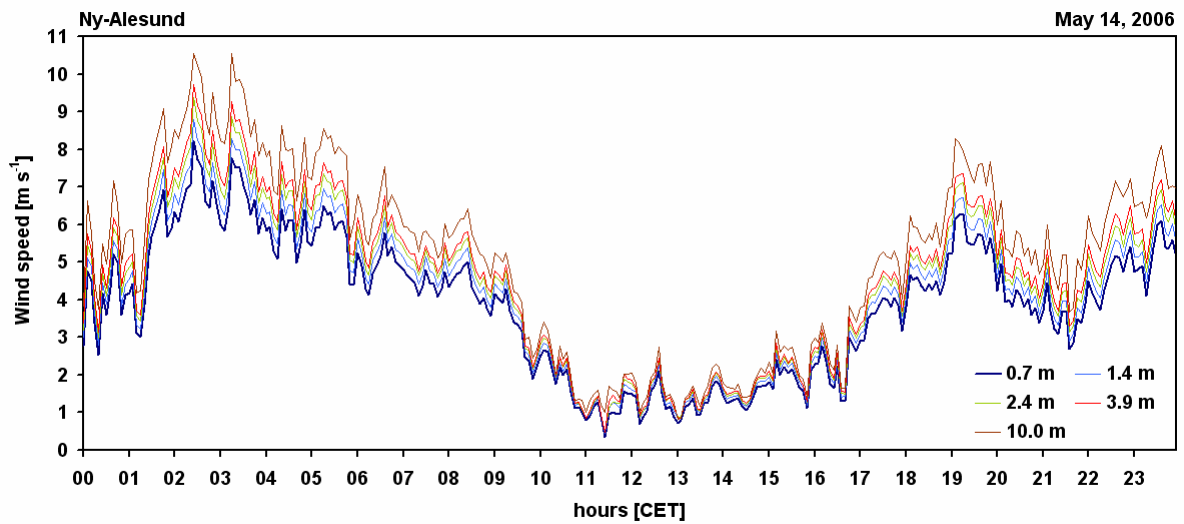
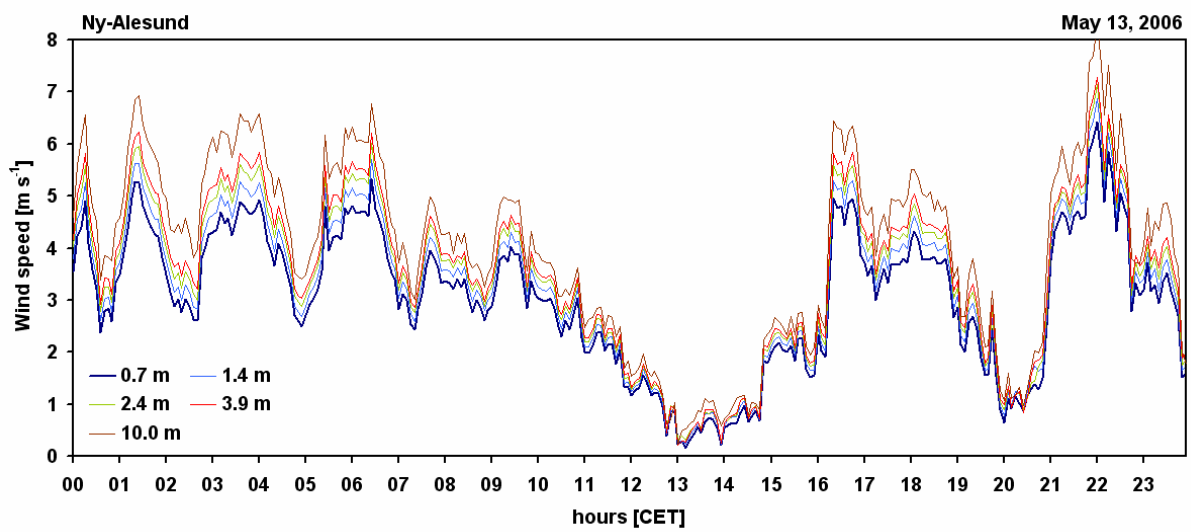
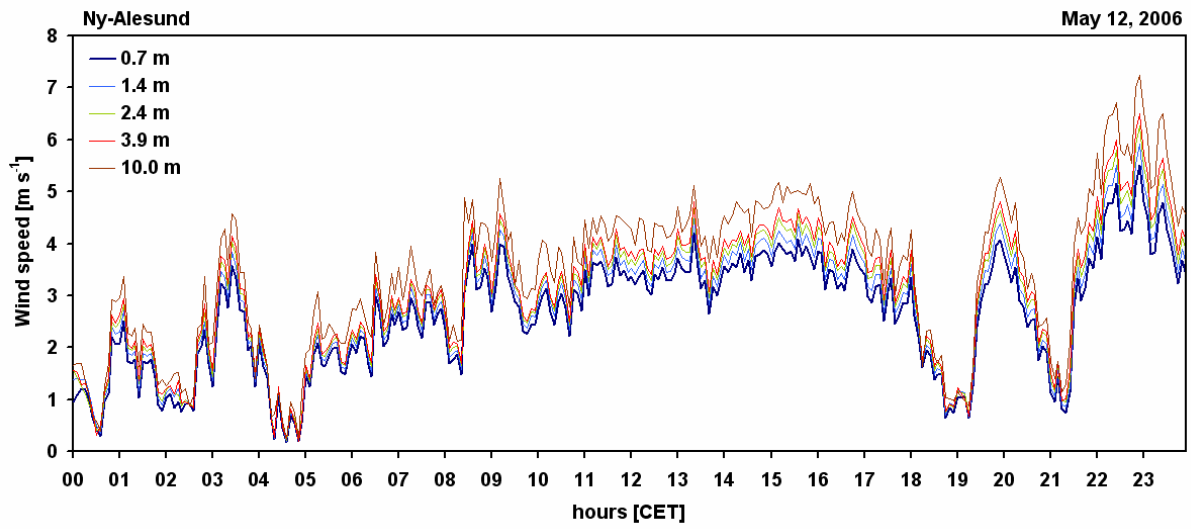
Wind speed

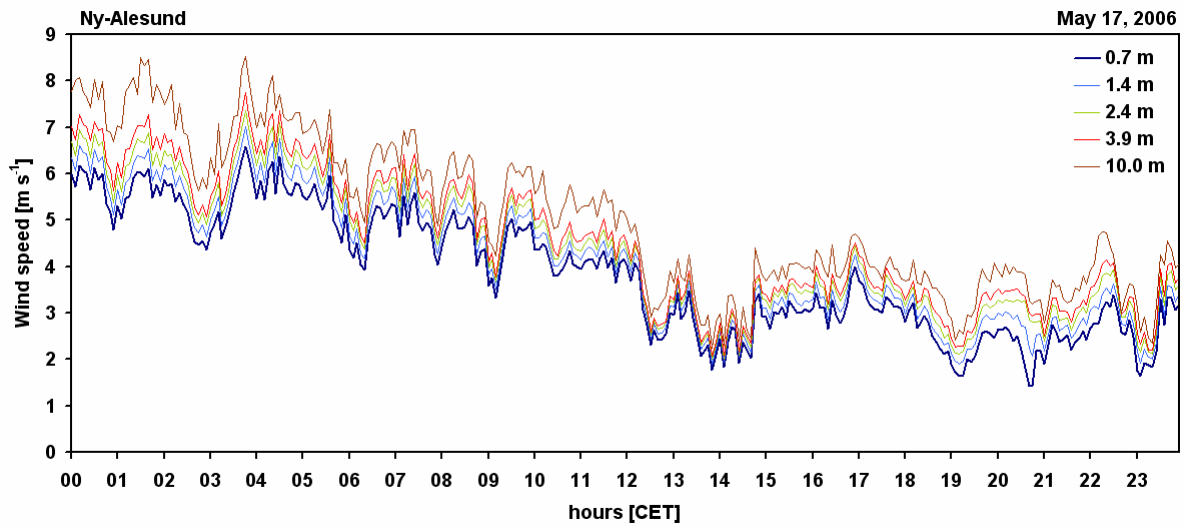
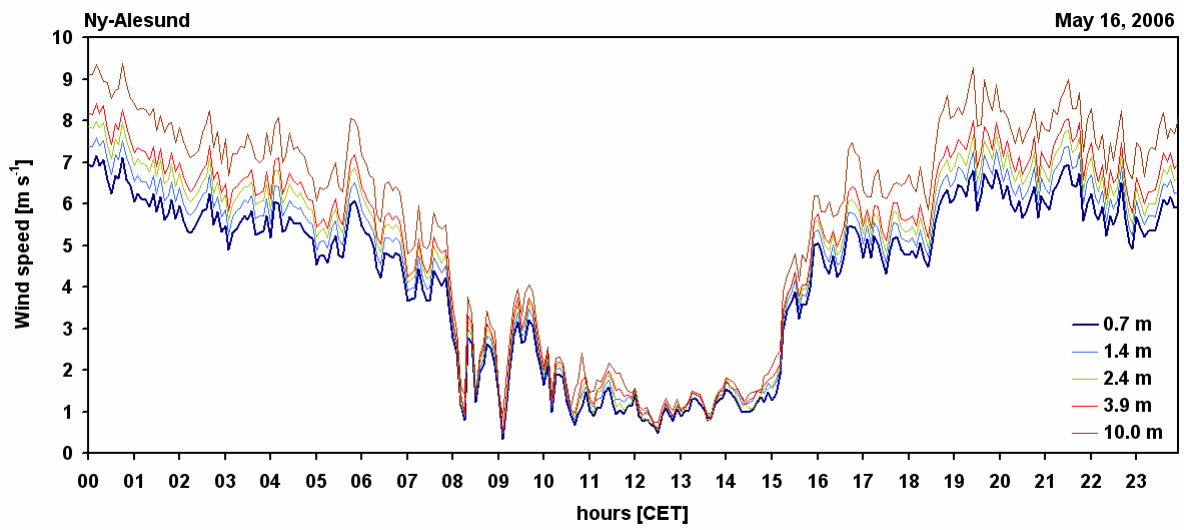
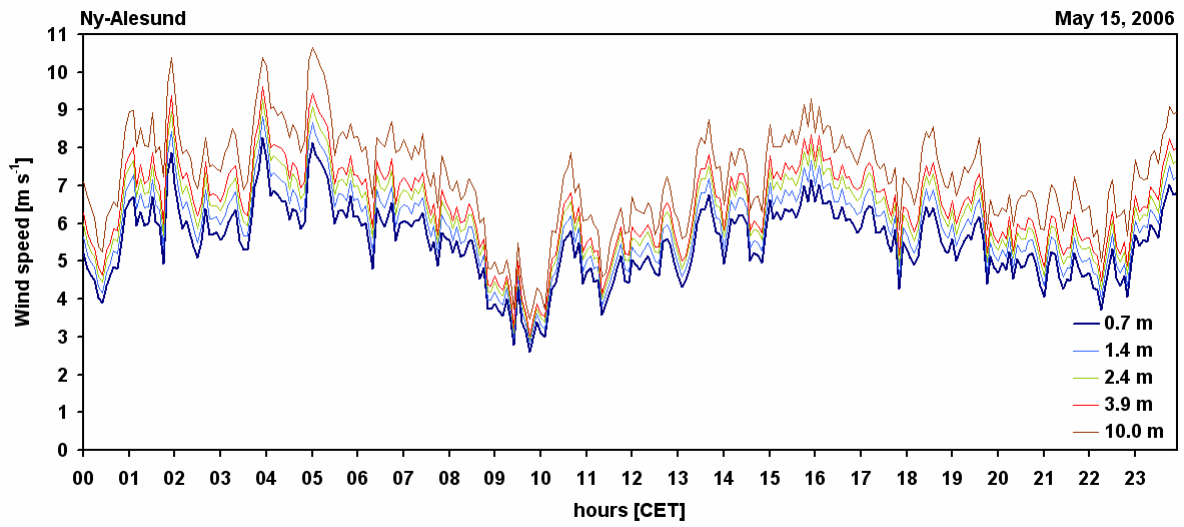
The wind speed was recorded in different heights above ground using cup anemometers. Most of the time the area around the gradient tower of the University of Bayreuth (MT2, measuring heights 0.7 m, 1.4m, 2.4 m and 3.9 m) and around the meteorological tower of the Alfred Wegener Institute for Polar and Marine Research (MT1, 10 m) was covered by 20 cm to 30 cm snow. The records of the cup anemometer mounted at 5.6 m had to be neglected because of a damage of the ball bearing after the storm event May 7, May 8.

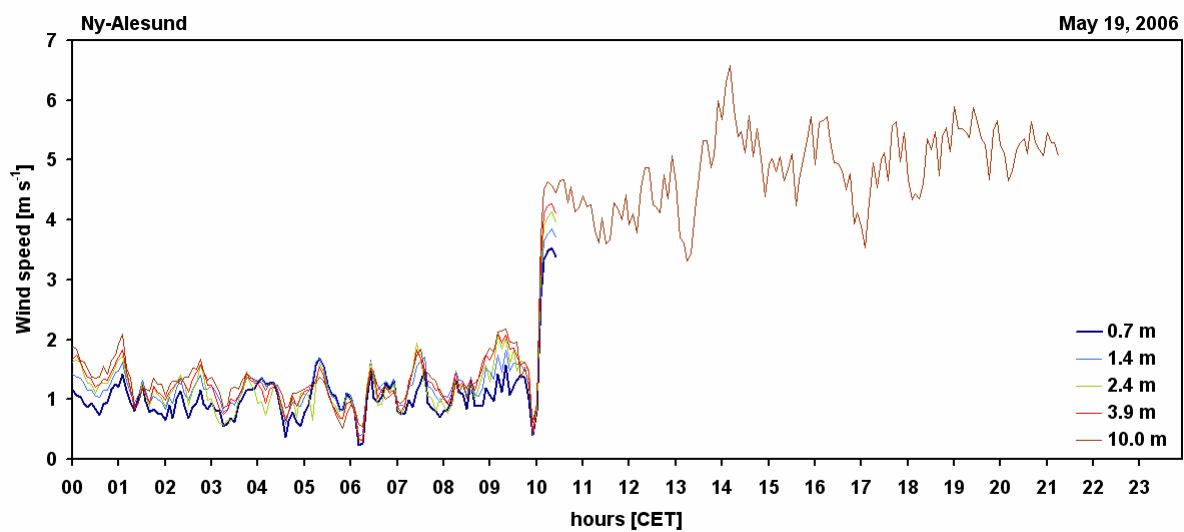
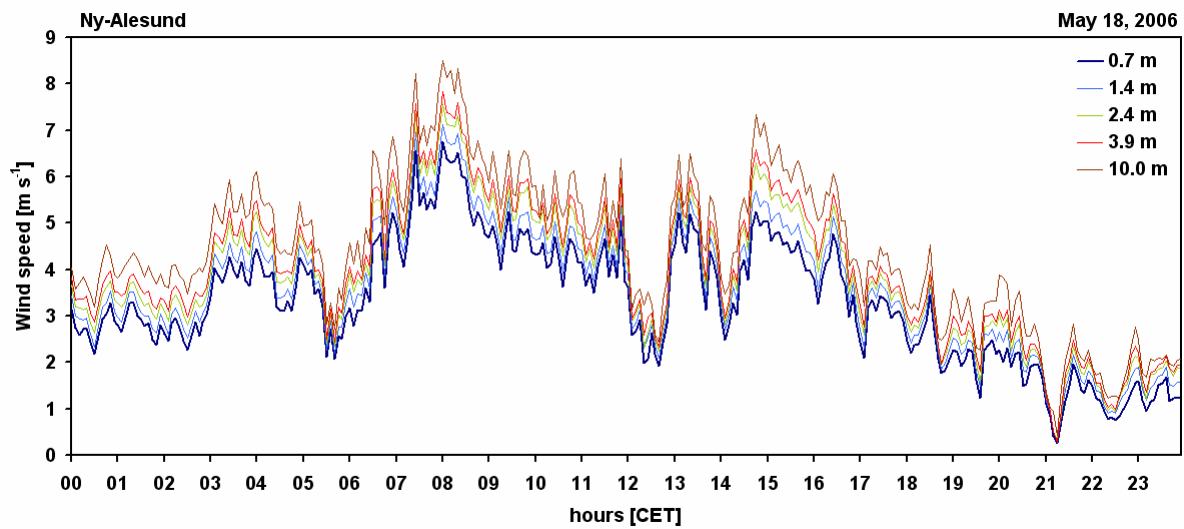










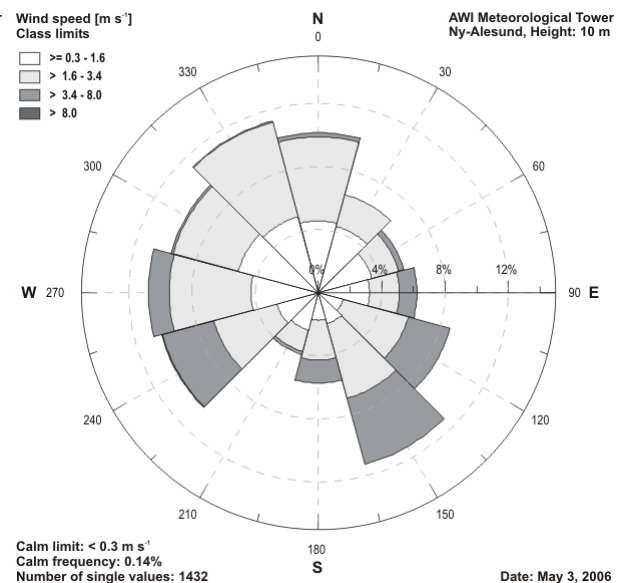
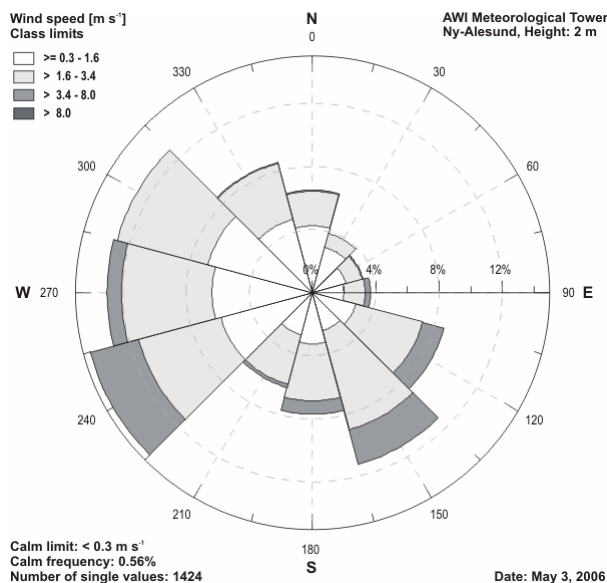
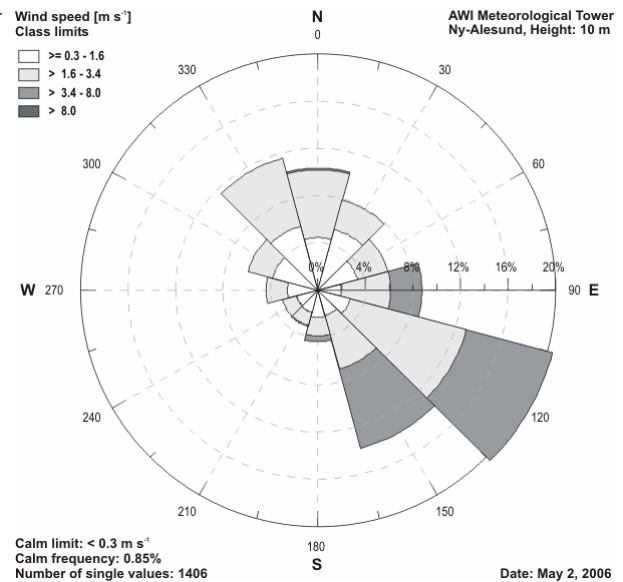
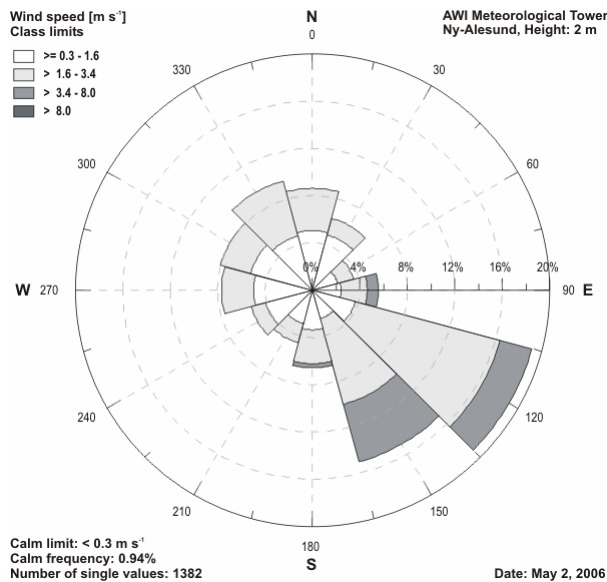
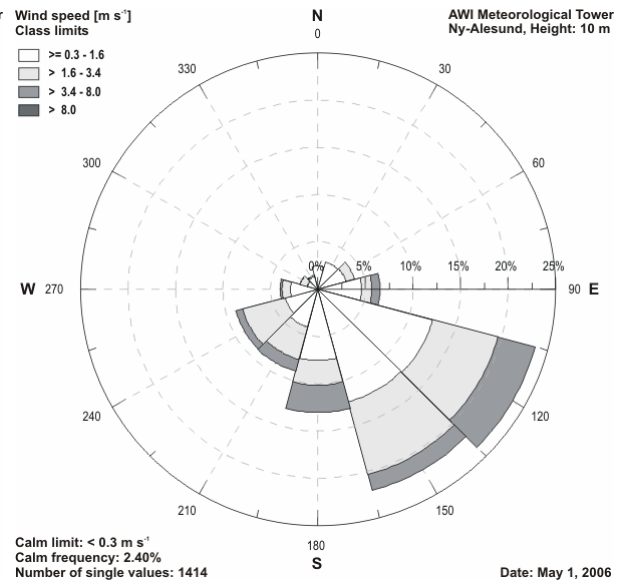
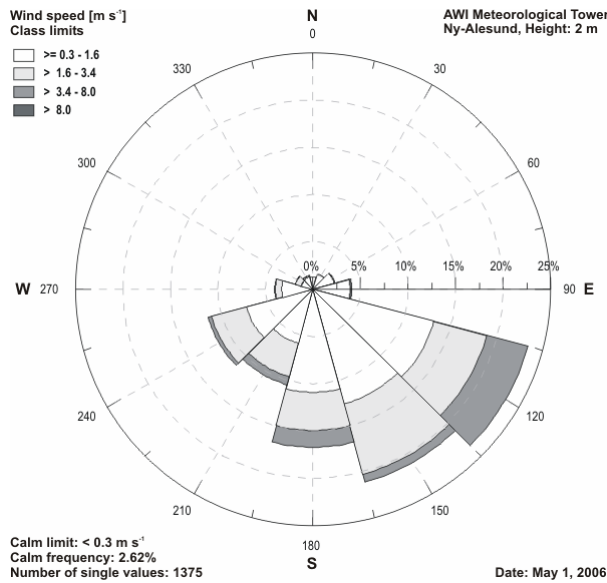


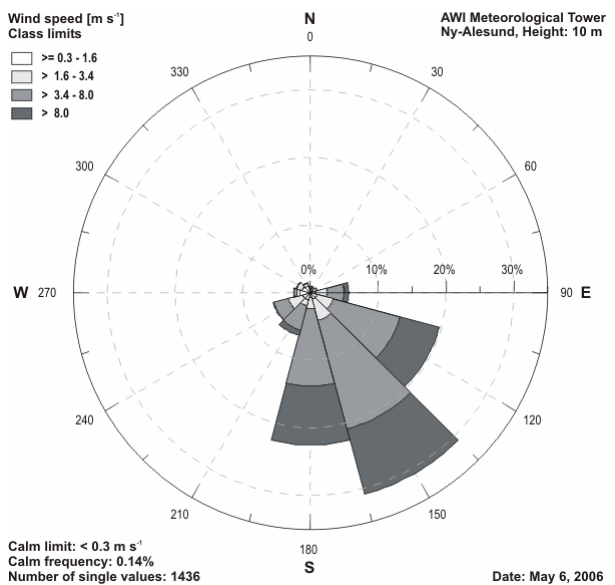
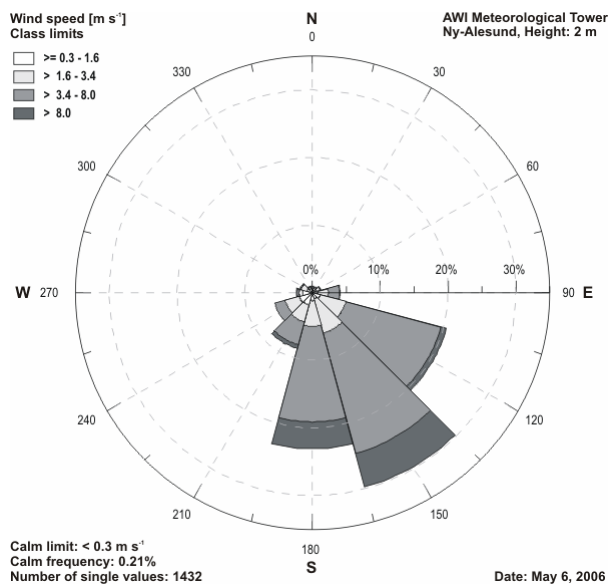
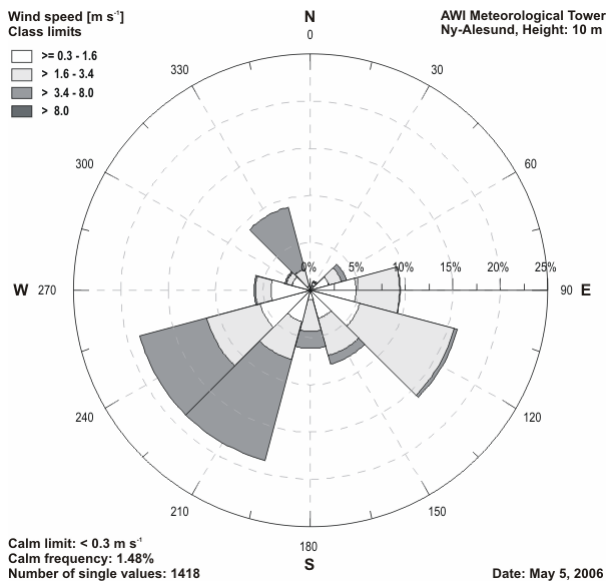
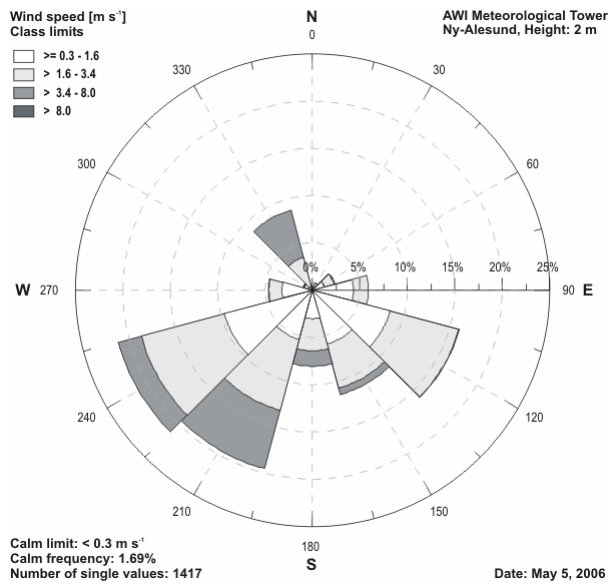
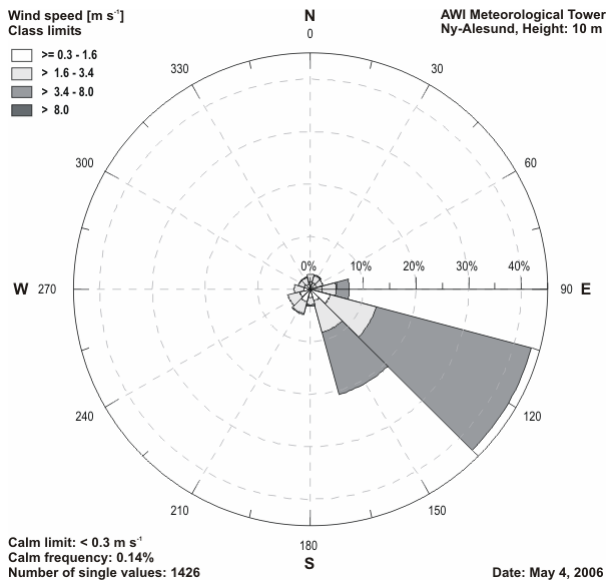
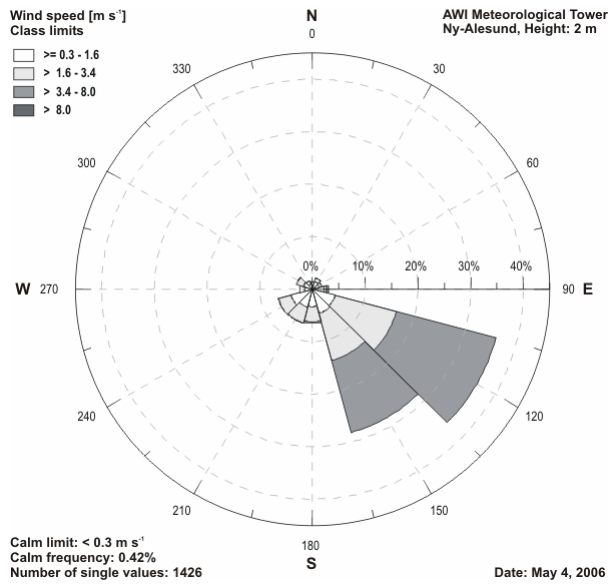
Wind direction

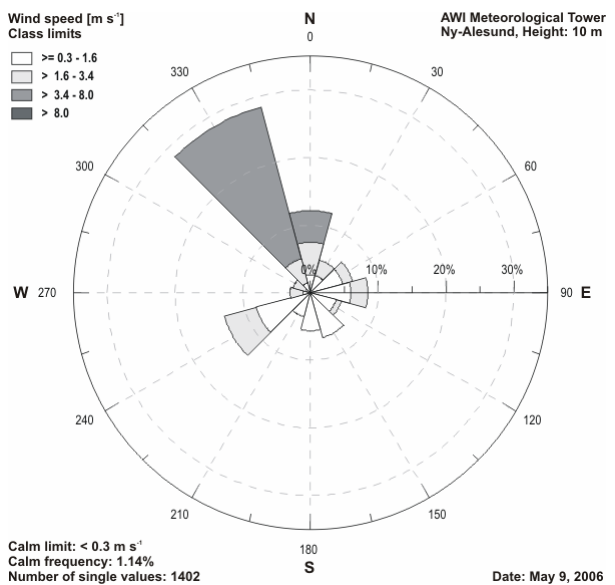
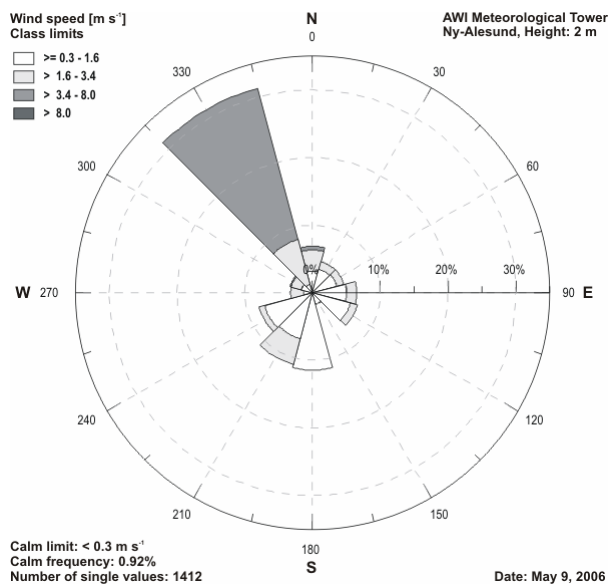
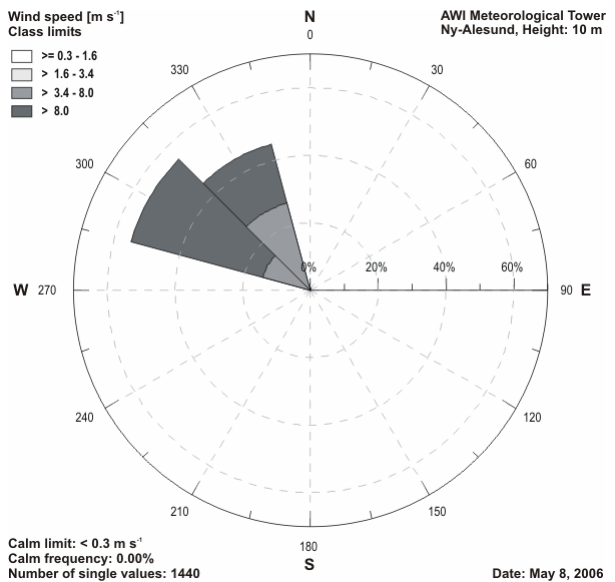
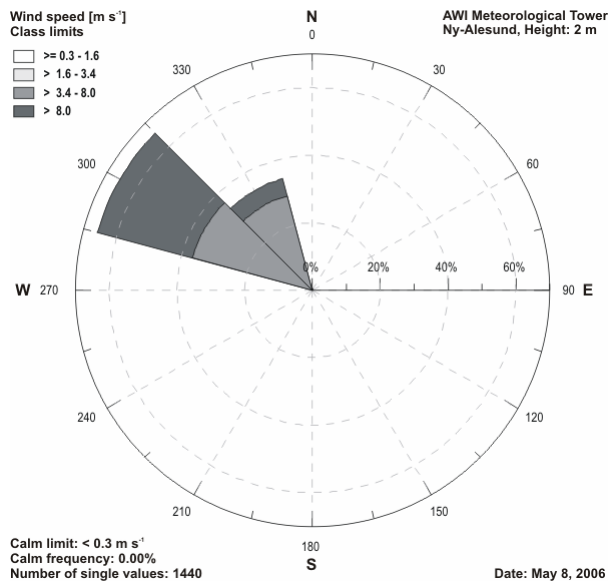
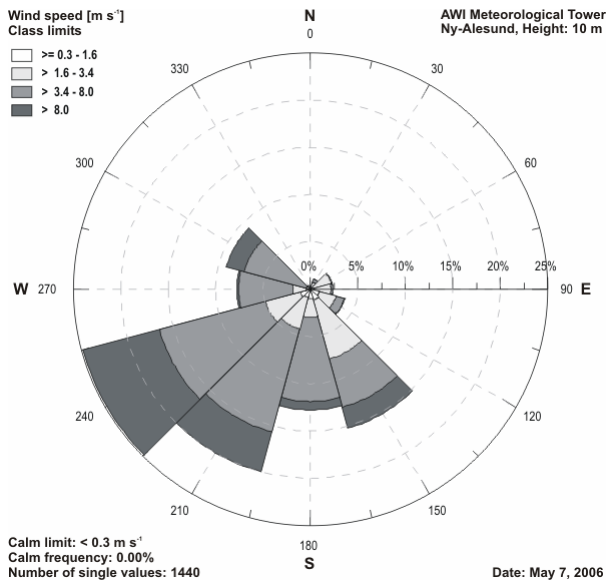
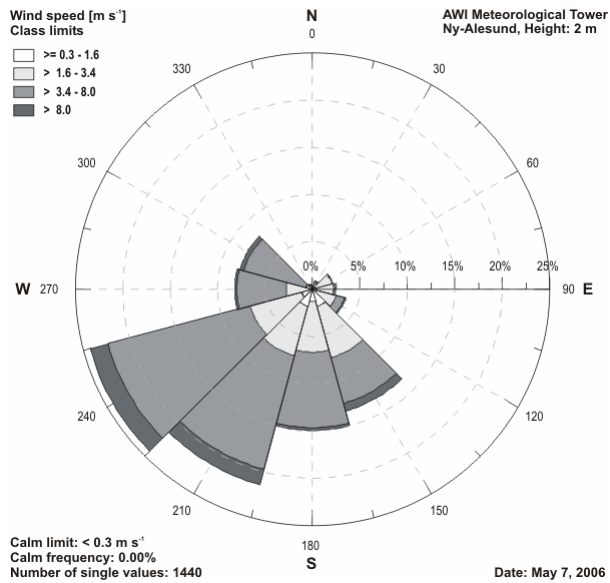
The wind direction was recorded with a wind vane at the meteorological tower of the Alfred Wegener Institute for Polar and Marine Research Ny-Ålesund (MT1) in 2 m and 10 m above the ground nearby the gradient tower and the eddy flux complex of the University of Bayreuth. The general calm limit was set to $< 0.3 \text{ m s}^{-1}$. At most of the days between May 1 and May 18 the percentage of calm events are below 1 % of all measurements per day.

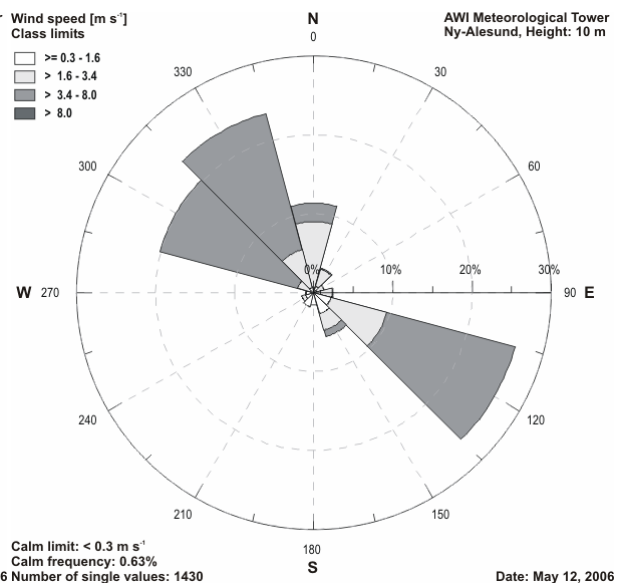
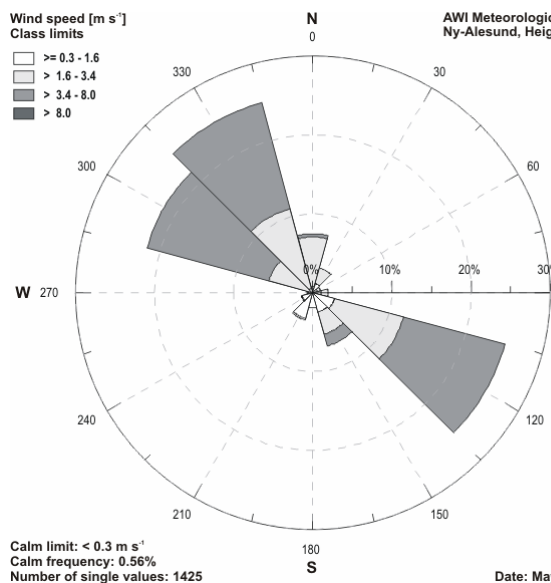
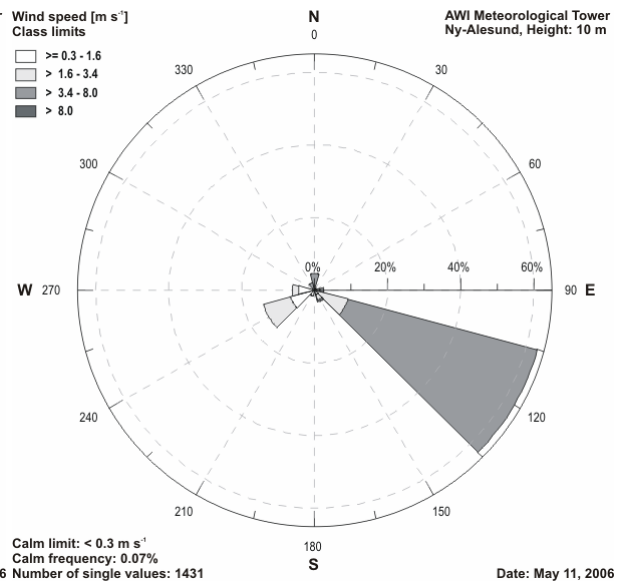
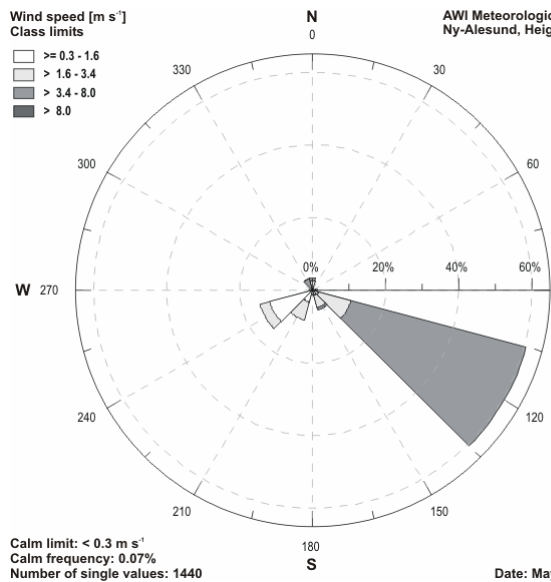
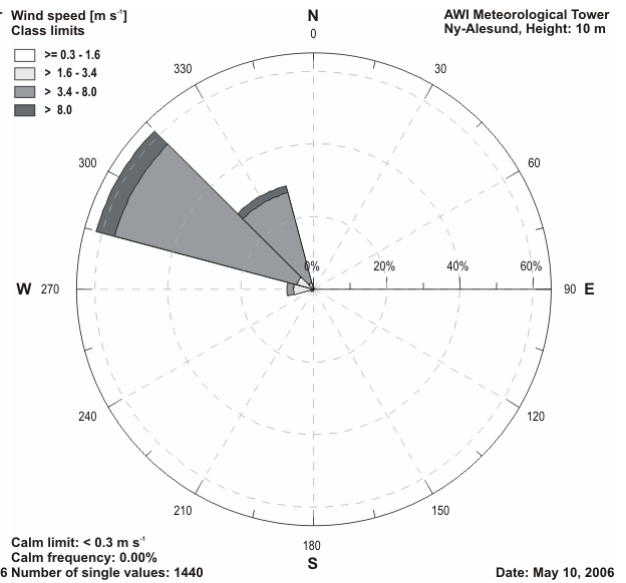
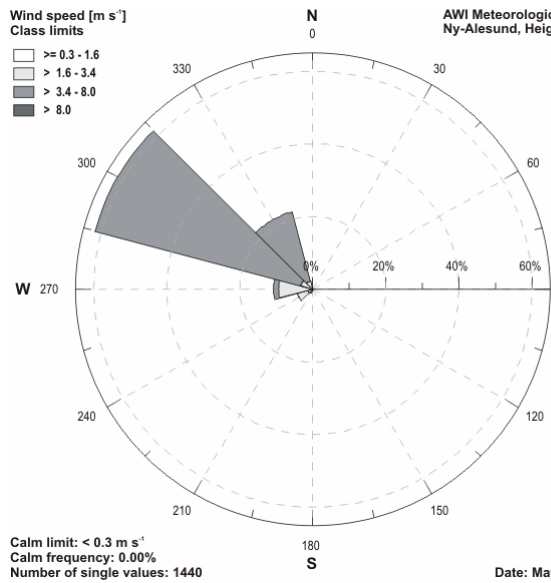
The wind rose plots are a combination of wind speed and related direction to succinctly show the daily distribution or frequency of particular directions separated in 12 sectors. The chosen wind speed class limits are ≥ 0.3 to 1.6, > 1.6 to 3.4, > 3.4 to 8.0 and $> 8.0 \text{ m s}^{-1}$.

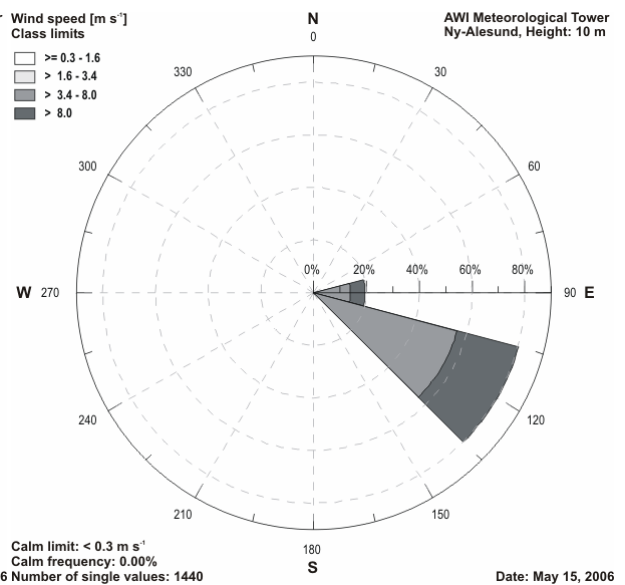
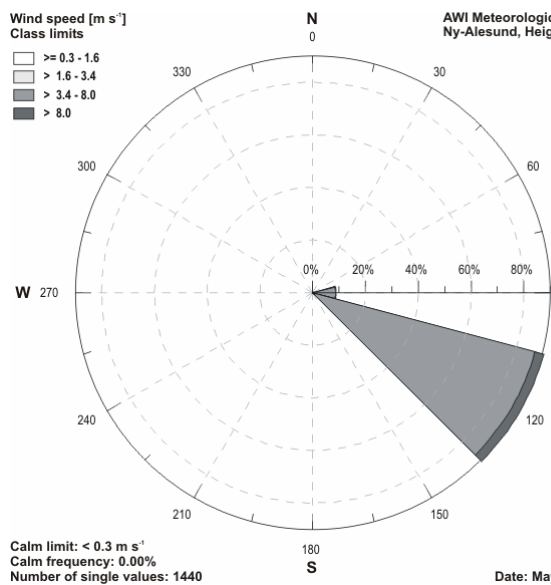
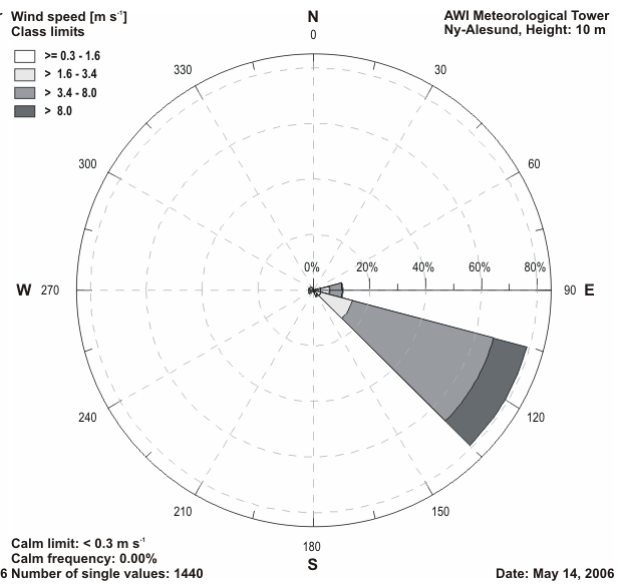
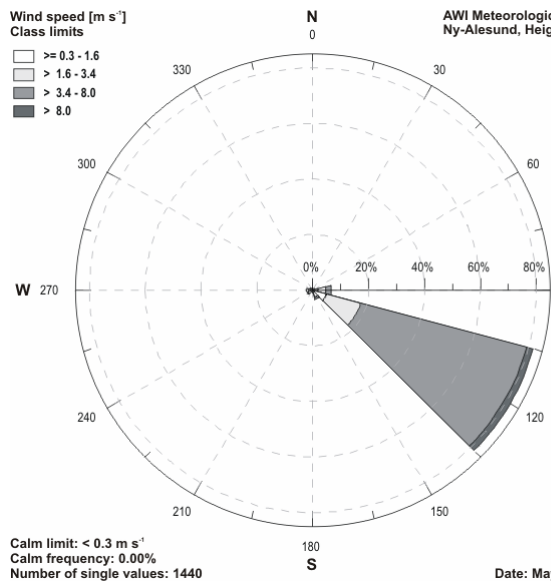
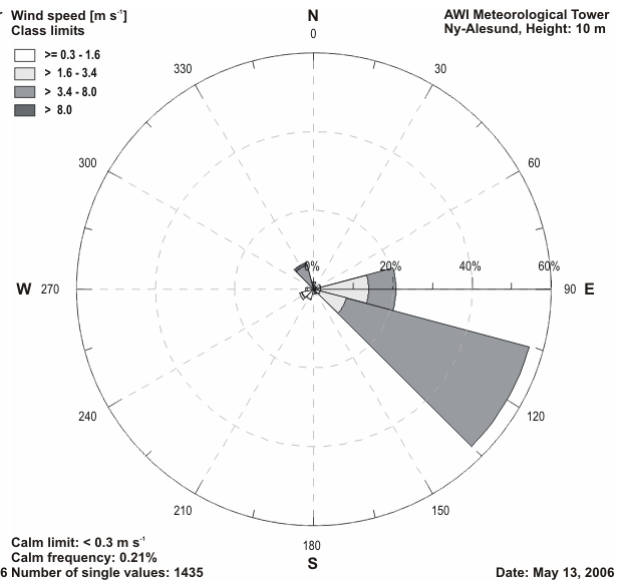
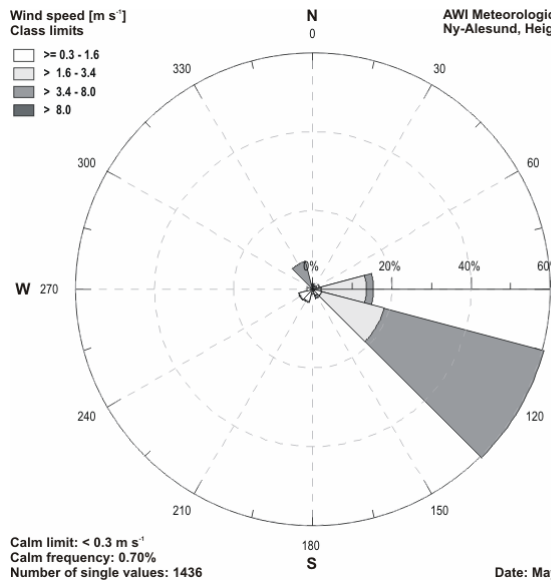
Noticeable are the offshore south-west components during weak wind especially at May 9 and May 11.

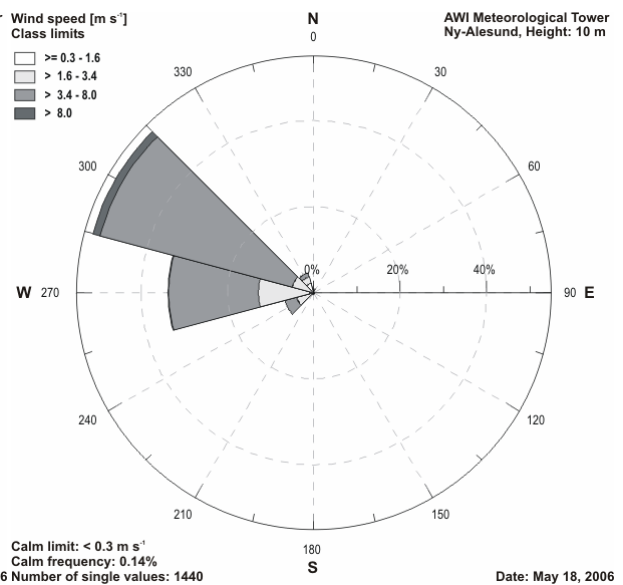
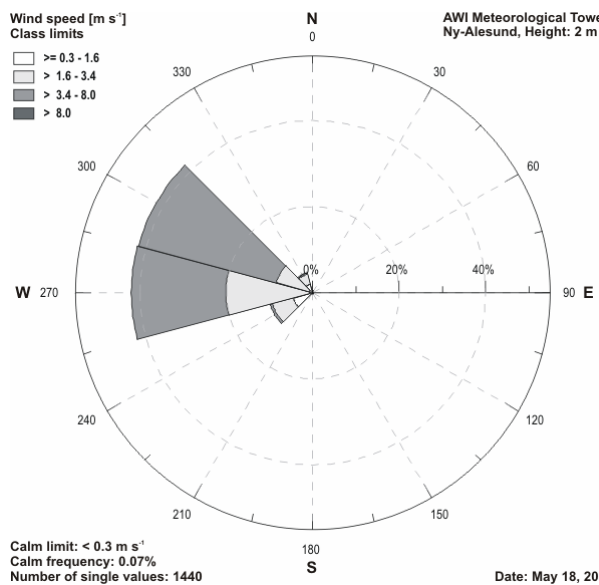
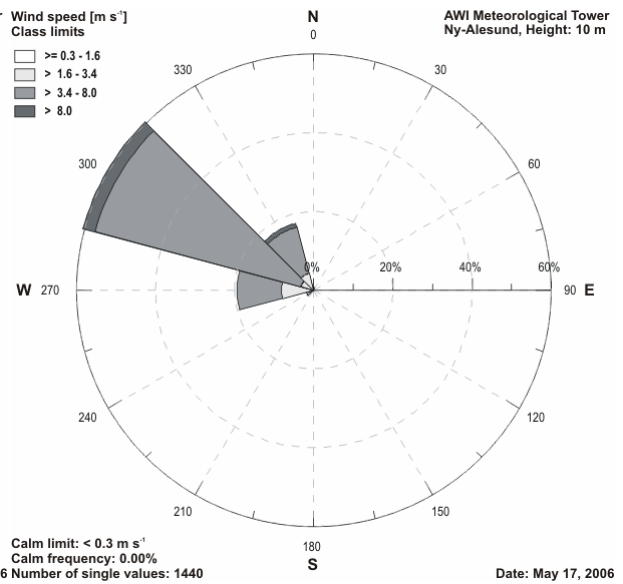
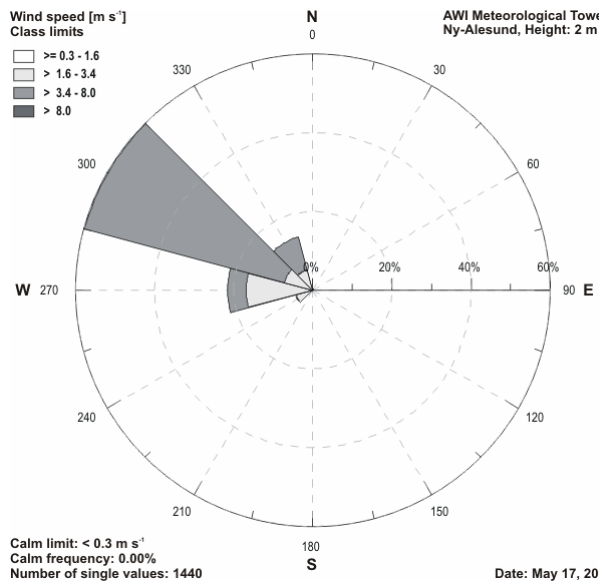
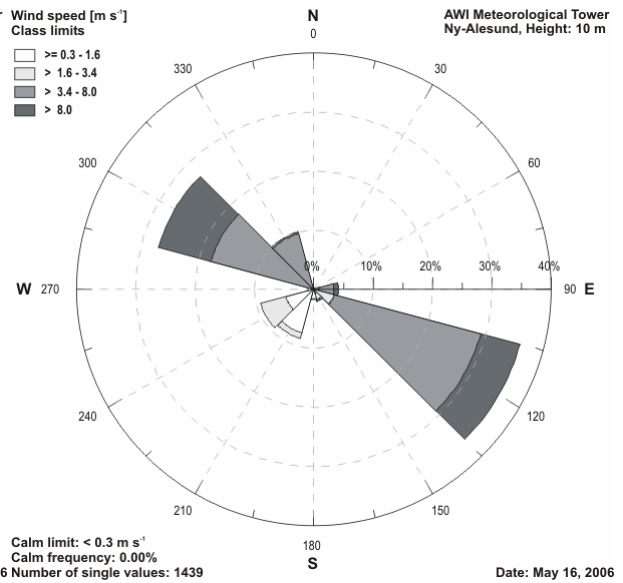
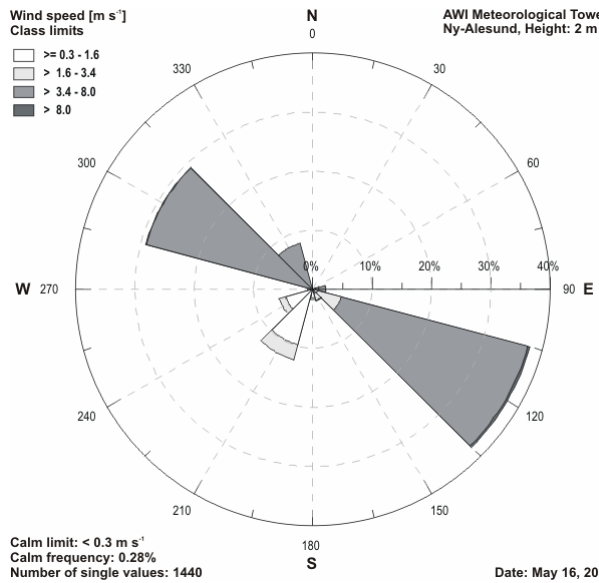






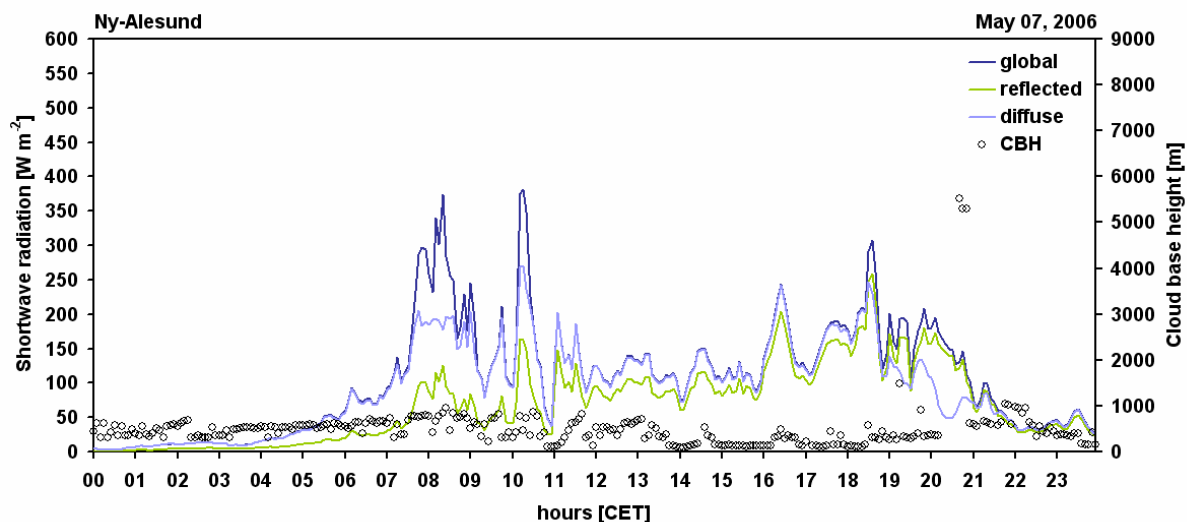
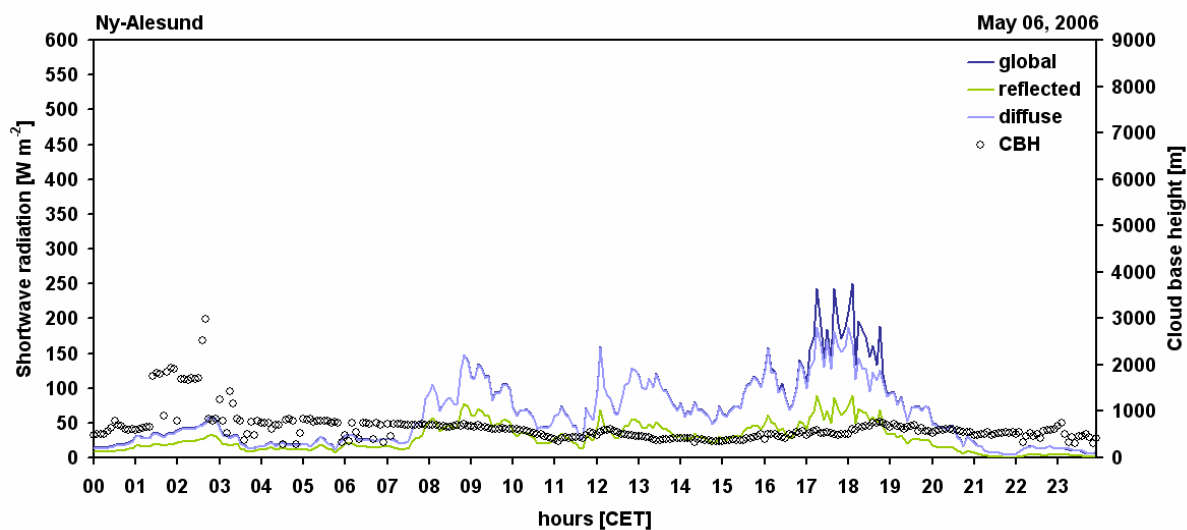
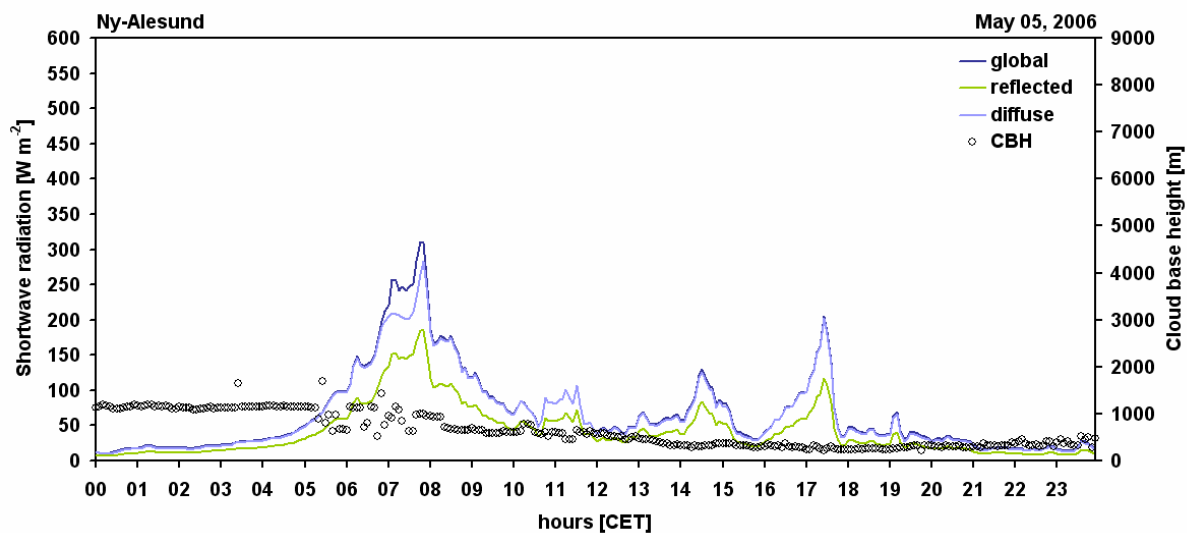


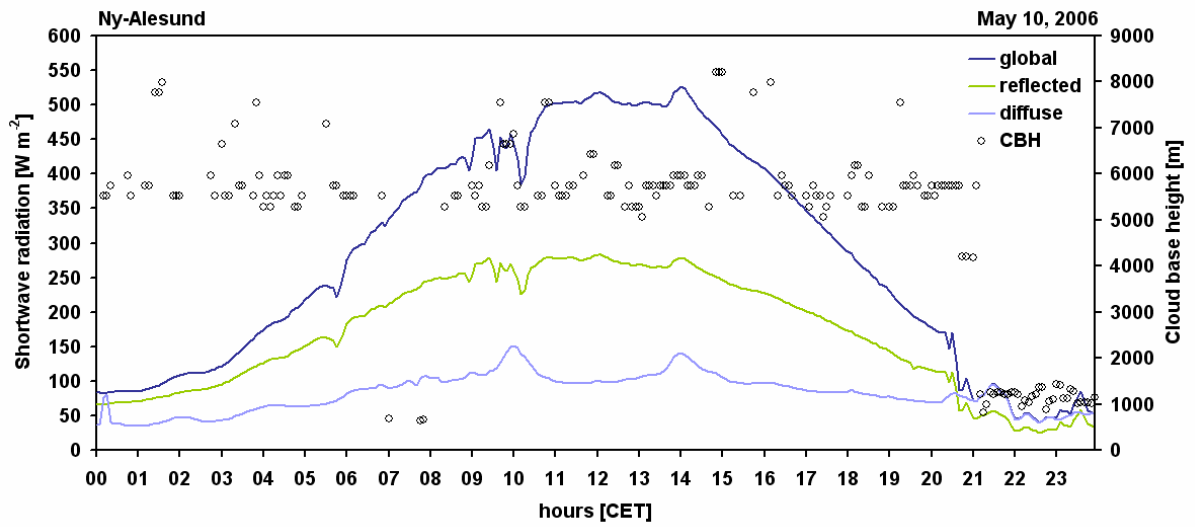
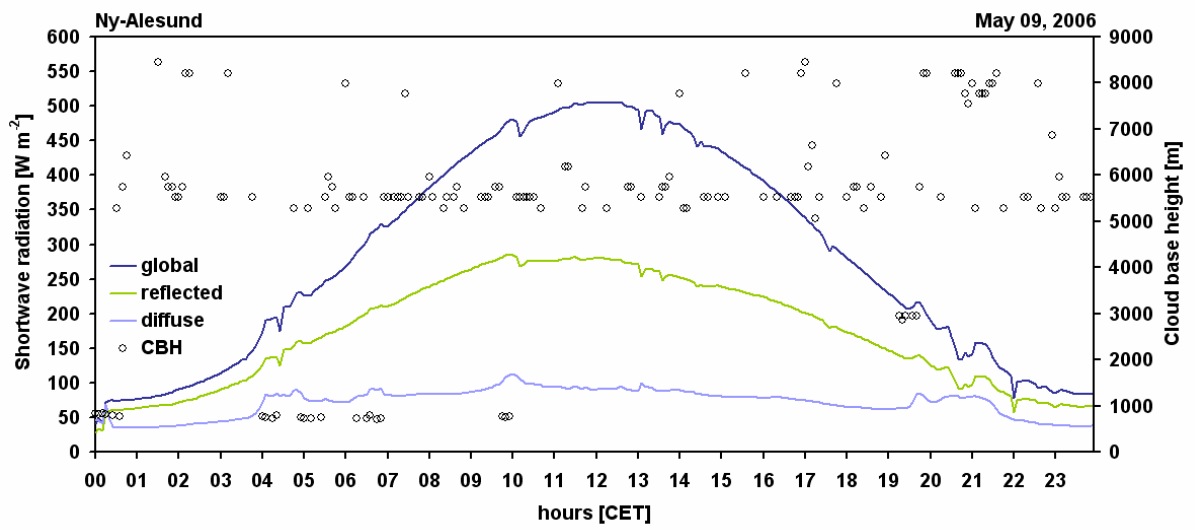
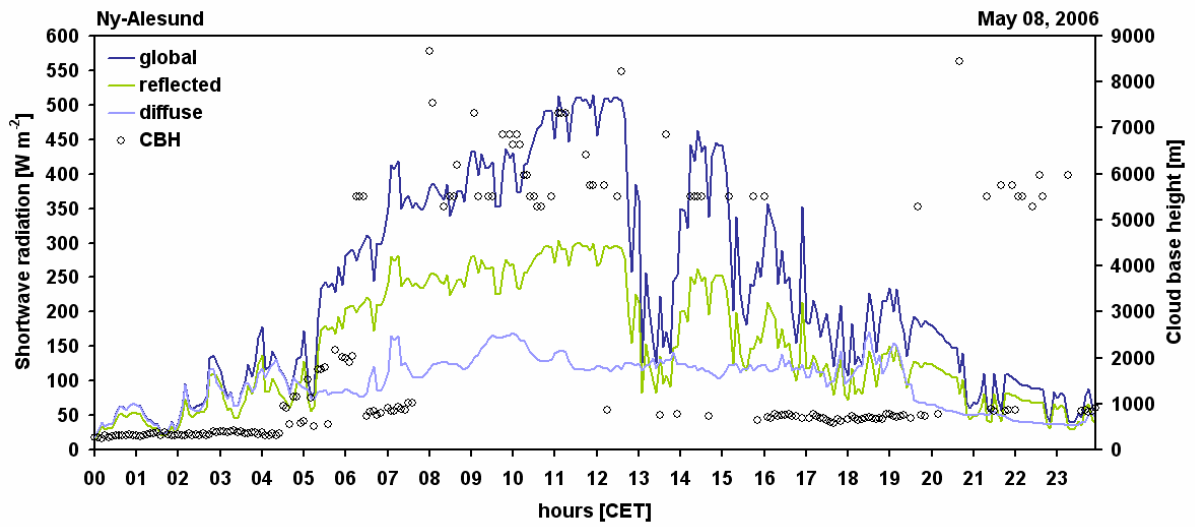


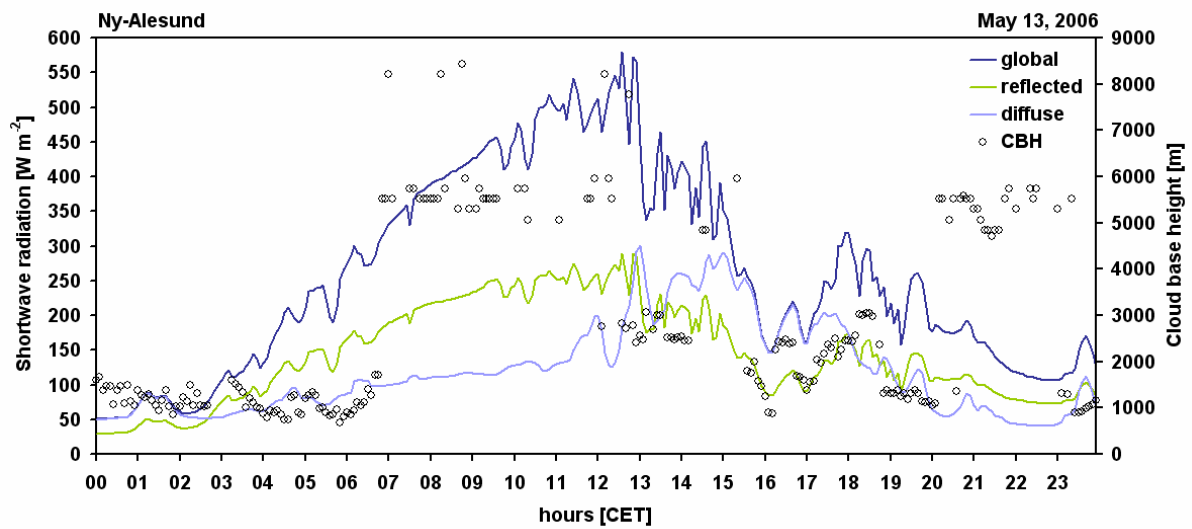
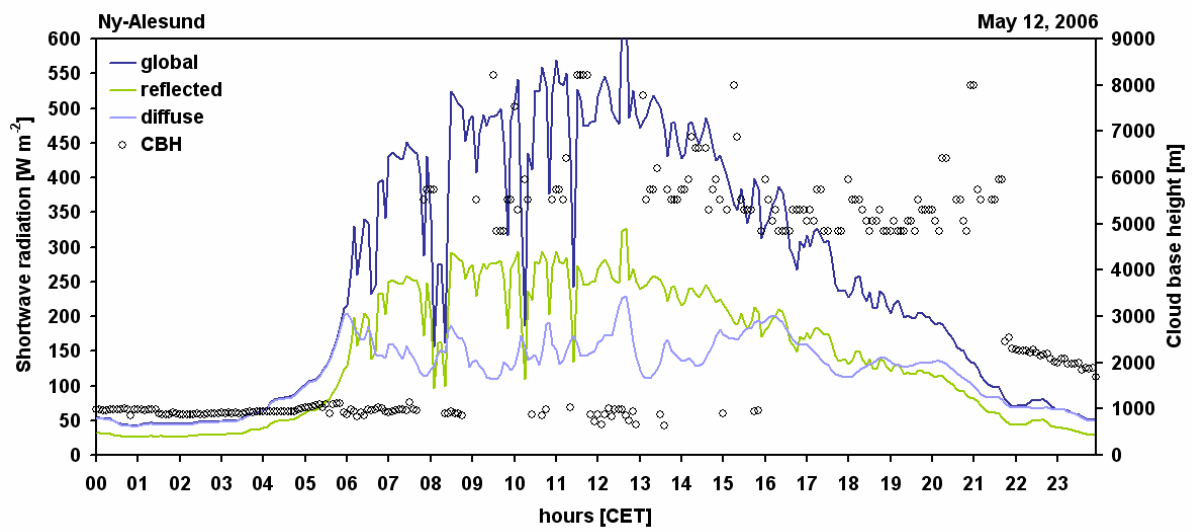
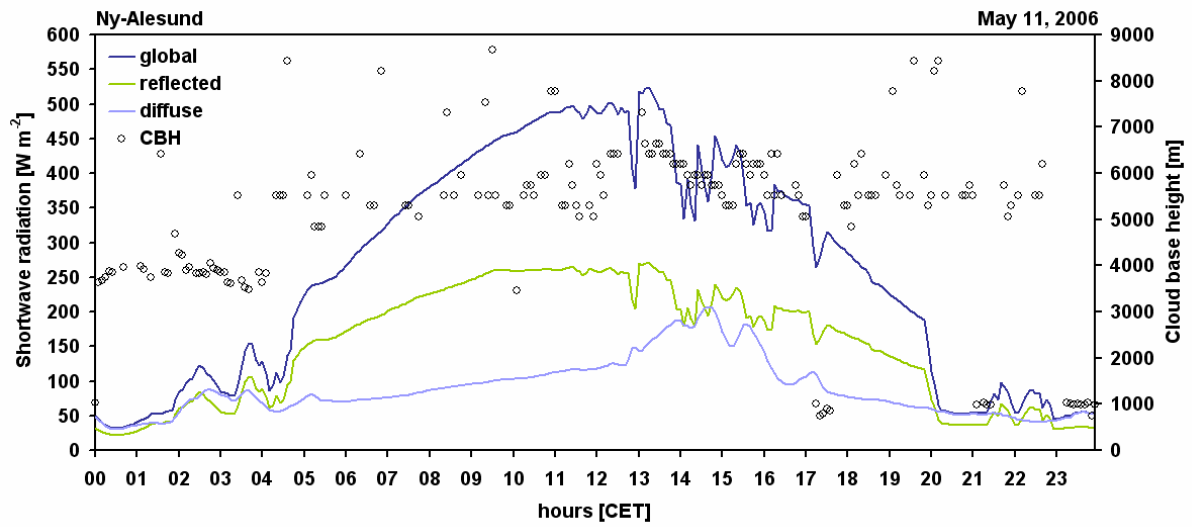


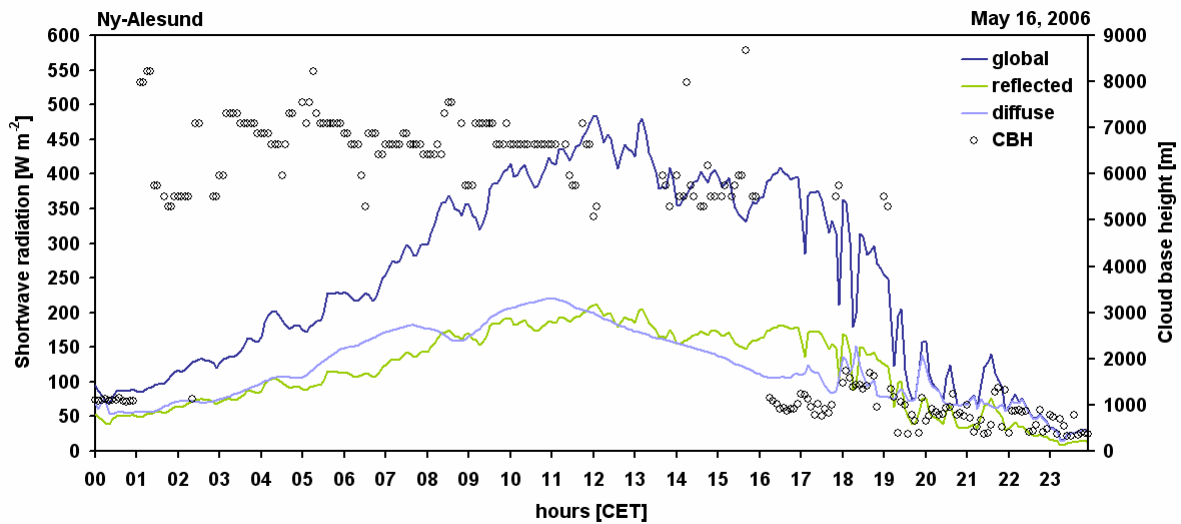
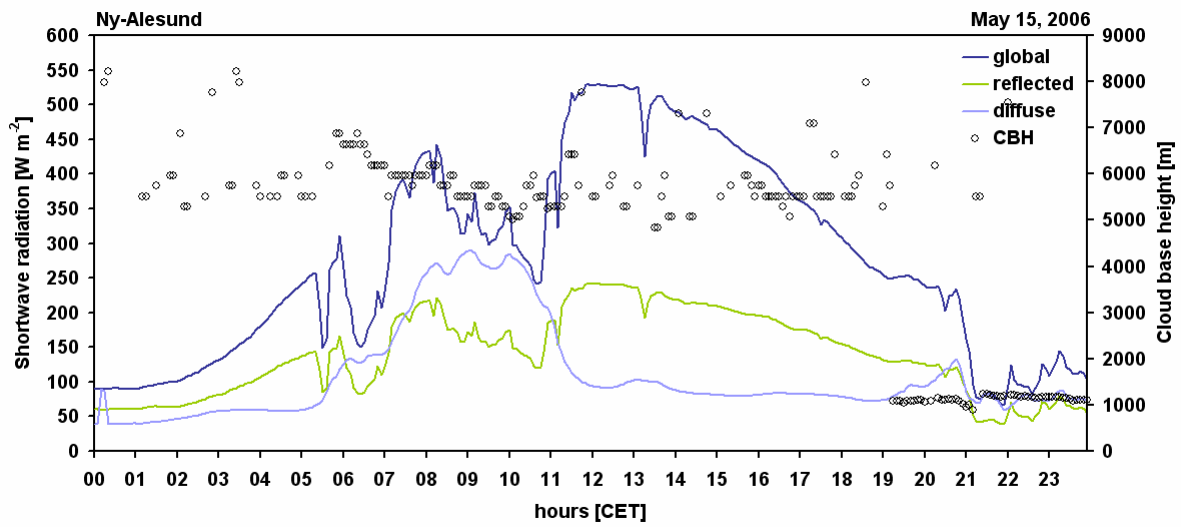
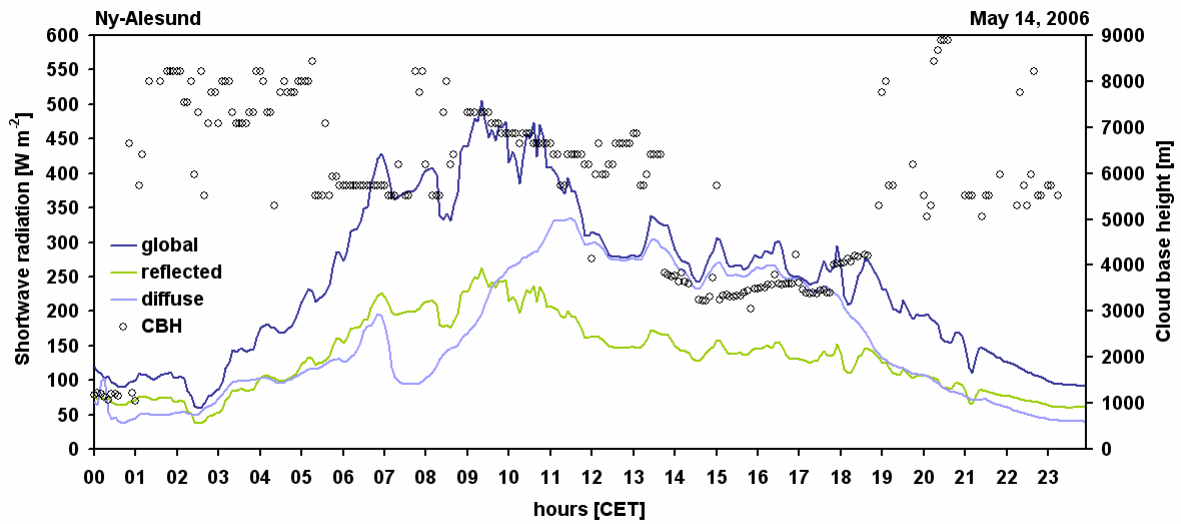
Shortwave radiation and cloud base height

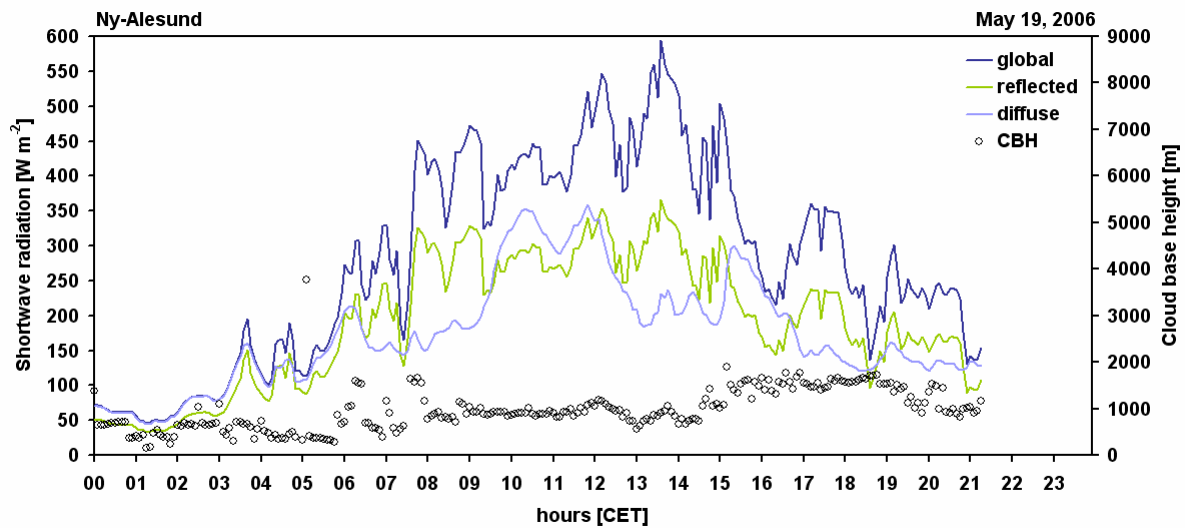
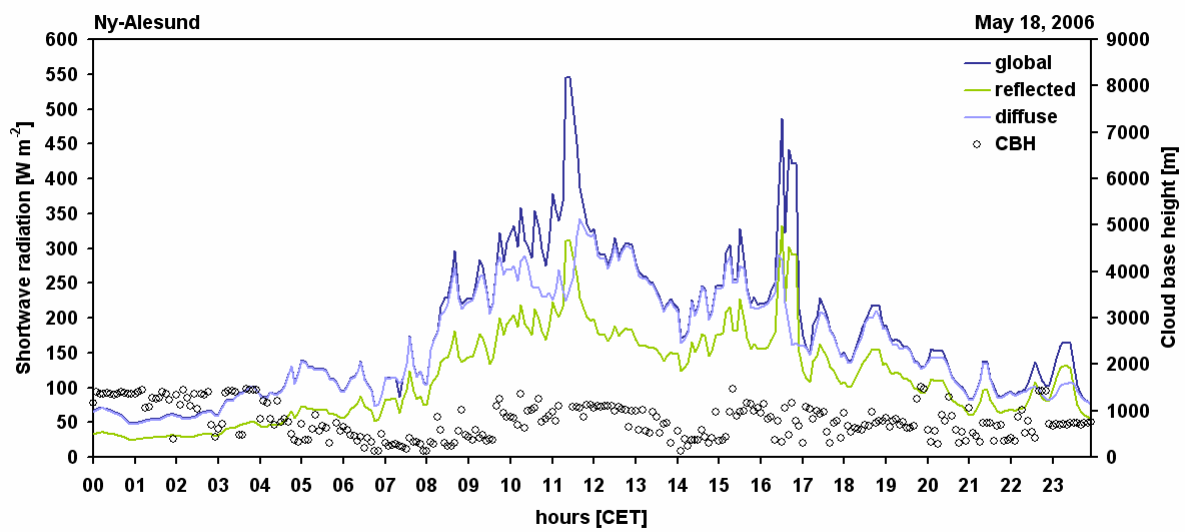
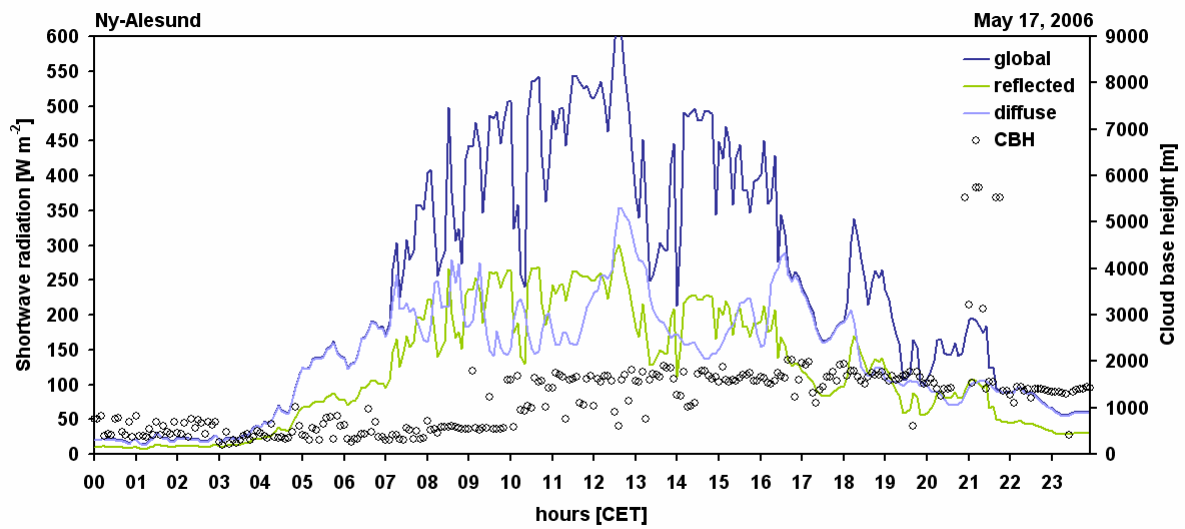
The presented recordings of the solar radiation and the cloud base height are obtained by the international standardized radiation measurements of the Baseline Surface Radiation Network (BSRN) and the laser ceilometer (cloud base height) both maintained by the Alfred Wegener Institute for Polar and Marine Research. The plots show the global (incoming), reflected and diffuse parts of the shortwave spectral range and the according cloud height.





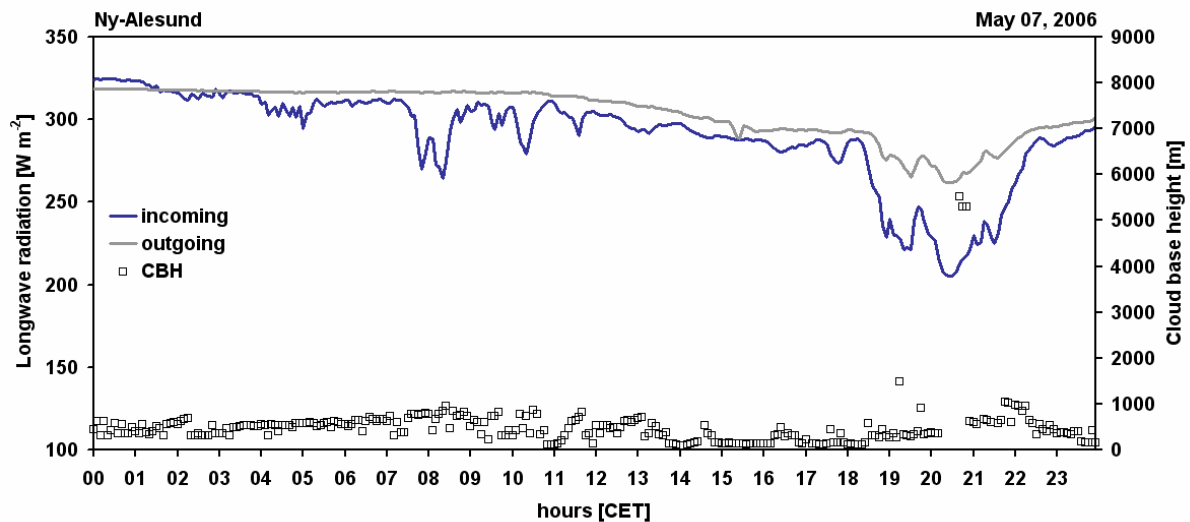
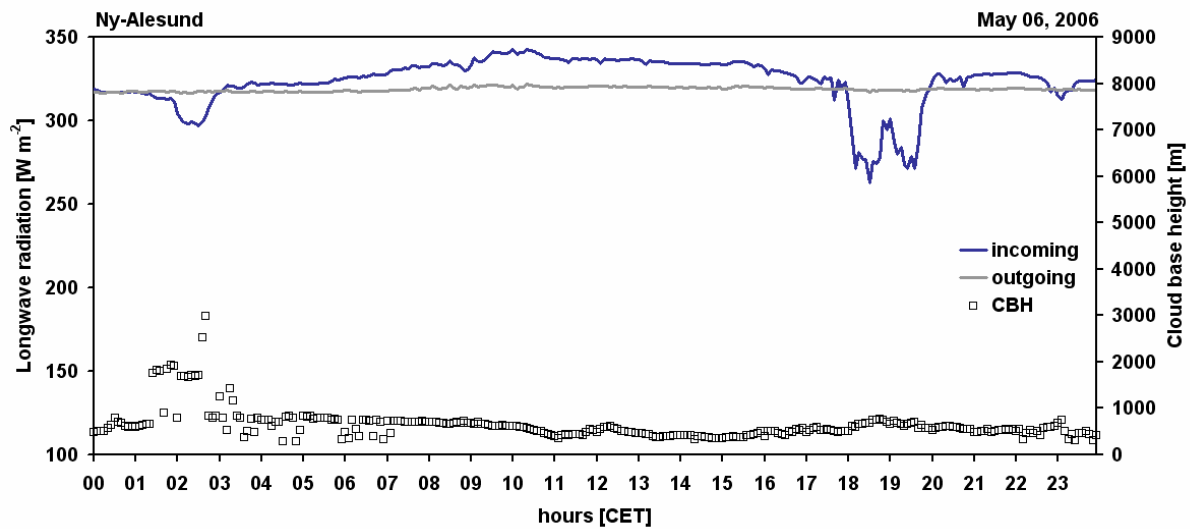
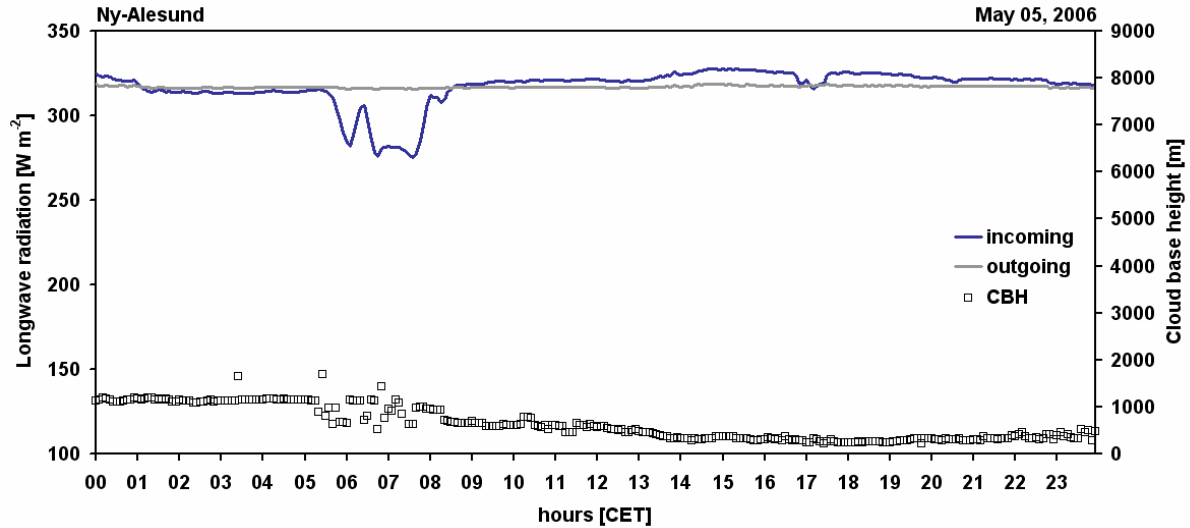


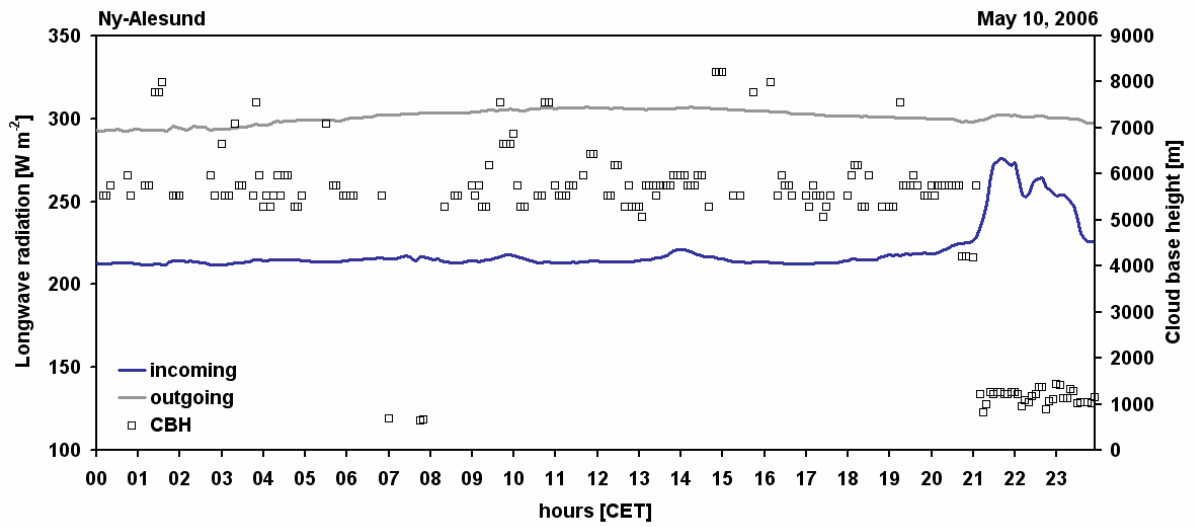
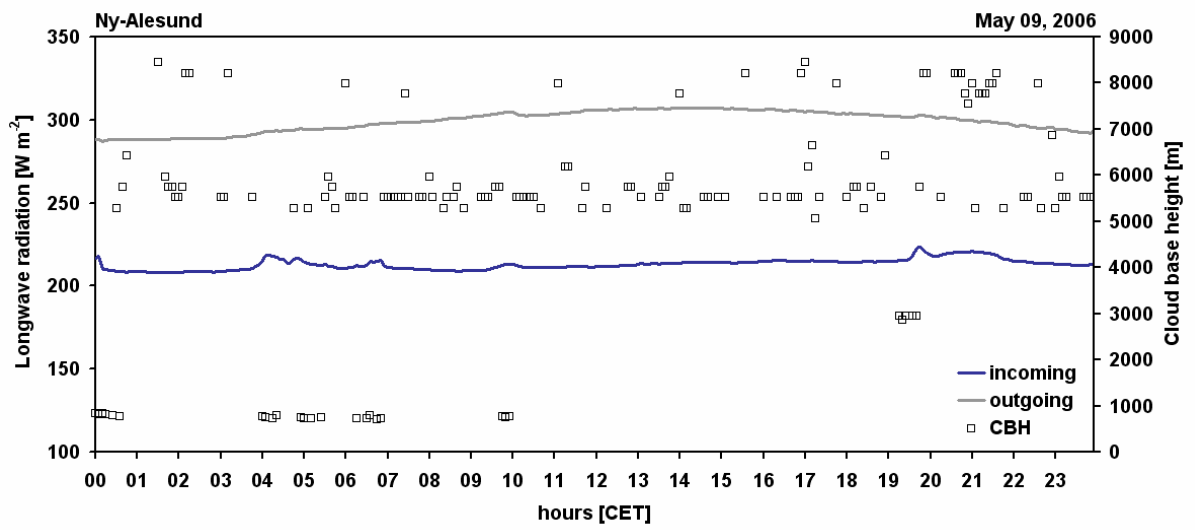
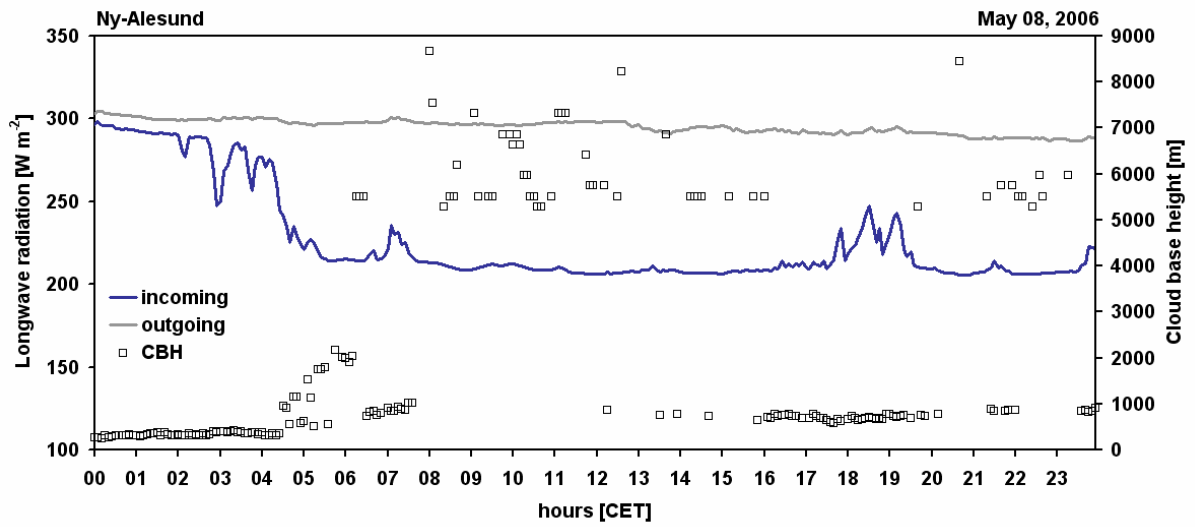


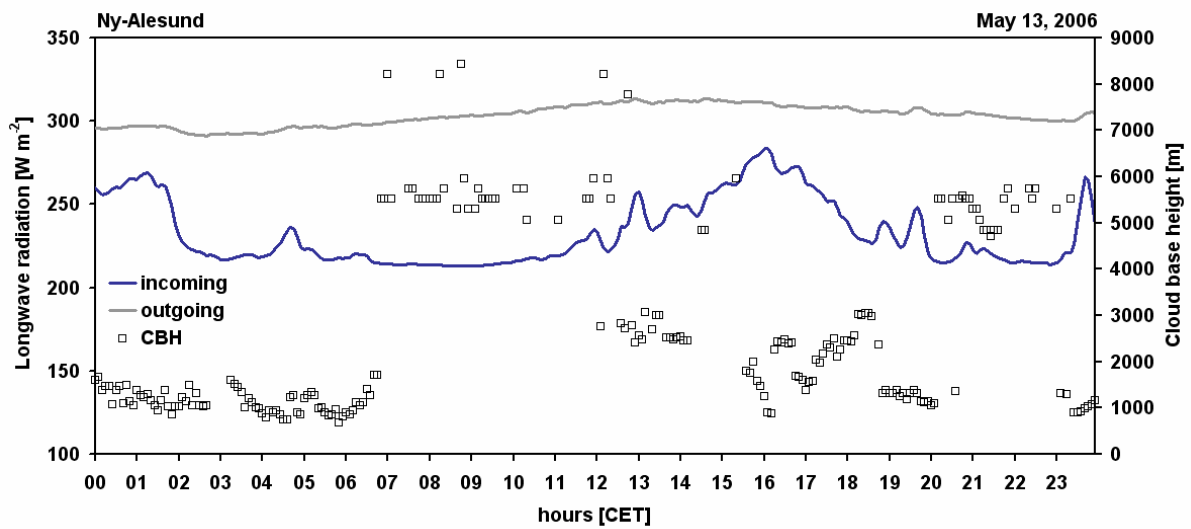
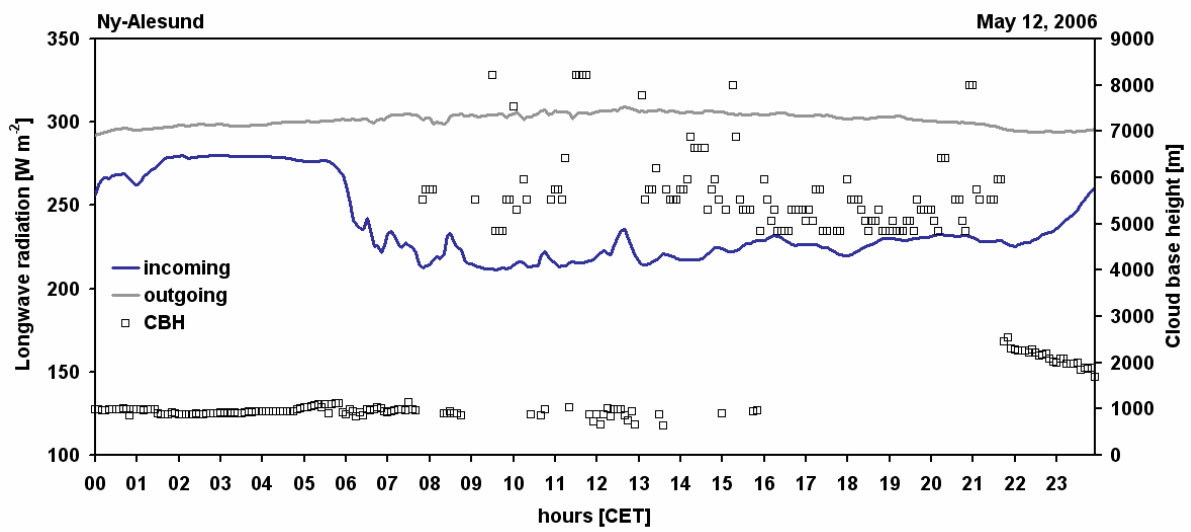
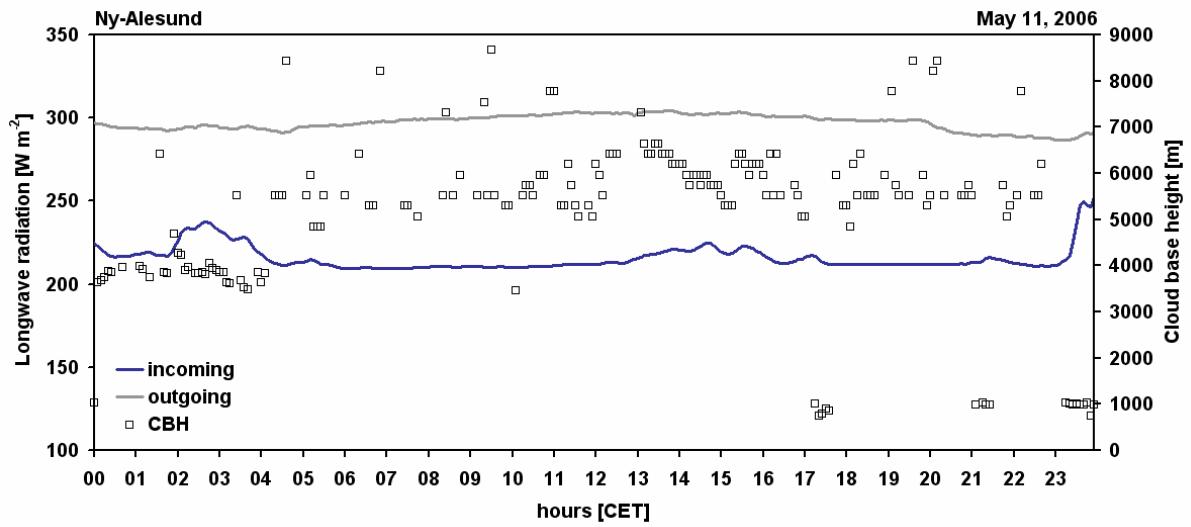


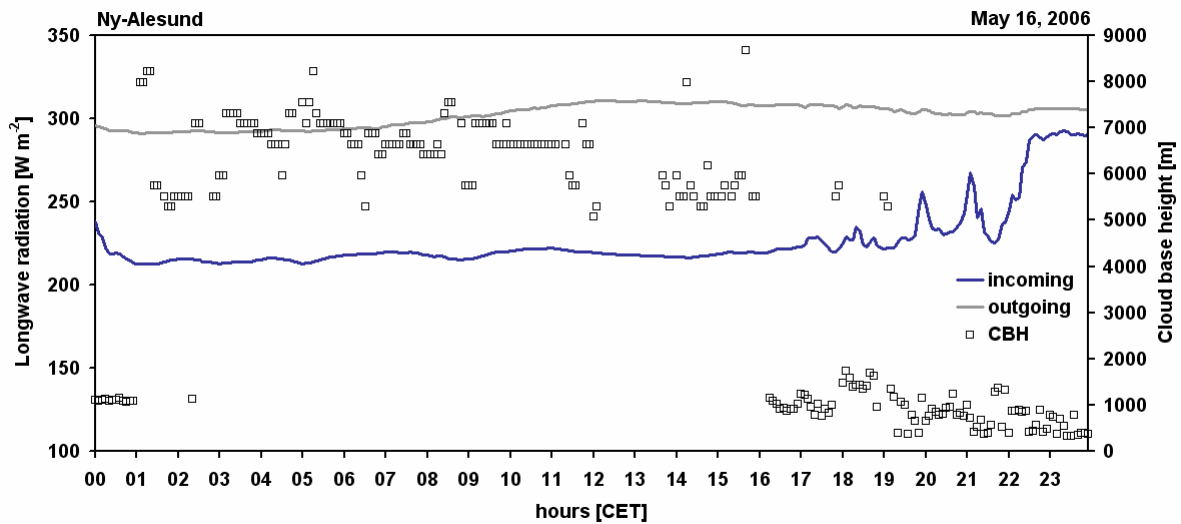
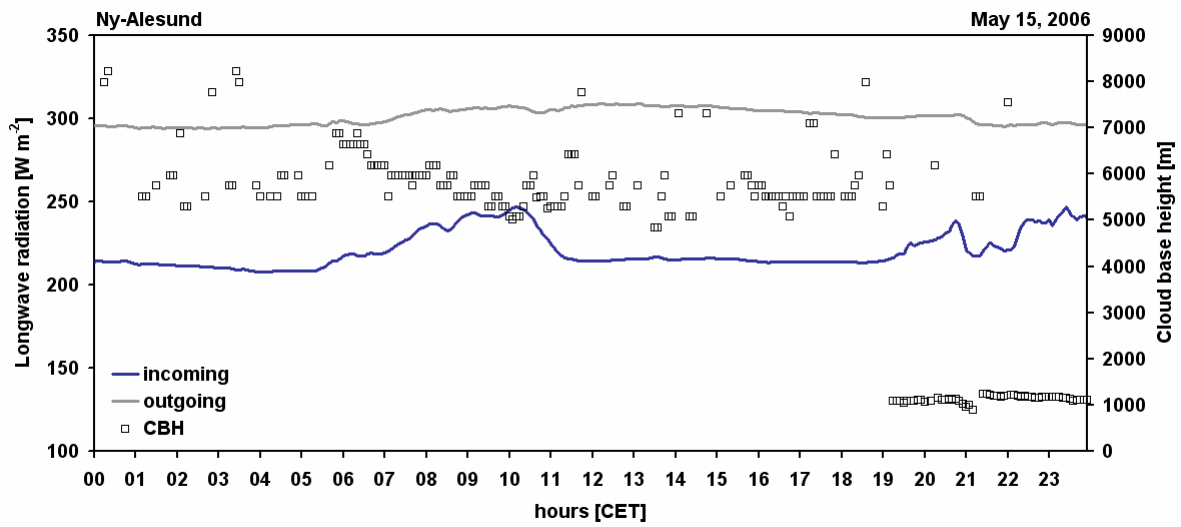
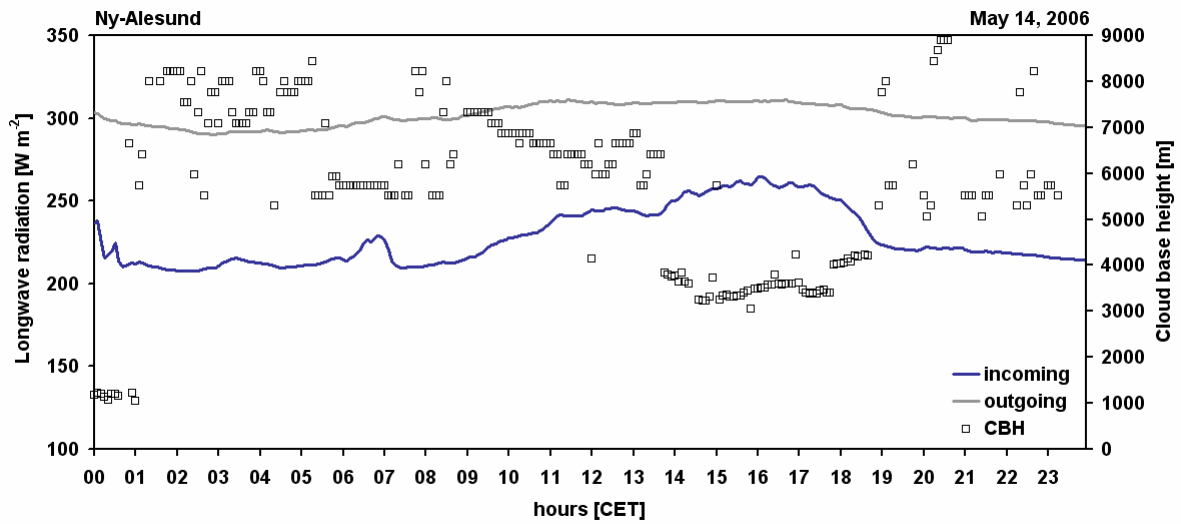
Longwave radiation

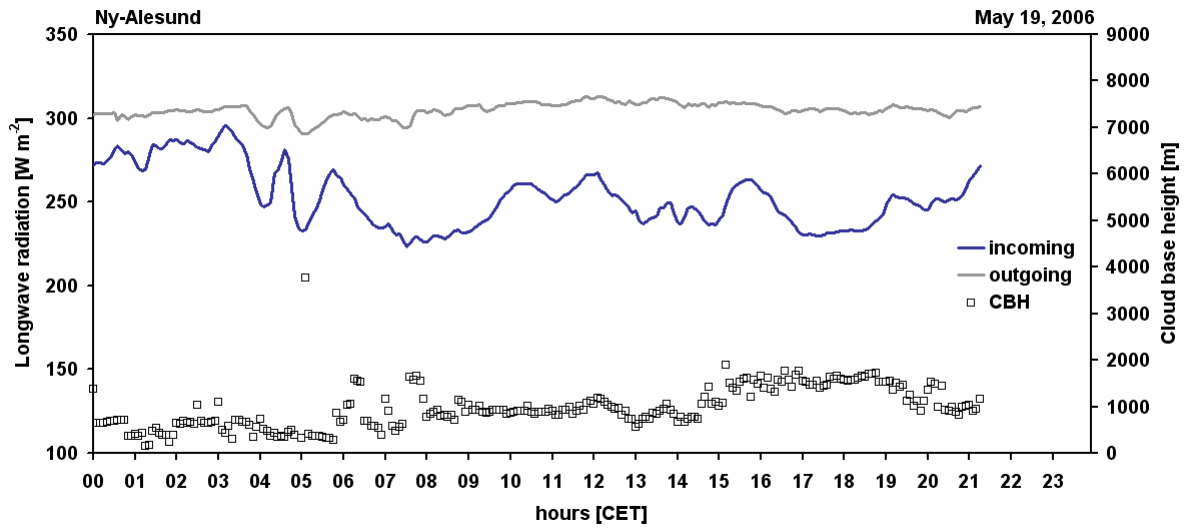
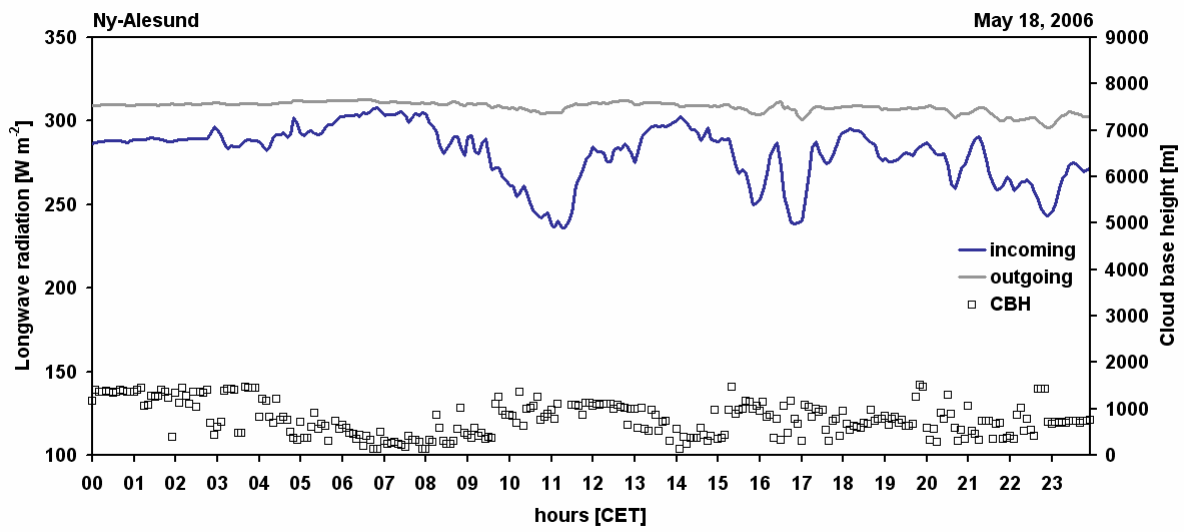
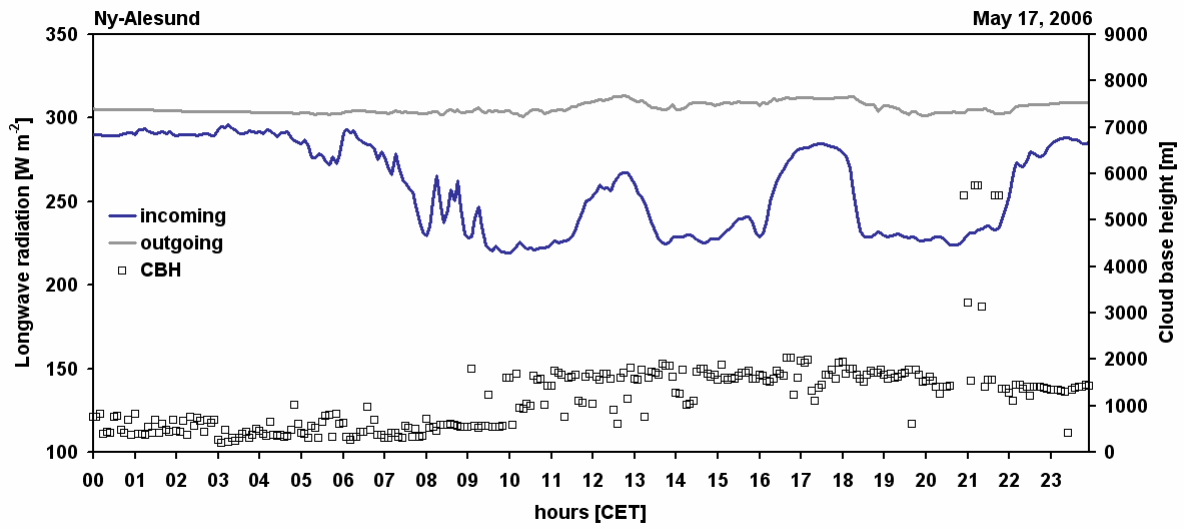
The presented recordings of the terrestrial radiation and the cloud base height are obtained by the international standardized radiation measurements of the Baseline Surface Radiation Network (BSRN) and the laser ceilometer (cloud base height) both maintained by the Alfred Wegener Institute for Polar and Marine Research. The plots show the incoming and outgoing fluxes in the longwave spectral range and the according cloud height.



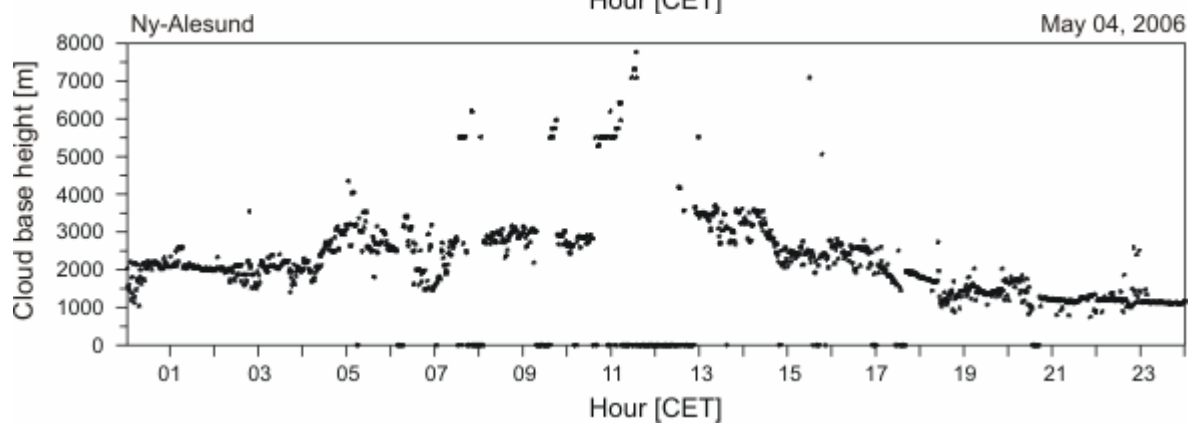
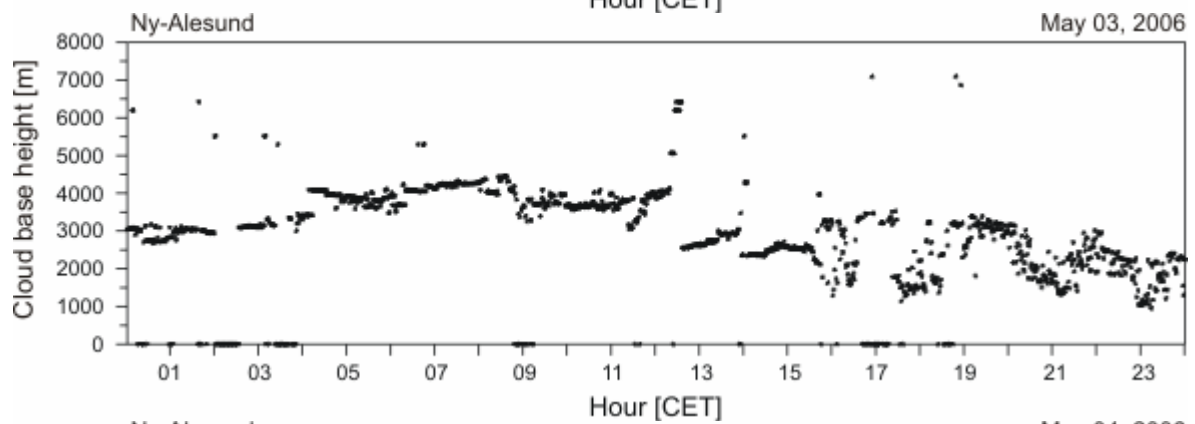
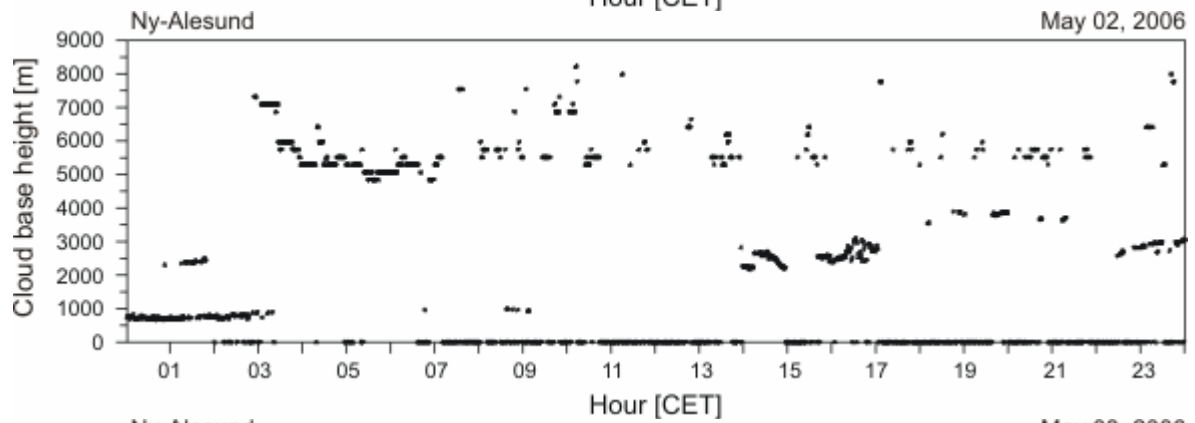
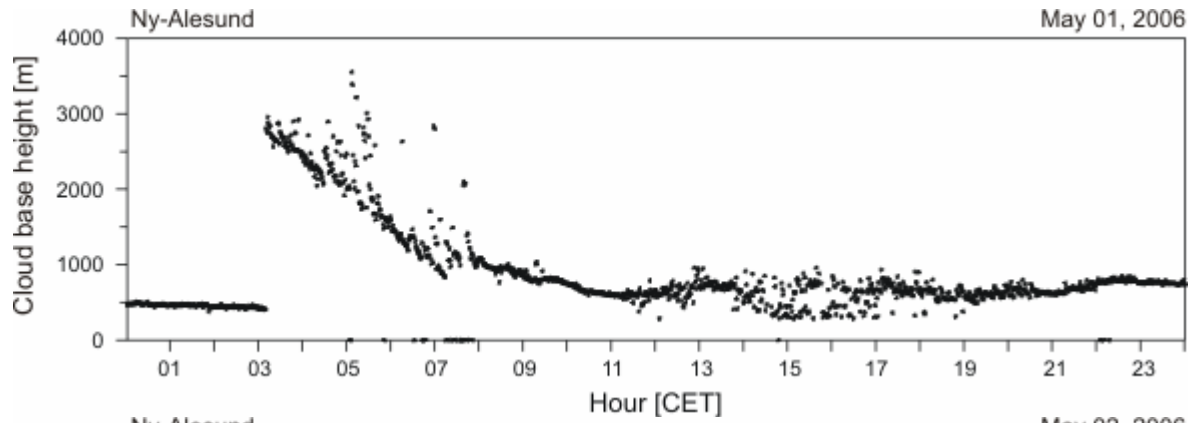


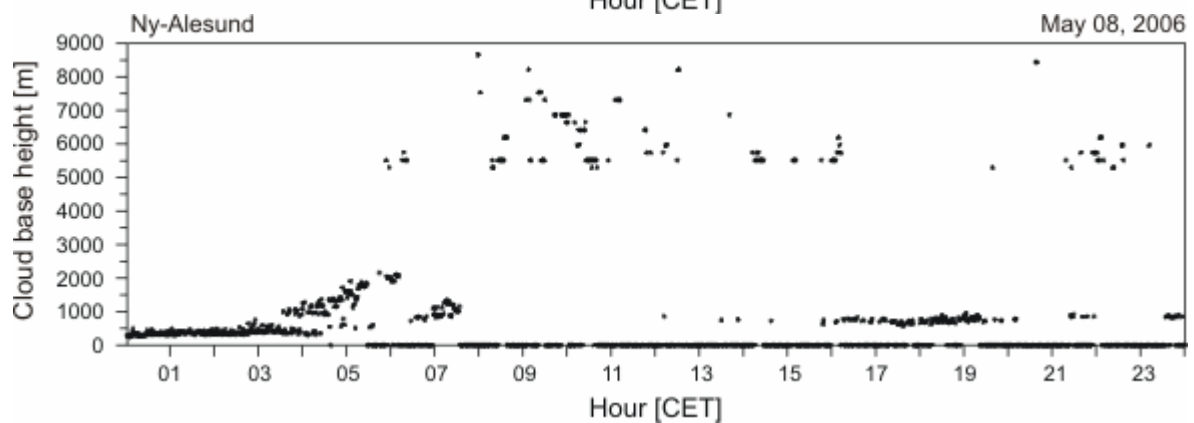
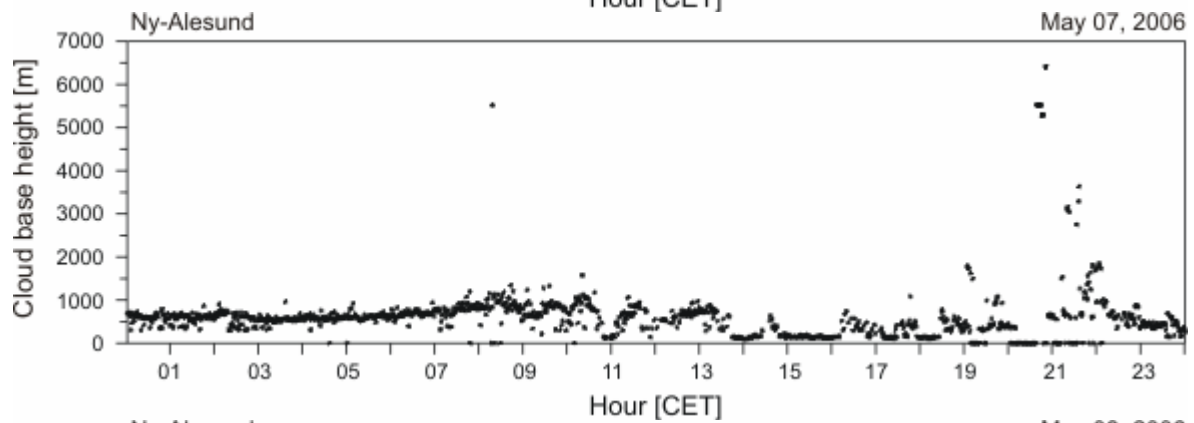
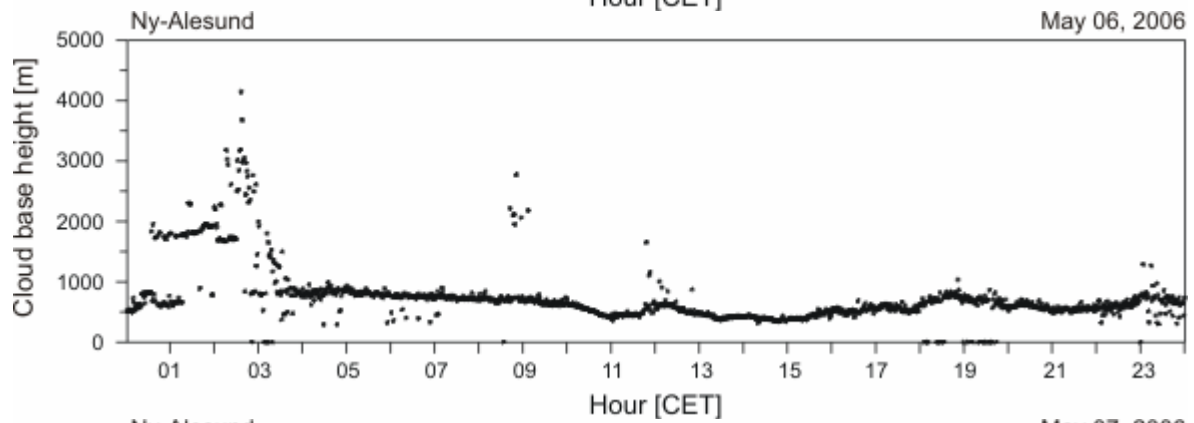
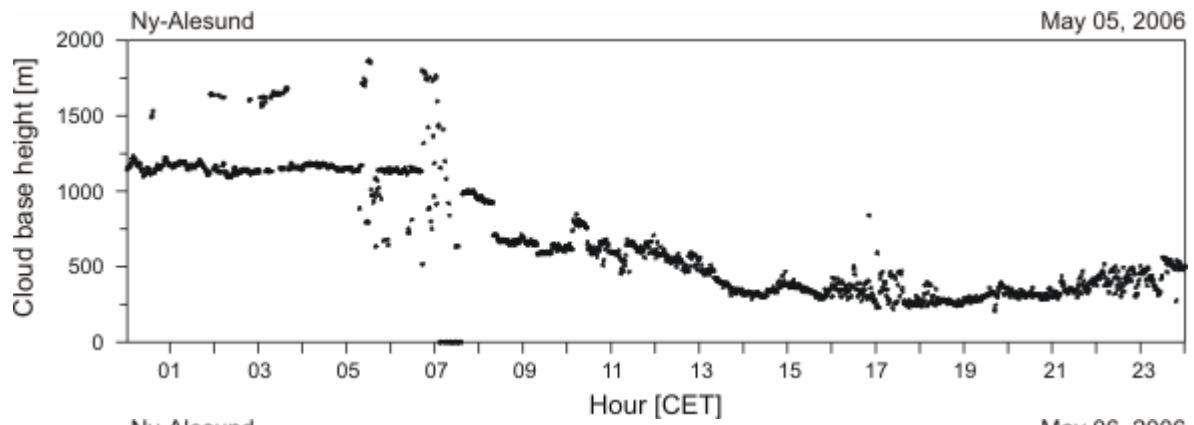


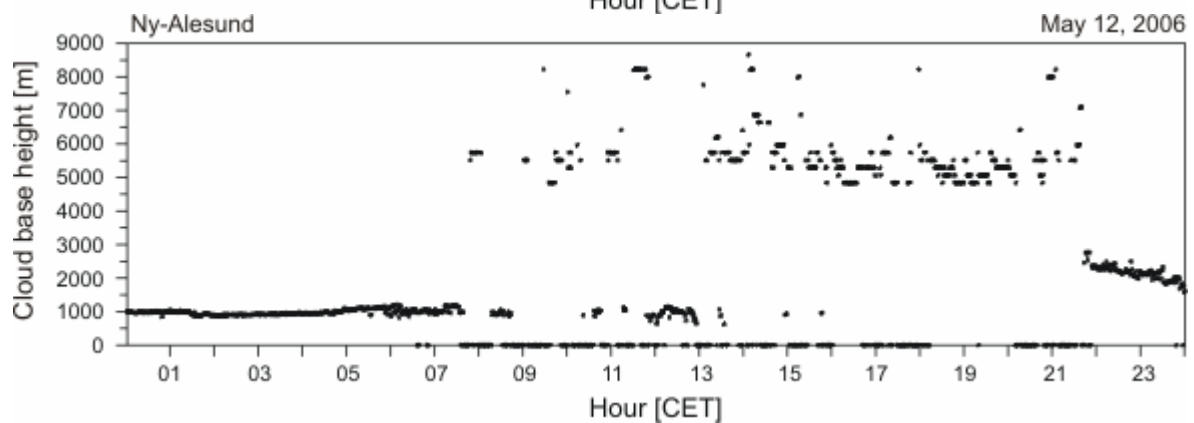
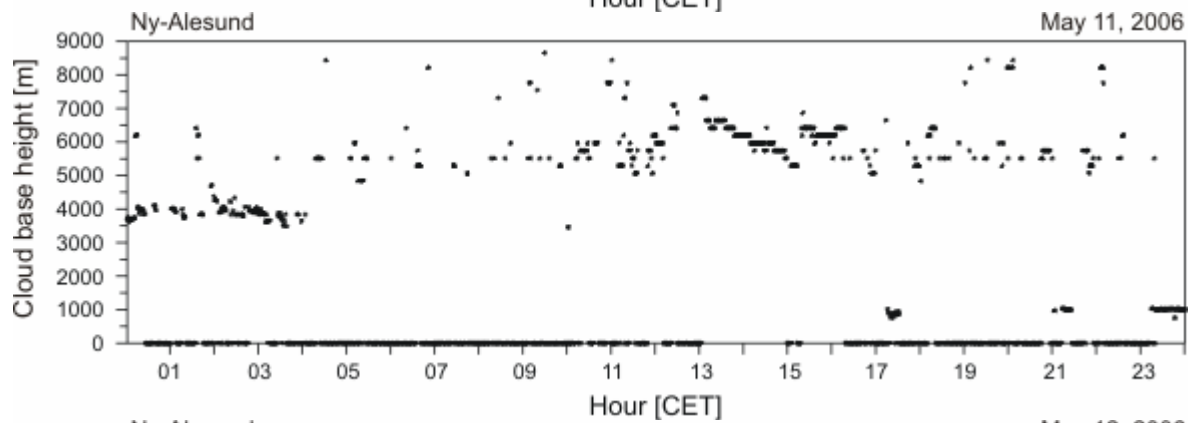
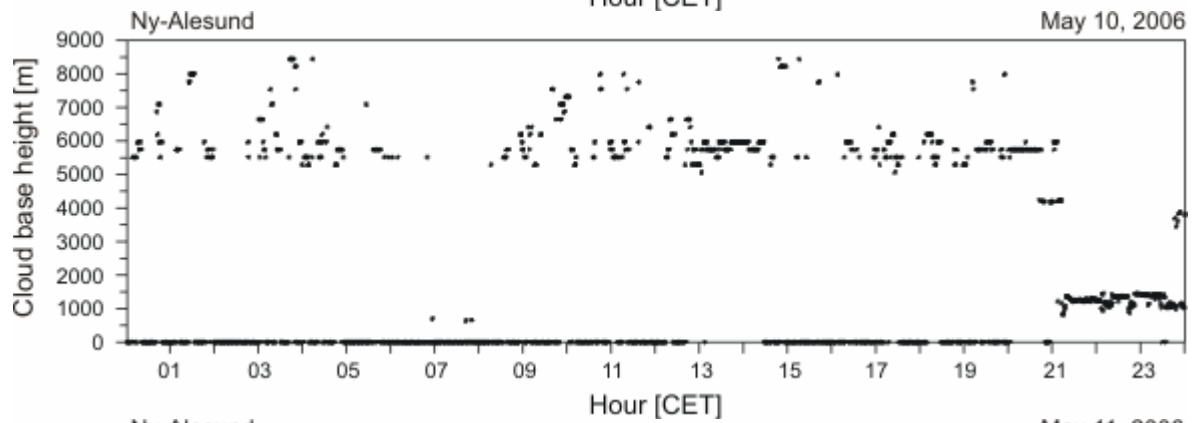
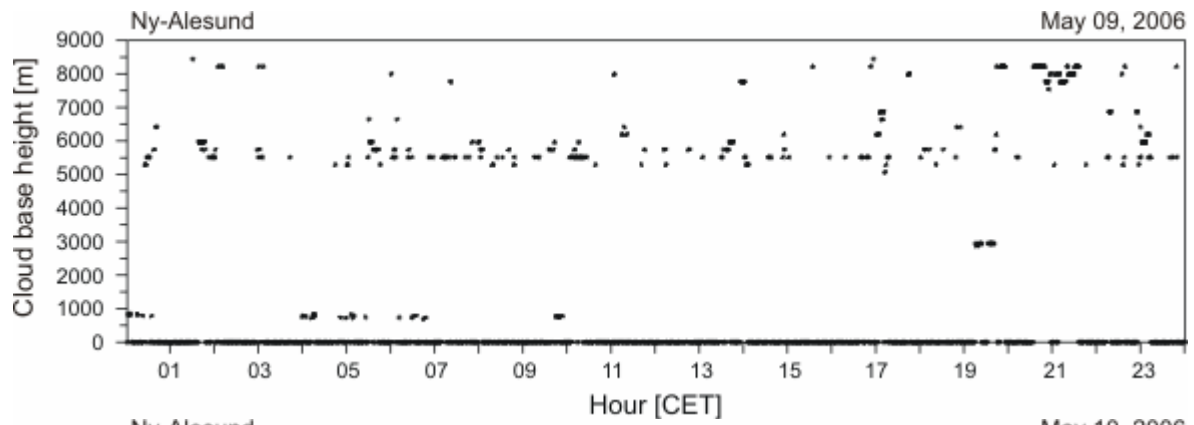


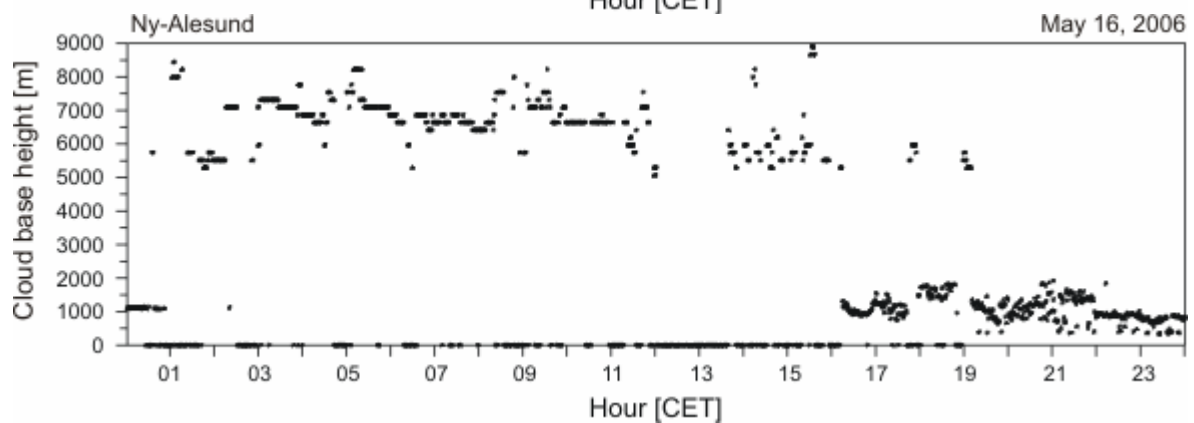
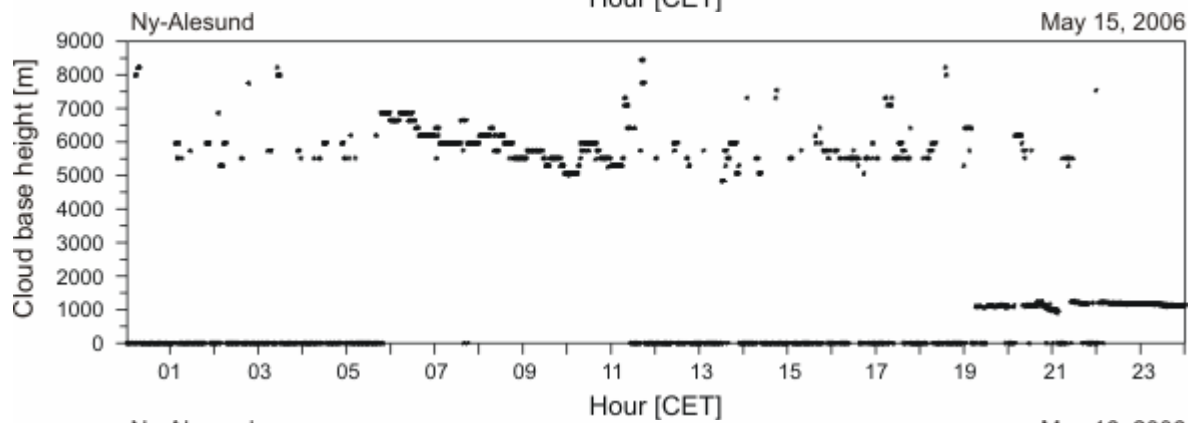
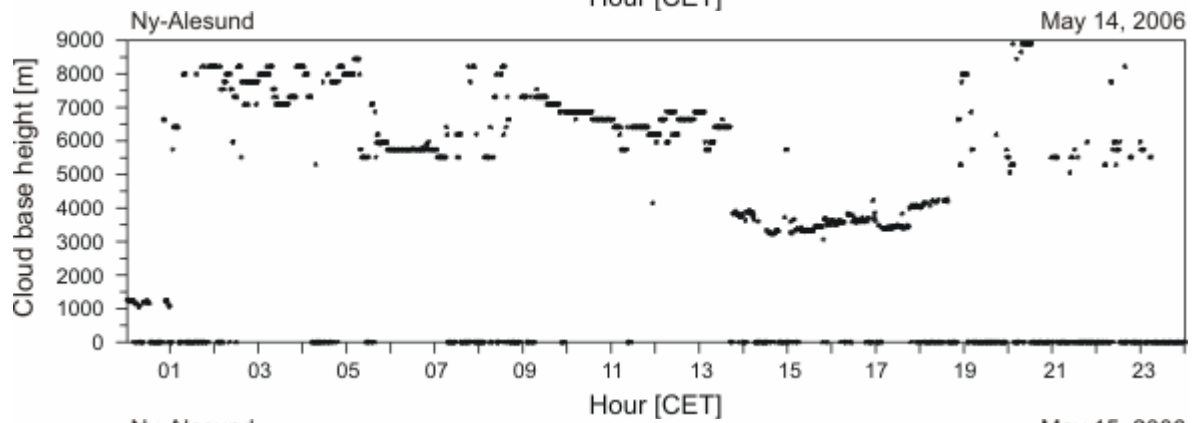
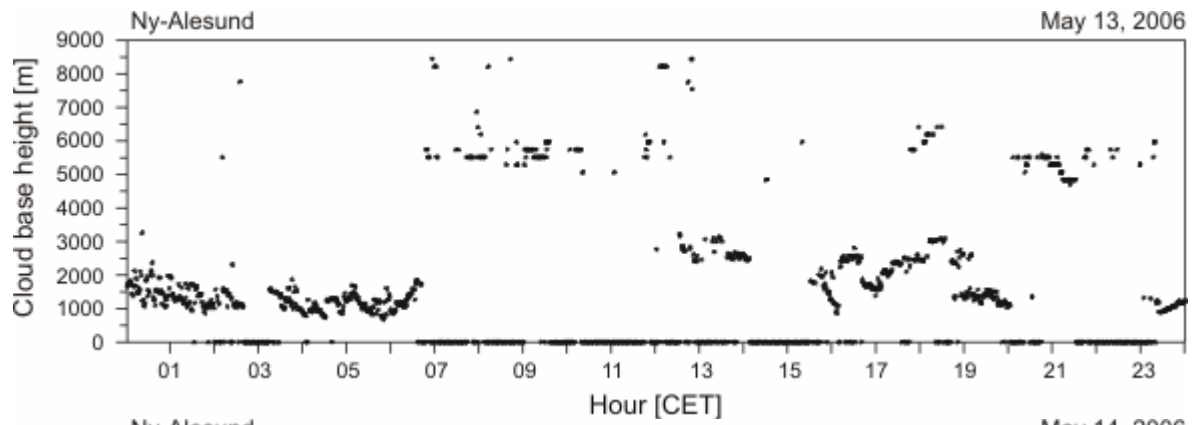


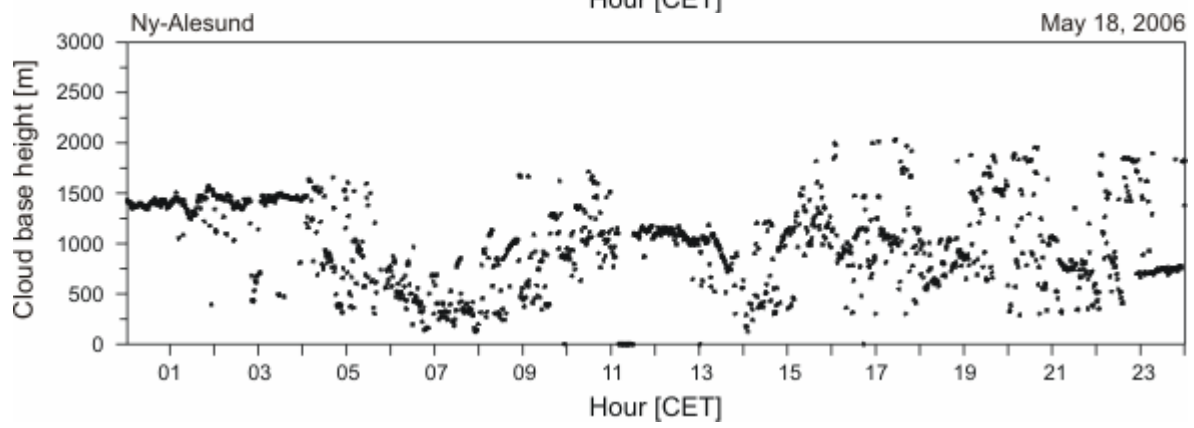
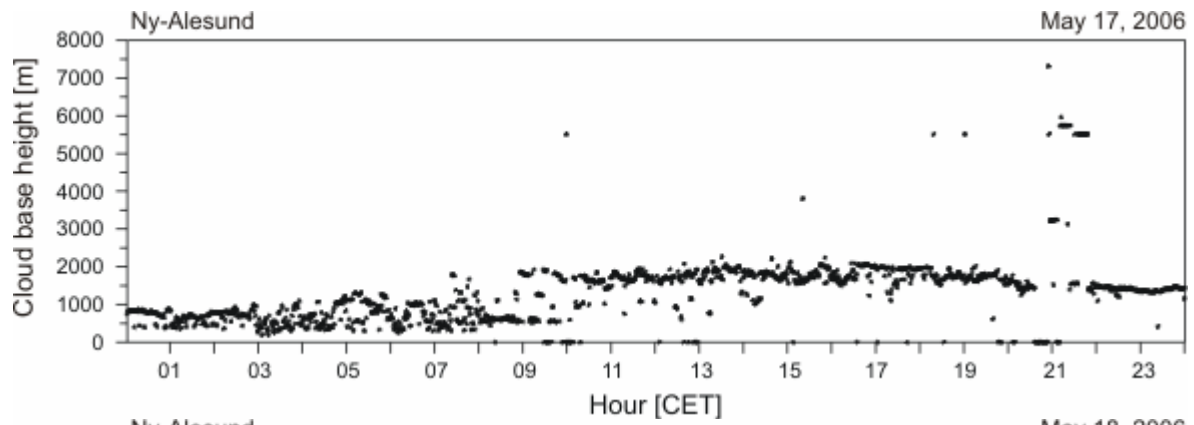
Cloud Base height in meter











5 Visualization of directly measured turbulence fluxes

5.1 Calculation of turbulent fluxes with the software package TK2

The turbulent fluxes were pre- and post-processed with the internationally standardized QA/QC software package TK2, developed by the Department of Micrometeorology, University of Bayreuth (Mauder et al., 2008; Mauder and Foken, 2004). The software package TK2 is based on 15 years of experiences. It was developed to calculate turbulent fluxes automatically for several international micrometeorological experiments since 1989. TK2 is capable of performing all of the post processing of turbulence measurements producing quality assured turbulent fluxes for a station automatically in one single run. It includes all corrections and tests, which are state of science (i.e. detection of spikes, application of Planar Fit method for coordinate transformation, determination of the time delay between sensors) and a quality assessment. The latter following a procedure proposed by Foken and Wichura (1996) and further developed by Foken et al. (2004).

Two quality tests were applied to the flux data. The Steady State test is designed to detect non steady state conditions, which are an assumption of the eddy covariance method. This test compares a 30-minute covariance with the arithmetic mean of the six 5-minute co-variances in this 30-minute interval. The agreement between both values is a measure of steady state conditions. The second test is based on the flux-variance similarity, which means that the ratio of the standard deviation of a turbulent parameter and its turbulent flux is nearly constant or a function, e.g. of the stability. These normalized standard deviations are called Integral Turbulence Characteristics (ITC). This test compares measured integral turbulence characteristics with modeled ones. The agreement between both values is a measure of well-developed turbulence. To check the sensible heat flux, models for normalized standard deviations of the vertical wind velocity w and sonic temperature T_s were applied.

Foken, T; Göckede, M; Mauder, M; Mahrt, L; Amiro, BD; Munger, JW (2004): Post-field data quality control. *in* Lee X., Massman W, Law B : Handbook of Micrometeorology: A Guide for Surface Flux Measurement and Analysis, Kluwer, Dordrecht, 181-208.

Foken, T; Wichura, B (1996): Tools for quality assessment of surface-based flux measurements. *Agric Forest Meteorology*, 78, 83-105.

Mauder, M; Foken, T (2004): Documentation and Instruction Manual of the Eddy Covariance Software Package TK2. Work report University of Bayreuth, Dept of Micrometeorology, 26, ISSN 1614-8916.

Mauder, M; Foken, T; Clement, R; Elbers, JA; Eugster, W; Grünwald, T; Heusinkveld, B; Kolle, O (2008): Quality control of CarboEurope flux data – Part 2: Inter-comparison of eddy-covariance software, *Biogeosciences*, 5, 451-462.

5.2 Entire observation period

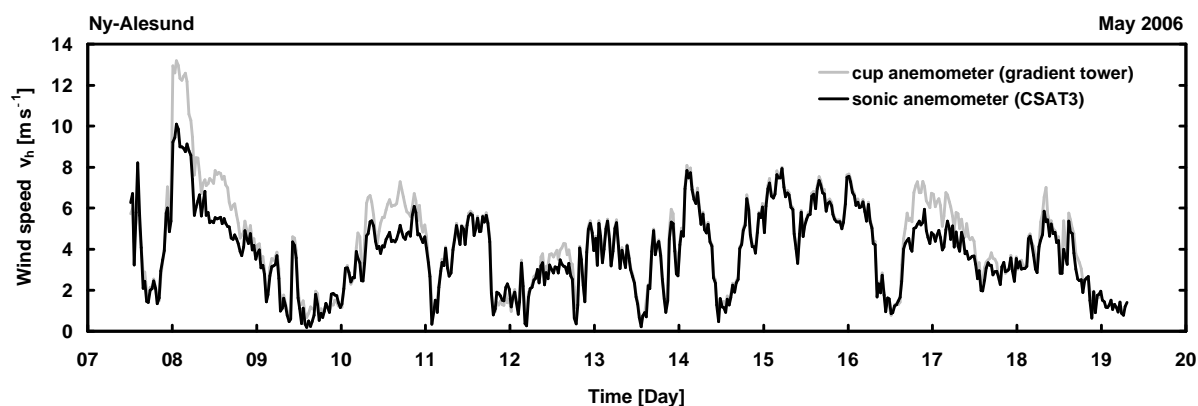


Figure 5.1: Comparison of wind speed measured with a cup anemometer in 2.4 m height above ground mounted at the gradient tower MT2 (grey line) and the CSAT3 sonic anemometer in 2.3 m a. g. of the eddy-flux measurement complex EF (black line) May 7 to May 19, 2006. Ny-Ålesund (Svalbard), ARCTEX-2006 campaign.

Figure 5.1 shows a quite well conformity between wind measurements obtained by a cup anemometer and a sonic anemometer, both mounted in app. 2.4 m height above ground and in the same vicinity at the ARCTEX-2006 monitoring area southeast of Ny-Ålesund. But some significant differences could be explained by a weak performance of the sonic measurement principle during precipitation events like on May 8 or May 17 or during a heavy, near ground drift of the fresh fallen snow, occurring on May 10.

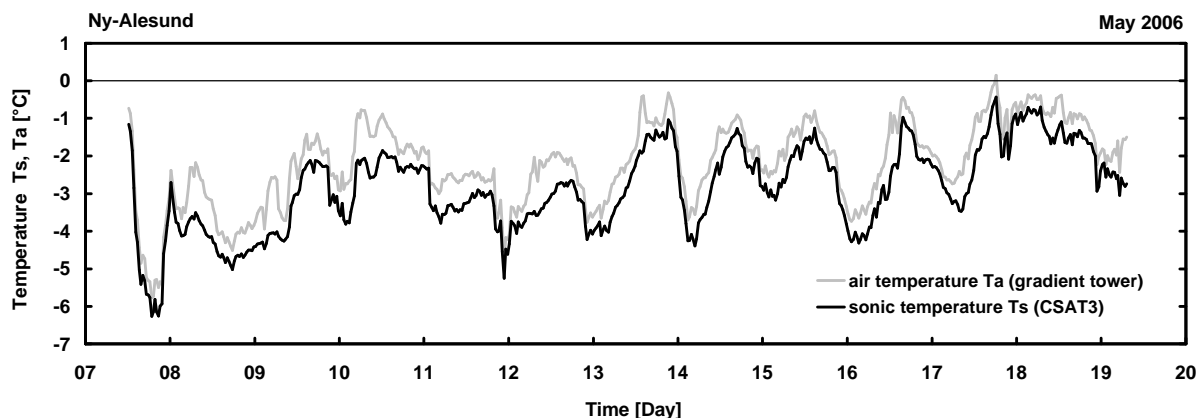


Figure 5.2: Comparison of temperature measured with a ventilated thermometer in 2.4 m height above ground mounted at the gradient tower MT2 (air temperature T_a , grey line) and the CSAT3 sonic anemometer in 2.3 m a. g. of the eddy-flux measurement complex EF (sonic temperature T_s , black line) May 7 to May 19, 2006. Ny-Ålesund (Svalbard), ARCTEX-2006 campaign.

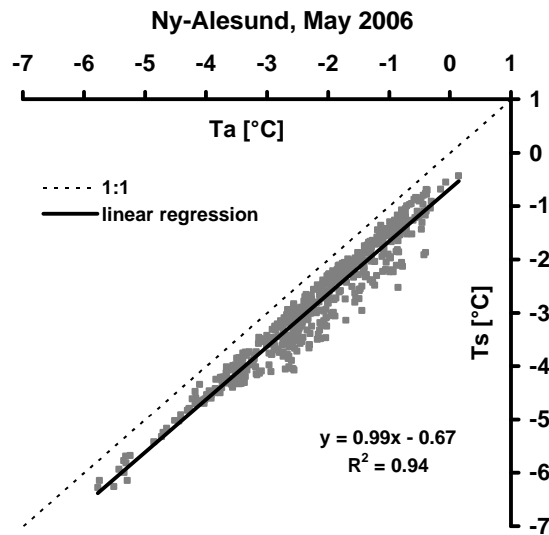


Figure 5.3: Correlation between temperature measured with a ventilated thermometer in 2.4 m height above ground mounted at the gradient tower MT2 (air temperature T_a) and measured with the CSAT3 sonic anemometer in 2.3 m a. g. of the eddy-flux measurement complex EF (sonic temperature T_s), based on data from May 7 to May 19, 2006. Ny-Ålesund (Svalbard), ARCTEX-2006 campaign.

The comparison between air temperature and sonic temperature (Figure 5.2 and Figure 5.3) gives an example that the CSAT3 shows no dependence on the reference temperature. The relation between air temperature and the temperature derived from the sonic speed of the CSAT3 is close to 1:1 with a slight, more or less constant offset of a little bit more than half a degree K. This is in total agreement with results found by Mauder et al. (2007).

The influence of the dependency of the sonic speed regarding air density or amount of water vapor respectively is relatively small due to the observed low absolute humidity between 2 g m^{-3} and 4 g m^{-3} (Figure 5.4) during the whole ARCTEX-2006 campaign. Accordingly, the effect of the correction of the covariance of the vertical wind component and the sonic temperature (buoyancy flux Q_{HB}) to obtain the proper sensible heat flux (Q_H) as recommended by Schotanus et al. (1983) and Liu et al. (2001) is very limited.

Liu, H; Peters, G; Foken, T (2001): New equations for sonic temperature variance and buoyancy heat flux with an omnidirectional sonic anemometer. *Boundary-Layer Meteorology*, 100: 459-468.

Mauder, M; Oncley, SP; Vogt, R; Weidinger, T; Riberio, L; Bernhofer, C; Foken, T; Kohsiek, W; DeBruin, H; Liu, H (2007): The Energy Balance Experiment EBEX-2000. Part II: Intercomparison of eddy covariance sensors and post-field data processing methods; *Boundary-Layer Meteorology*, 123, 29-54.

Schotanus, P; Nieuwstadt, F.T.M; De Bruin, H.A.R (1983): Temperature Measurement with a Sonic Anemometer and its Application to Heat and Moisture Fluctuations; *Boundary-Layer Meteorology*, 26, 81-93.

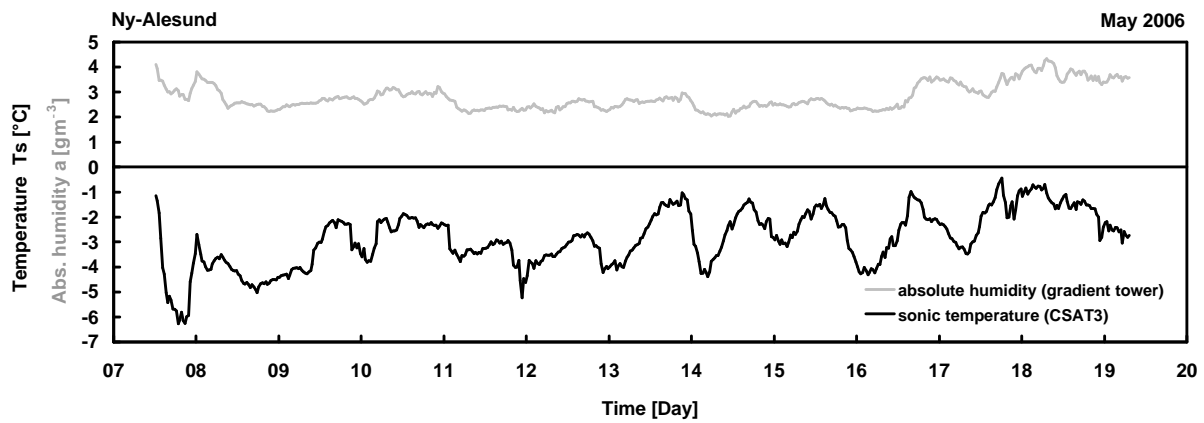


Figure 5.4: Absolute air humidity a (grey line) derived from measurements of relative humidity (gradient tower MT1) at 1.85 m above ground (snow) and the sonic temperature T_s (black line) derived from the CSAT3 sonic anemometer in 2.3 m a. g. of the eddy-flux measurement complex EF. Ny-Ålesund (Svalbard), ARCTEX-2006 campaign.

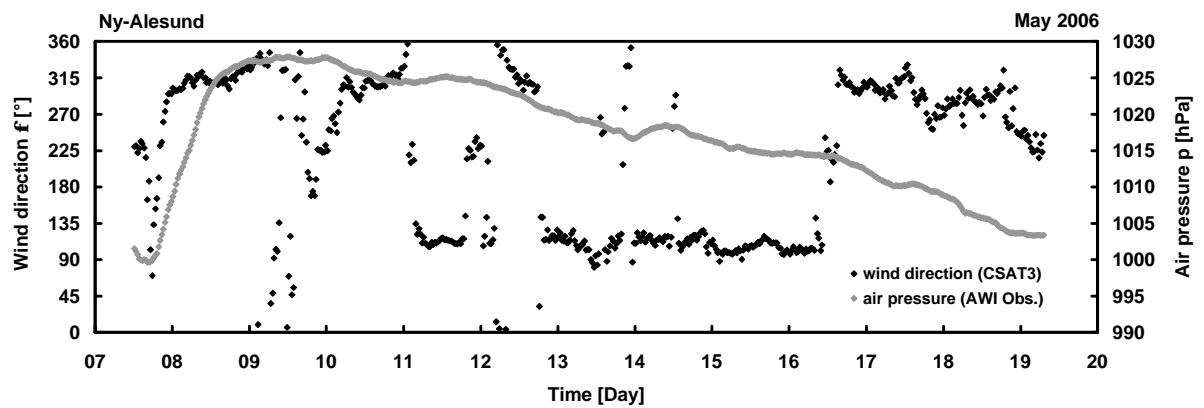


Figure 5.5: Surface air pressure p (grey dots) measured at the AWI-Meteorological Observatory and the wind direction in degree ϕ (black dots) derived from the CSAT3 sonic anemometer in 2.3 m a. g. of the eddy-flux measurement complex EF. Ny-Ålesund (Svalbard), ARCTEX-2006 campaign.

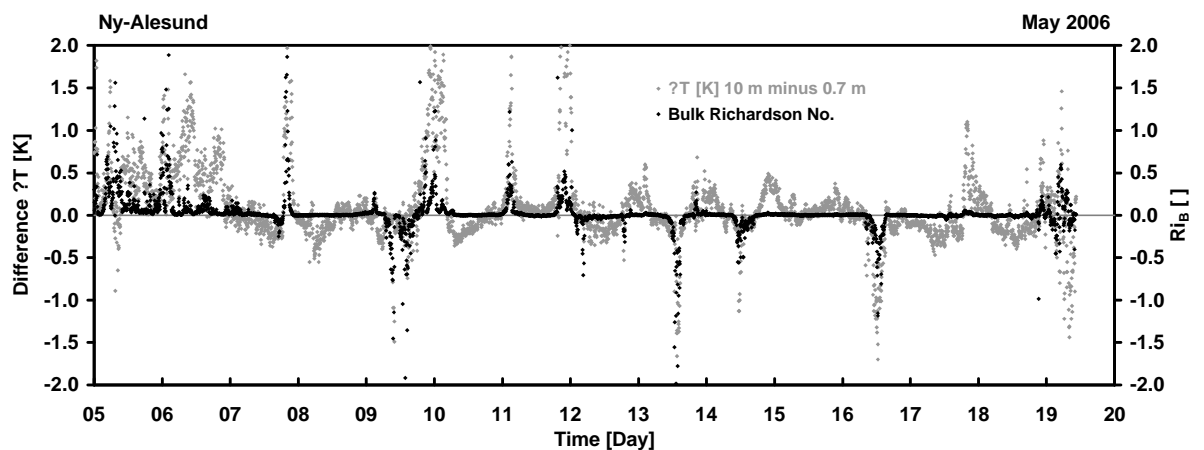


Figure 5.6: Comparison of the vertical gradient of air temperature ΔT obtained by ventilated thermometers mounted at 10 m and 0.7 m above ground (snow) and the bulk Richardson number Ri_B . For calculation of Ri_B the from the outgoing longwave radiation measurement (BSRN-station) deduced ground surface temperature and the wind velocity at 10 m height (gradient tower MT1) were used. Ny-Ålesund (Svalbard), ARCTEX-2006 campaign.

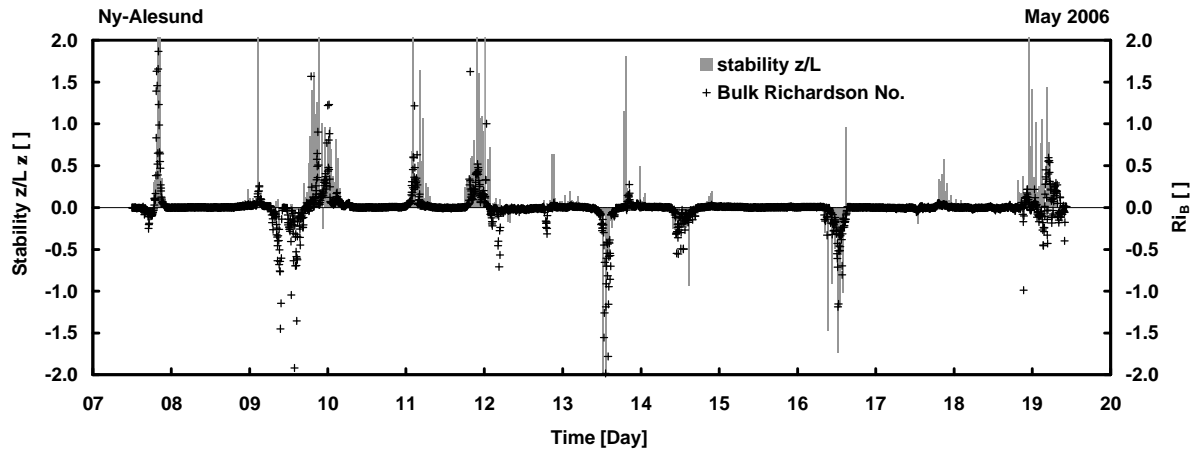


Figure 5.7: Comparison of the atmospheric stability parameter ζ (z/L) whereas L is the Obukhov-length and z is the measurement height (2.4 m), obtained by the eddy covariance complex EF and the independently determined bulk Richardson number Ri_B . For calculation of Ri_B the from the outgoing longwave radiation measurement (BSRN-station) deduced ground surface temperature and the wind velocity at 10 m height (gradient tower MT1) were used. Ny-Ålesund (Svalbard), ARCTEX-2006 campaign.

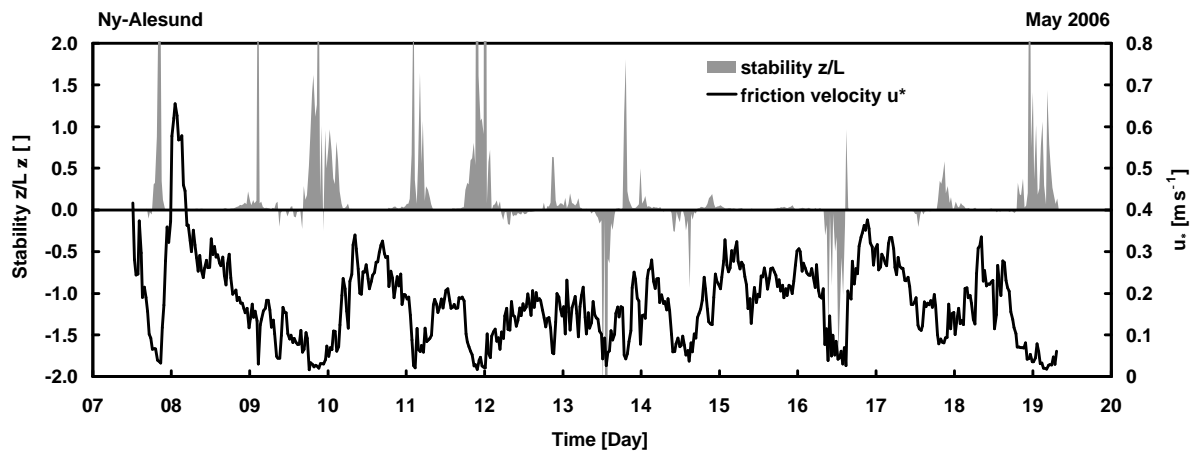


Figure 5.8: Comparison of the atmospheric stability parameter ζ (z/L), whereas L is the Obukhov-length and z is the measurement height (2.4 m), and the friction velocity u_* , both obtained by the eddy covariance complex EF. Ny-Ålesund (Svalbard), ARCTEX-2006 campaign.

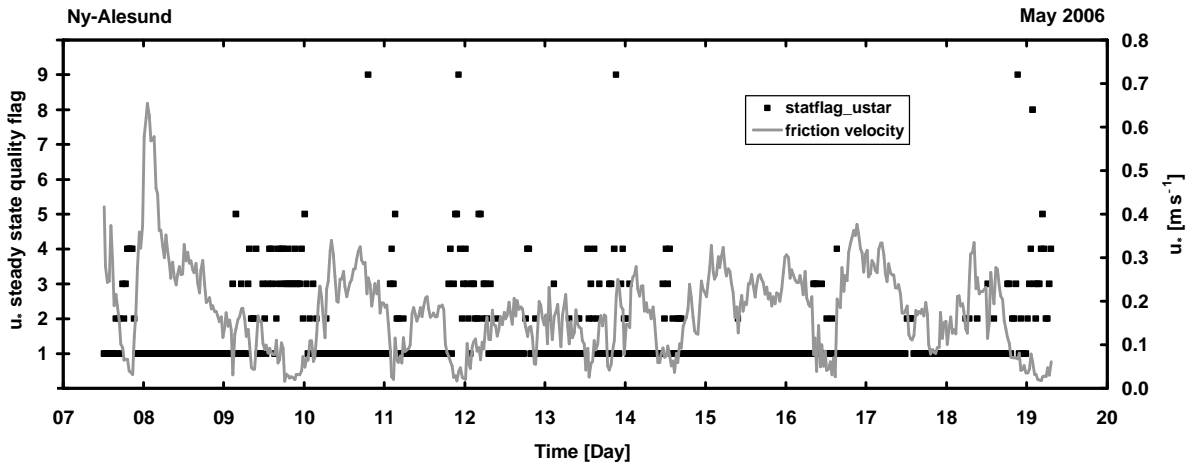


Figure 5.9: Friction velocity u_* (at 2.4 m above ground) obtained by the eddy covariance complex EF and the related quality flags of the Steady State test (Foken & Wichura, 1996; TK2-software) of the covariance of the fluctuations of the horizontal (u' , v') and vertical (w') wind components (statflag_ustar). The classes 1 to 3 are good quality, the classes 4 to 6 are usable quality, class 7 and 8 are only for orientation, 9 has to be neglected, May 7 to May 19, 2006. Ny-Ålesund (Svalbard), ARCTEX-2006 campaign.

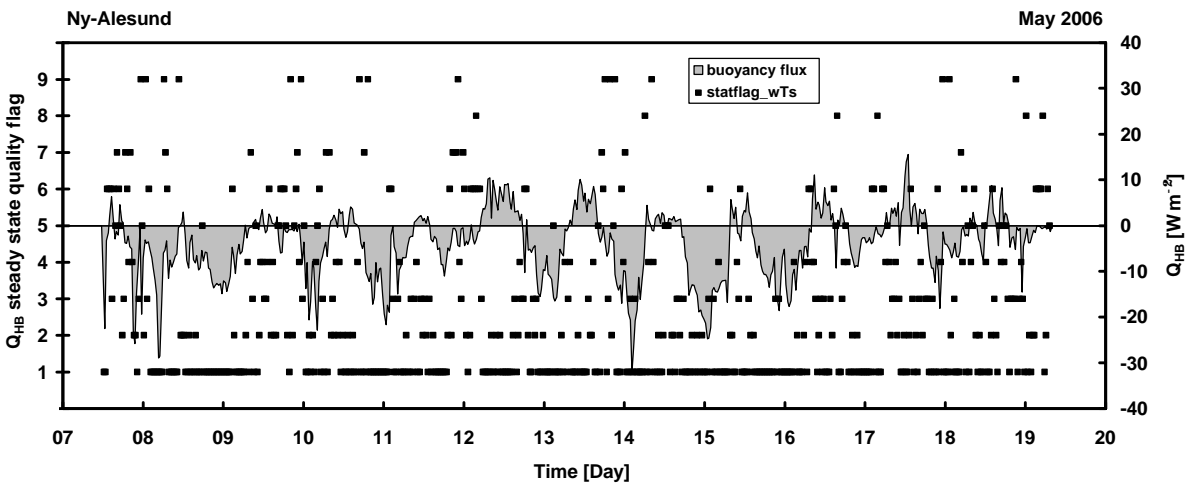


Figure 5.10: Buoyancy flux Q_{HB} (due to the very low water vapor content during May 2006 equatable to the real sensible heat flux Q_H) at 2.4 m above ground obtained by the eddy covariance complex EF and the related quality flags of the Steady State test (Foken & Wichura, 1996; TK2-software) of the covariance of the fluctuations of the sonic temperature (T_s') and vertical (w') wind component (statflag_wTs). The classes 1 to 3 are good quality, the classes 4 to 6 are usable quality, class 7 and 8 are only for orientation, 9 has to be neglected, May 7 to May 19, 2006. Ny-Ålesund (Svalbard), ARCTEX-2006 campaign.

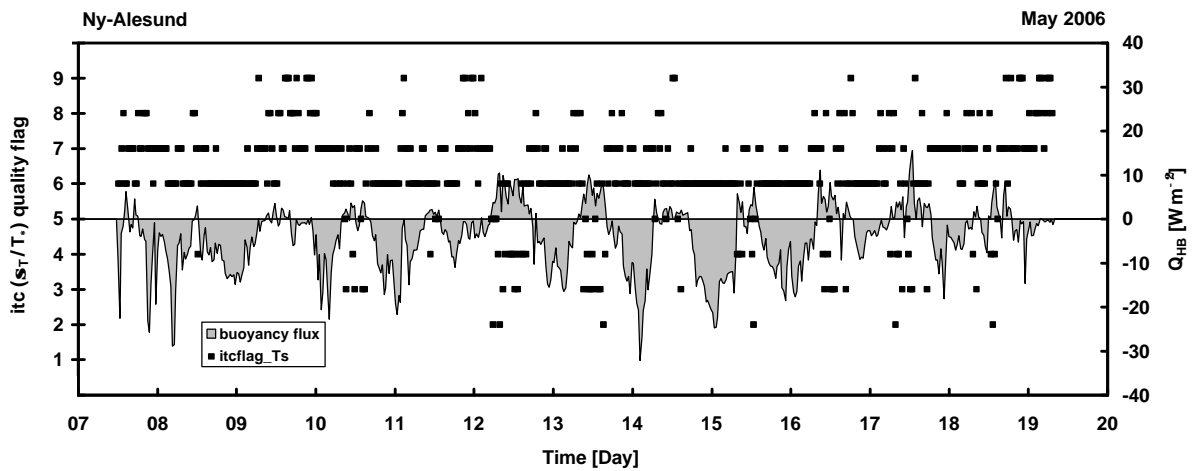


Figure 5.11: Buoyancy flux Q_{HB} (due to the very low water vapor content during May 2006 equatable to the real sensible heat flux Q_H) at 2.4 m above ground obtained by the eddy covariance complex EF and the related quality flags of the Integral Turbulence Characteristic test (ITC-test, Foken & Wichura, 1996; TK2-software) of the standard deviation (σ_{T_s}) normalized by its dynamical parameter T_* (itcflag_Ts). The classes 1 to 3 are good quality, the classes 4 to 6 are usable quality, class 7 and 8 are only for orientation, 9 has to be neglected, May 7 to May 19, 2006. Ny-Ålesund (Svalbard), ARCTEX-2006 campaign.

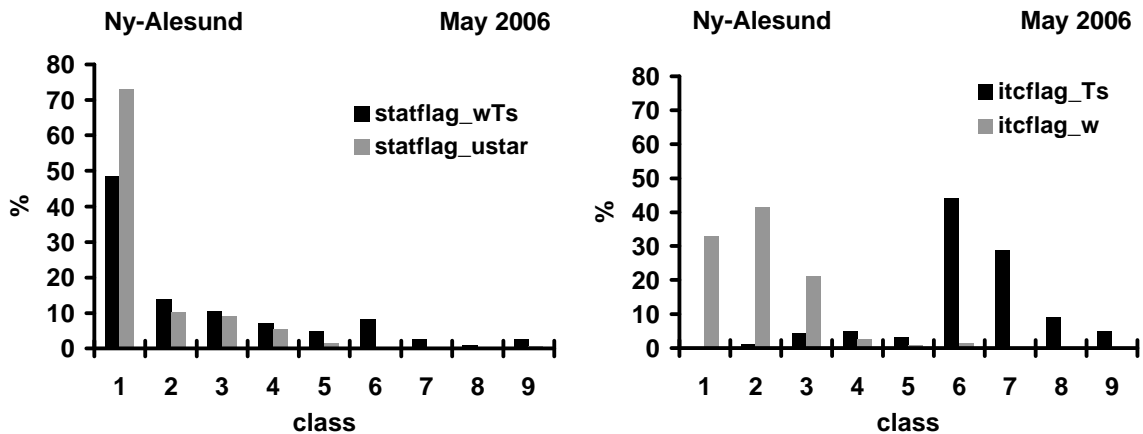


Figure 5.12: Quality control using the quality flag system after Foken & Wichura (1996) by applying the TK2-software. Left: Steady State test of the covariance of the fluctuations of a) the horizontal wind components (u' , v') and b) the sonic temperature (T_s') and the vertical (w') wind component (statflag_ustar and statflag_wTs). Right: Integral Turbulence Characteristic test (ITC-test) of the standard deviations (σ_w and σ_{T_s}) normalized by their dynamical parameters u_* and T_* (itcflag_w and itcflag_Ts). The classes 1 to 3 are good quality, the classes 4 to 6 are usable quality, class 7 and 8 are only for orientation, 9 has to be neglected, May 7 to May 19, 2006. Ny-Ålesund (Svalbard), ARCTEX-2006 campaign.

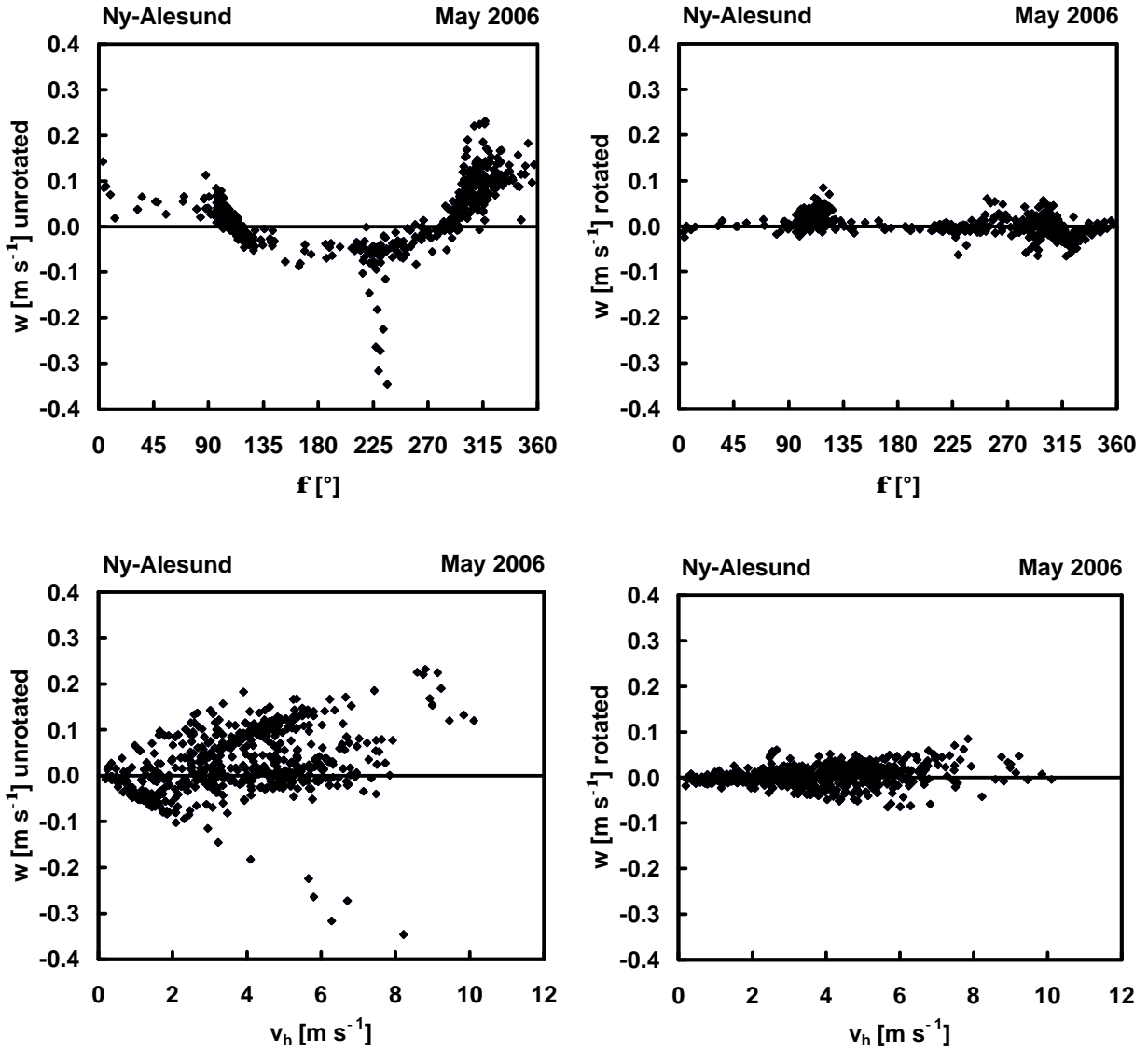


Figure 5.13: Quality control of the turbulent fluxes obtained by the eddy covariance complex EF applying the Planar Fit coordinate rotation method after Wilczak et al. (2001) ideally resulting in a w -value of zero averaged over the whole data set May 7 to May 18, 2006. The plots show the correction effect (left with unrotated, right with rotated coordinate matrix) regarding the vertical wind component w in relation to the according wind direction ϕ (above) and regarding the vertical wind component w in relation to the according horizontal wind speed v_h (below). Ny-Ålesund (Svalbard), ARCTEX-2006 campaign.

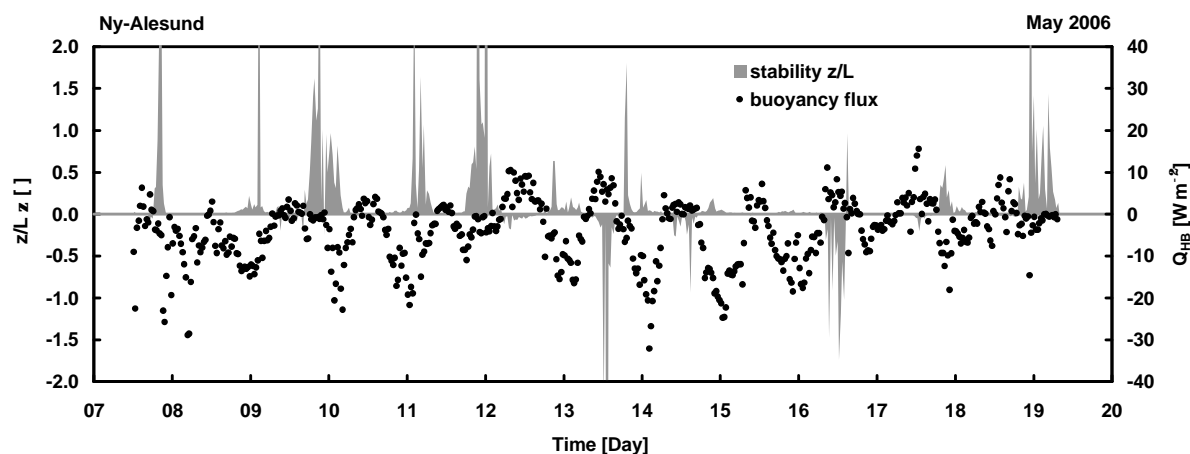


Figure 5.14: Buoyancy flux Q_{HB} (due to the very low water vapor content during May 2006 equatable to the real sensible heat flux Q_H) at 2.4 m above ground (black dots) and the related atmospheric stability parameter ζ (z/L), whereas L is the Obukhov-length and z is the measurement height (2.4 m), both obtained by the eddy covariance complex EF. Ny-Ålesund (Svalbard), ARCTEX-2006 campaign.

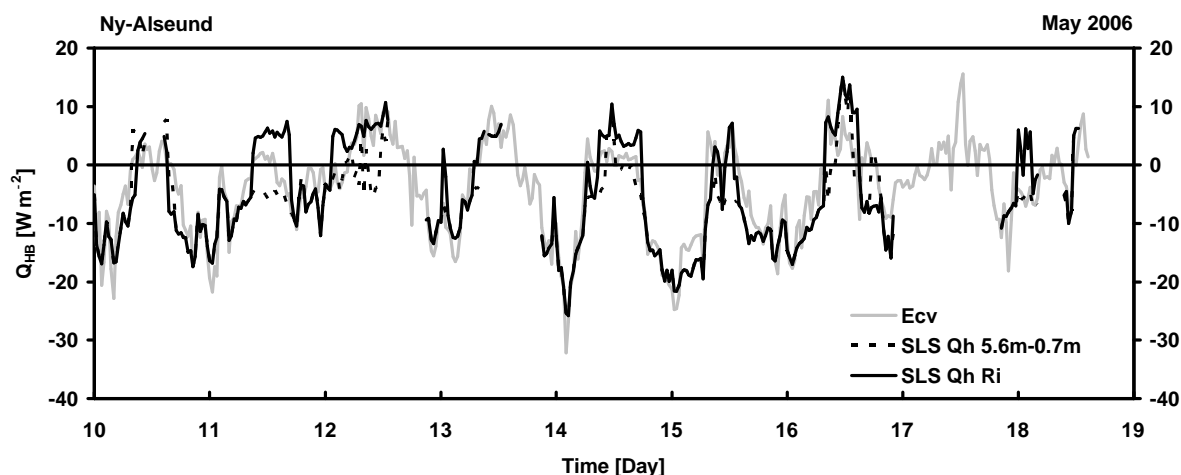


Figure 5.15: Comparison of the sensible heat flux obtained by two independent measurement systems during May 7 and May 19, 2006, nearby Ny-Ålesund (Svalbard). The grey line (Ecv) indicates the sensible heat flux Q_H at 2.4 m above ground obtained by the eddy covariance complex EF using a Campbell CAST3. The solid and dotted black lines indicate the sensible heat flux along a 104 m long laser scintillometer pathway (Scintec SLS-20) 1.5 m above ground covering the same fetch as the sonic-anemometer. For the solid line (SLS Q_H Ri) the bulk Richardson number was used and for the dotted line (SLS Q_H 5.6m–0.7m) the vertical gradient of air temperature between 5.6 m and 0.7 m was used to decide the appropriate flux directions. To calculate the Ri-Number and the temperature gradient the data of both gradient towers MT1 and MT2 were used. Ny-Ålesund (Svalbard), ARCTEX-2006 campaign.

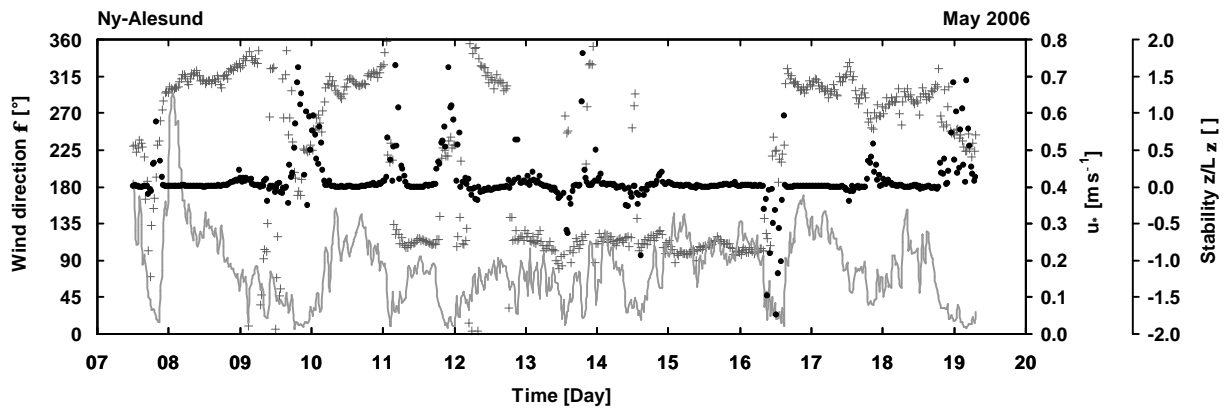


Figure 5.16: Recorded wind direction ϕ (crosses) and the friction velocity u_* (grey line), and the related atmospheric stability parameter ζ (z/L , black dots, pos. values = stable, neg. values = unstable), whereas L is the Obukhov-length and z is the measurement height (2.4 m), all obtained by the eddy covariance complex EF, May 7 to May 19, 2006. Ny-Ålesund (Svalbard), ARCTEX-2006 campaign.

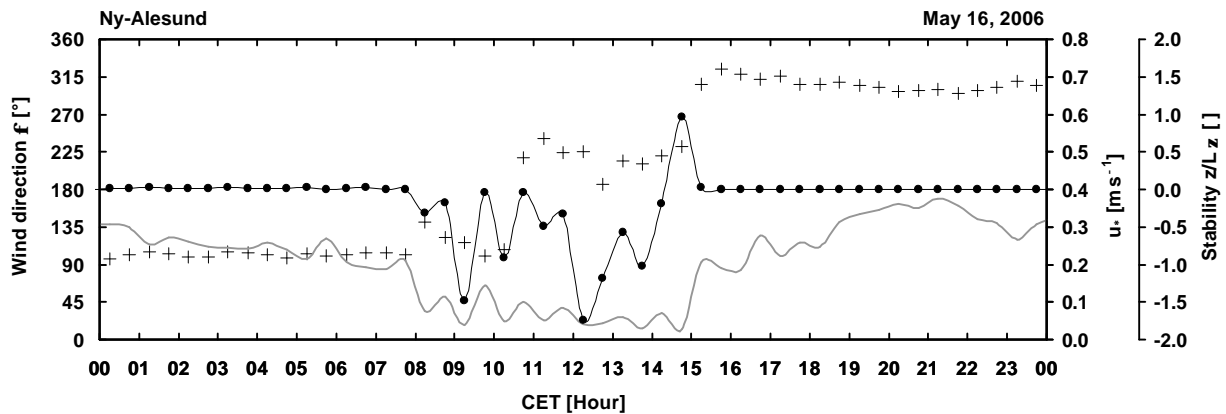


Figure 5.17: Recorded wind direction ϕ (crosses) and the friction velocity u_* (grey line), and the related atmospheric stability parameter ζ (z/L , black dots, pos. values = stable, neg. values = unstable), whereas L is the Obukhov-length and z is the measurement height (2.4 m), all obtained by the eddy covariance complex EF, selected day May 16, 2006. Ny-Ålesund (Svalbard), ARCTEX-2006 campaign.

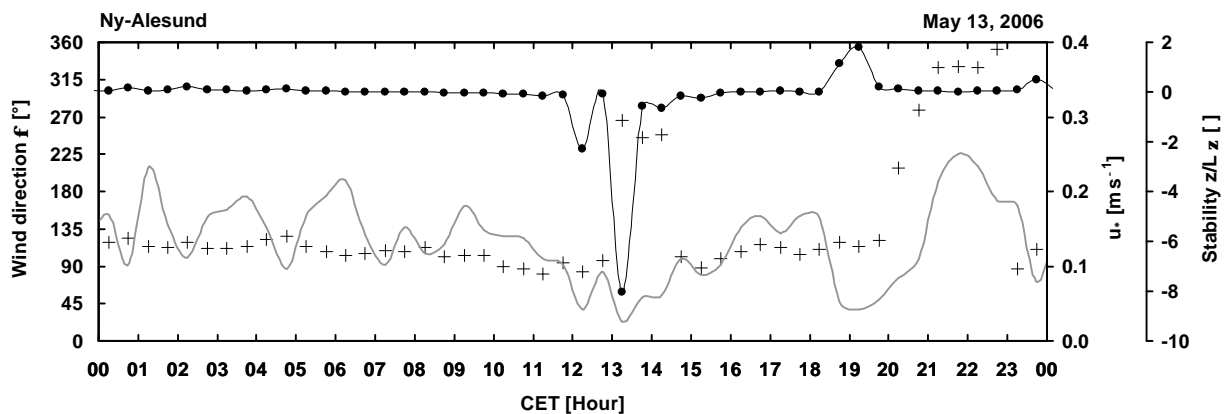
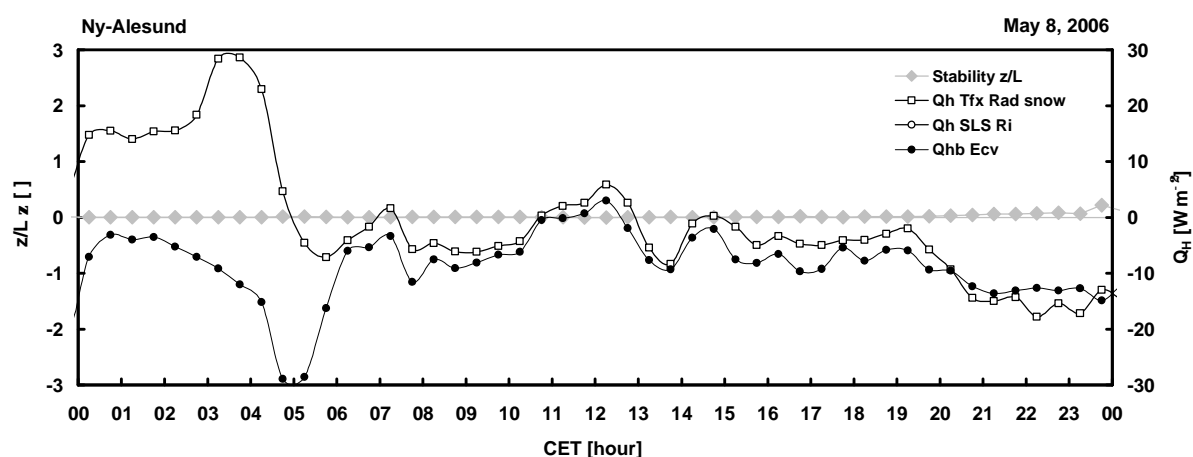
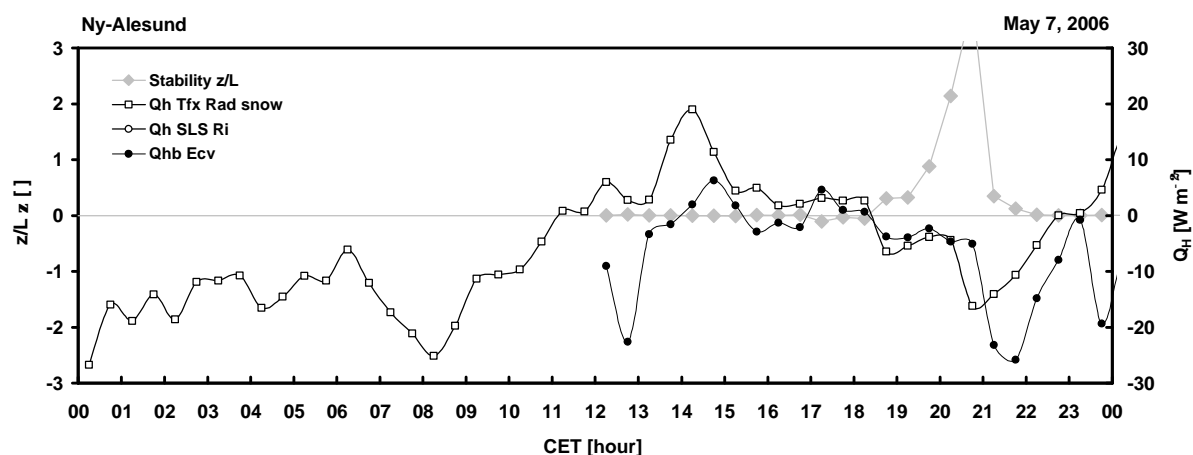
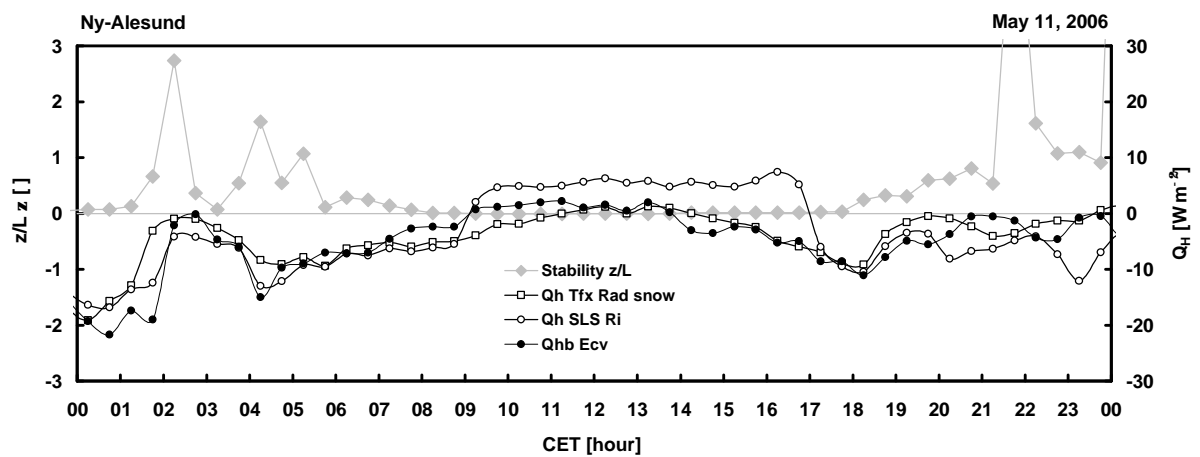
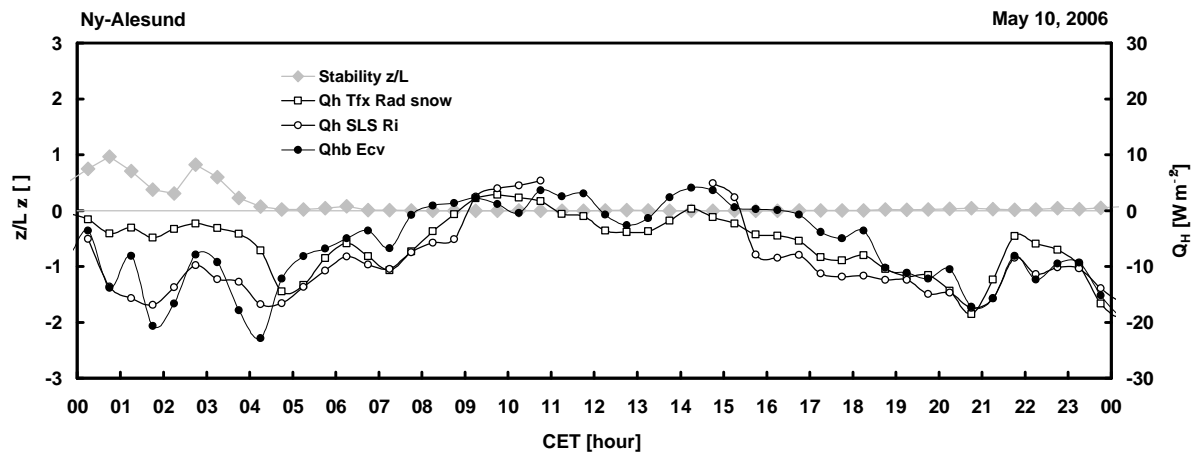
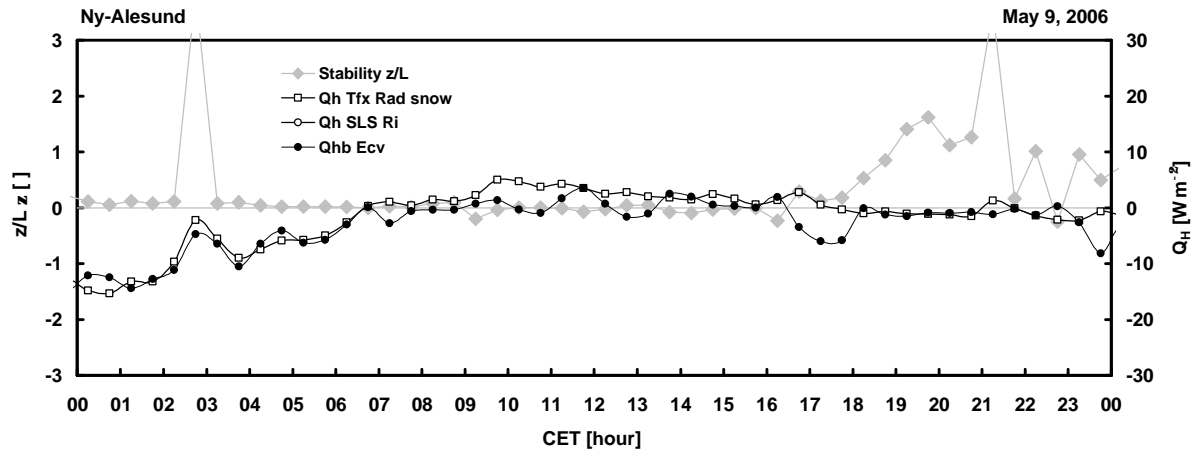


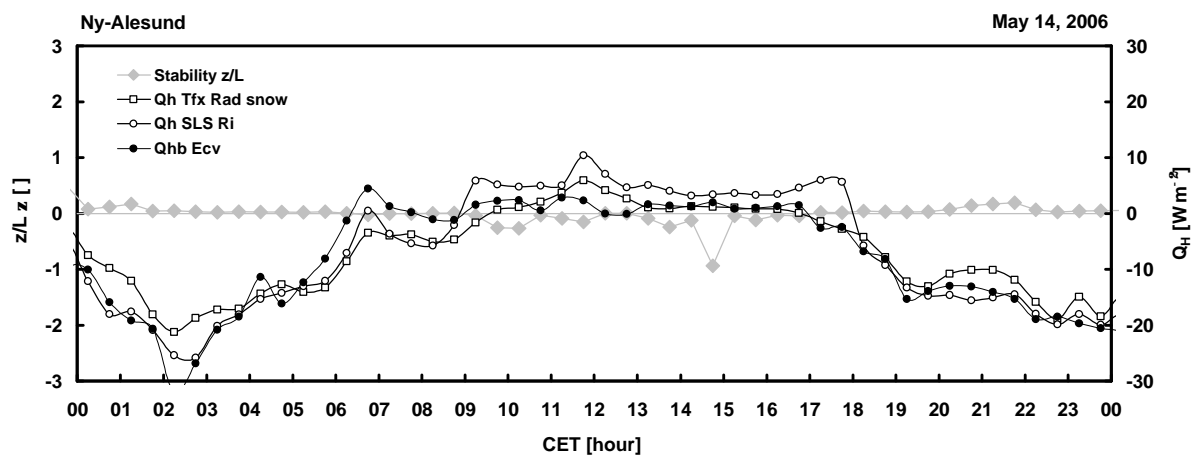
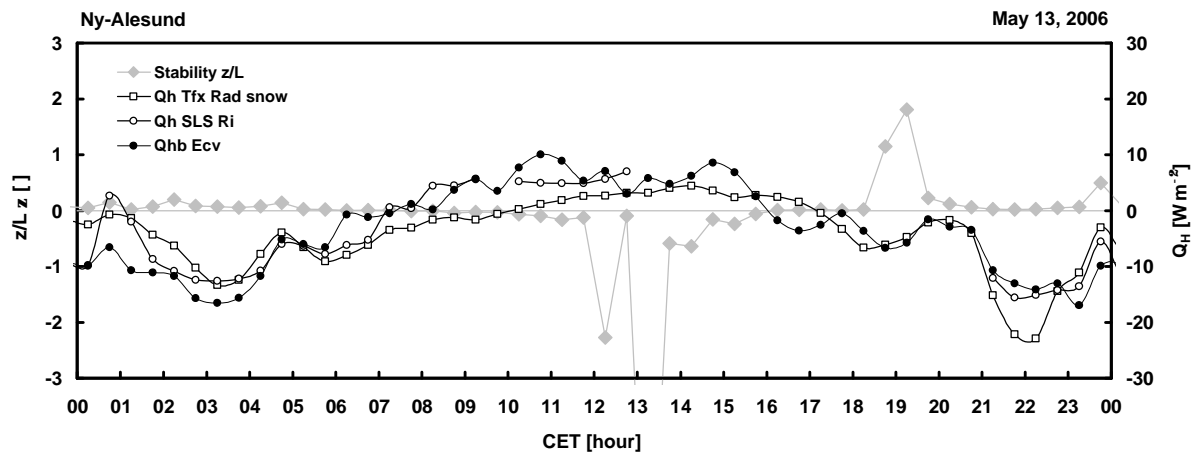
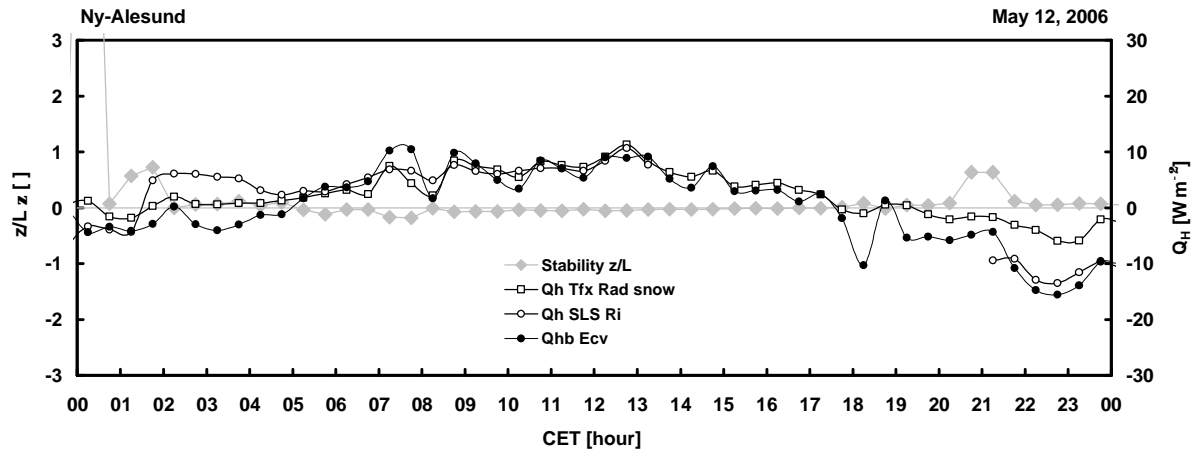
Figure 5.18: Recorded wind direction ϕ (crosses) and the friction velocity u_* (grey line), and the related atmospheric stability parameter ζ (z/L , black dots, pos. values = stable, neg. values = unstable), whereas L is the Obukhov-length and z is the measurement height (2.4 m), all obtained by the eddy covariance complex EF, selected day May 13, 2006. Ny-Ålesund (Svalbard), ARCTEX-2006 campaign.

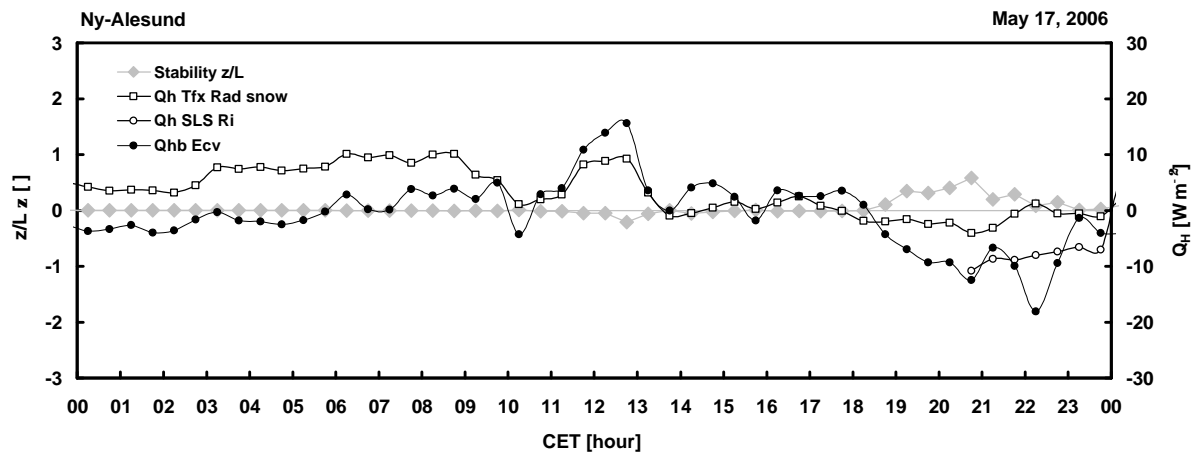
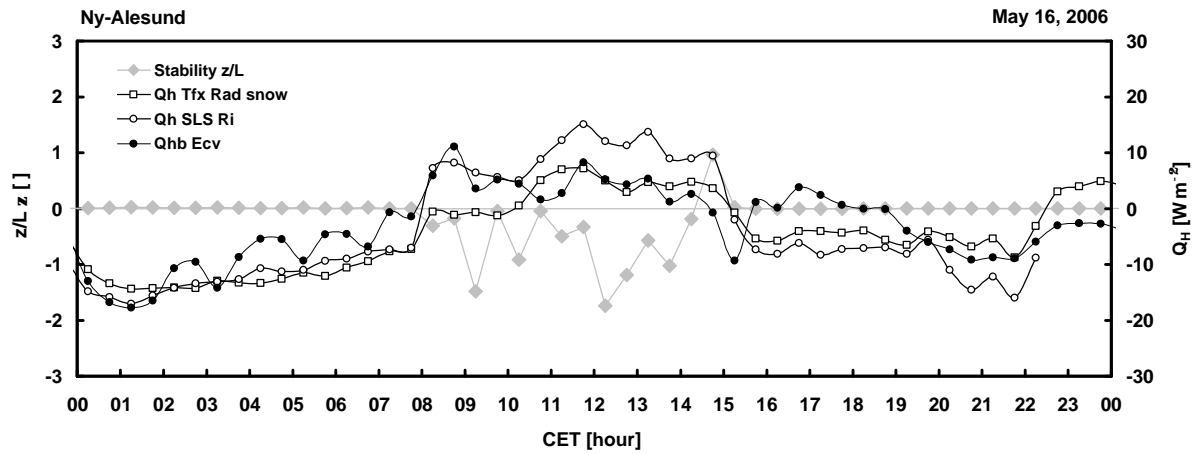
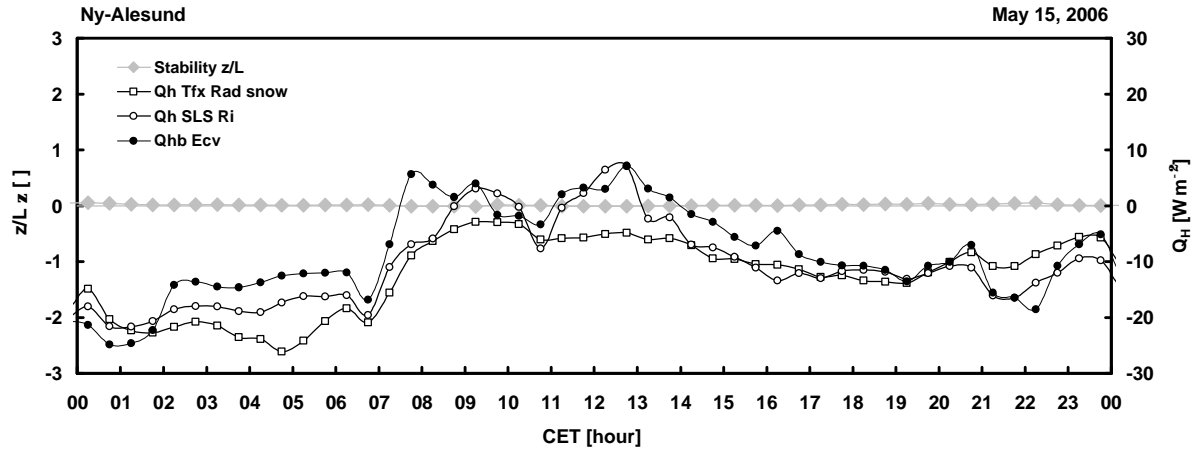
5.3 Daily charts

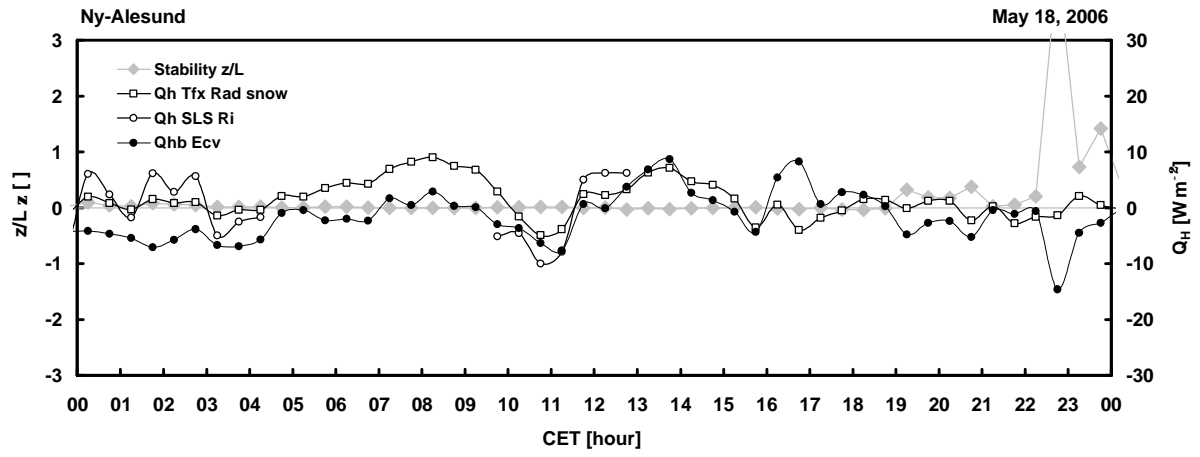
The figures in this chapter present the two directly measured sensible heat fluxes including the atmospheric stability parameter ζ (z/L) during the ARCTEX-2006 campaign May 7 to May 18 and the calculated sensible heat flux applying the model approach of Launiainen & Cheng, 1995 (Turbflx). For the latter approach the eddy covariance independent meteorological measurements of both gradient towers MT1 and MT2 as well as the BSRN-station were used. As input for the Turbflx-model the required ground (snow) surface temperature was recalculated from the outgoing longwave radiation values of the nearby BSRN-station. To determine the drag coefficient or bulk transfer coefficient a snow/ice covered land surface was assumed (Q_H Tfx Rad snow). The two direct approaches utilized a) the CSAT3 eddy covariance complex EF (Q_{HB} Ecv) and b) the laser-scintillometer section (Q_H SLS Ri). For the analysis of the scintillometer measurements the bulk Richardson number was used to decide the appropriate flux directions instead the usual vertical gradient of air temperature.











6 Data archived at Ny-Ålesund (CDs)

CD-Nummer		CD-Inhalt
CD1		Rohdaten CSAT3, ARCTEX-Gradientmast und Strahlungsbock, AWI-Met-Turm, Radiosonden
CD2		CSAT3-Originale und ausgelesene Dateien mit CSAT_B2A.EXE (Teil 1), 07.05.2006 bis 10.05.2006
CD3		CSAT3 ausgelesene Dateien mit CSAT_B2A.EXE (Teil 2), 11.05.2006 bis 15.05.2006
CD4		CSAT3 ausgelesene Dateien mit CSAT_B2A.EXE (Teil 3), 16.05.2006 bis 19.05.2006
CD5		TK 2 Eingabe- und Ausgabedateien (Teil 1), AT_0001.dat bis AT_0006.dat
CD6		TK 2 Eingabe- und Ausgabedateien (Teil 2), AT_0007.dat bis AT_0011.dat
CD7		TK 2 Eingabe- und Ausgabedateien (Teil 3), AT_0010.dat bis AT_0013.dat + Fesselballondaten + Scintillometer

Bisher erschienene Arbeiten der Reihe "Arbeitsergebnisse Universität Bayreuth, Abteilung Mikrometeorologie":

Nr	Author(s)	Title	Year
01	Foken	Der Bayreuther Turbulenzknecht	01/1999
02	Foken	Methode zur Bestimmung der trockenen Deposition von Bor	02/1999
03	Liu	Error analysis of the modified Bowen ratio method	02/1999
04	Foken et al.	Nachfrostgefährdung des ÖBG	03/1999
05	Hierteis	Dokumentation des Experimentes Dlouhá Louka	03/1999
06	Mangold	Dokumentation des Experimentes am Standort Weidenbrunnen, Juli/August 1998	07/1999
07	Heinz et al.	Strukturanalyse der atmosphärischen Turbulenz mittels Wavelet-Verfahren zur Bestimmung von Austauschprozessen über dem antarktischen Schelfeis	07/1999
08	Foken	Comparison of the sonic anemometer Young Model 81000 during VOITEX-99	10/1999
09	Foken et al.	Lufthygienisch-bioklimatische Kennzeichnung des oberen Egertales, Zwischenbericht 1999	11/1999
10	Sodemann	Stationsdatenbank zum BStMLU-Projekt Lufthygienisch-bioklimatische Kennzeichnung des oberen Egertales	03/2000
11	Neuner	Dokumentation zur Erstellung der meteorologischen Eingabedaten für das Modell BEKLIMA	10/2000
12	Foken et al.	Dokumentation des Experimentes VOITEX-99	10/2000
13	Bruckmeier et al.	Documentation of the experiment EBEX-2000, July 20 to August 24, 2000	01/2001
14	Foken et al.	Lufthygienisch-bioklimatische Kennzeichnung des oberen Egertales	02/2001
15	Göckede	Die Verwendung des Footprint-Modells nach Schmid (1997) zur stabilitätsabhängigen Bestimmung der Rauheitslänge	03/2001
16	Neuner	Berechnung der Evaporation im ÖBG (Universität Bayreuth) mit dem SVAT-Modell BEKLIMA	05/2001
17	Sodemann	Dokumentation der Software zur Bearbeitung der FINTUREX-Daten	08/2002
18	Göckede et al.	Dokumentation des Experiments STINHO-1	08/2002
19	Göckede et al.	Dokumentation des Experiments STINHO-2	12/2002
20	Göckede et al.	Characterisation of a complex measuring site for flux measurements	12/2002
21	Liebenthal	Strahlungsmessgerätevergleich während des Experiments STINHO-1	01/2003
22	Mauder et al.	Dokumentation des Experiments EVA_GRIPS	03/2003
23	Mauder et al.	Dokumentation des Experimentes LITFASS-2003, Dokumentation des Experimentes GRASATEM-2003	12/2003
24	Thomas et al.	Documentation of the WALDATEM-2003 Experiment	05/2004
25	Göckede et al.	Qualitätsbegutachtung komplexer mikrometeorologischer Messstationen im Rahmen des VERTIKO-Projekts	11/2004
26	Mauder & Foken	Documentation and instruction manual of the eddy covariance software package TK2	12/2004
27	Herold et al.	The OP-2 open path infrared gas analyser for CO ₂ and H ₂ O	01/2005
28	Ruppert	ATEM software for atmospheric turbulent exchange measurements using eddy covariance and relaxed eddy accumulation systems and Bayreuth whole-air REA system setup	04/2005
29	Foken (Ed.)	Klimatologische und mikrometeorologische Forschungen im Rahmen des Bayreuther Institutes für Terrestrische Ökosystemforschung (BITÖK), 1989-2004	06/2005
30	Siebeke & Serafimovich	Ultraschallanemometer-Überprüfung im Windkanal der TU Dresden 2007	04/2007
31	Lüers & Bareiss	The Arctic Turbulence Experiment 2006 PART 1: Technical documentation of the ARCTEX 2006 campaign, May, 2nd to May, 20th 2006	07/2007
32	Lüers & Bareiss	The Arctic Turbulence Experiment 2006 PART 2: Near surface measurements during the ARCTEX 2006 campaign, May, 2nd to May, 20th 2006	07/2007
33	Bareiss & Lüers	The Arctic Turbulence Experiment 2006 PART 3: Aerological measurements during the ARCTEX 2006 campaign, May, 2nd to May, 20th 2006	07/2007